Structure – Basicity Relationships of 4-Aryl Pyridine Moieties

ROHAN AJIT VAZE

Durham University Department of Chemistry

Structure – Basicity Relationships of 4-Aryl Pyridine Moieties

by

Rohan Vaze

2017

A thesis submitted to the

Department of Chemistry

in fulfilment of the requirements for the

Degree of Master of Science

ABSTRACT

To examine the transmission and relative magnitude of substituent effects in biphenyl compounds, we have used 4-aryl pyridine moieties as probes. Accordingly, 58 4-aryl pyridine type compounds have been synthesized, characterised and the acid dissociation constants of their conjugate acids have been determined at 298 kelvin.

The parameter *d*ΔG has been introduced and used to quantify substituent effects. It has been shown that a dichotomy exists between the transmission of electron-withdrawing substituents and electron donating substituents. Electron withdrawing groups in the 3 and 4 position exhibit effects of a similar magnitude while those in the 2 position exert a stronger effect. In contrast, electron donating groups have been shown to exert a significant effect only in the 2 and 4 position. Additionally, it has been found that the cyano substituent in the 2 position exerts an unexpectedly powerful effect while the nitro group in the same position exerts an unexpectedly weak effect. Crystal structures suggest the latter observation is due to the nitro group in the 2 position being twisted out of plane. These results indicate that secondary electronic effects and rotational freedom of functional groups might affect biphenyl geometry. Substituent effects in 4-aryl-3-picoline and 4-aryl-3,5-lutidine compounds have been found to be significantly weaker than in the analogous 4-aryl pyridine compounds, which suggests that resonance interactions between the two aryl rings are at least partially responsible for transmission of substituent effects.

ACKNOWLEDGEMENT

I must begin by expressing my gratitude to Professor Baxendale for giving me the opportunity to gain valuable research experience in his lab. The past year has been very fruitful and would not have been so without the Professor's guidance.

Thanks also to Dr. Marcus Baumann for being the in-house guru, to Dr. Ann-Marie O'Donoghue for her help and encouragement during the (long) process of pK_a measurement, to Dr. Batsanov for the crystal structures, and to the PhD students in our group- James, Michele, Laura, Laurens, Carl, Te and Seger for all their advice.

I would also like to express my gratitude to Alex Nicholls for helping me finish this thesis.

Last but not least, I must thank all the undergraduates in the group for making the lab a fun, music filled place to work in.

STATEMENT OF COPYRIGHT

LIST OF ABBREVIATIONS

1. ^{o}C – degrees Centigrade
2. h – hour(s)
3. min – minutes
4. RT – room temperature
5. mol – moles
6. eq. – equivalent(s)
7. UV-vis – ultraviolet-visible
8. δ - chemical shift
9. ν – wavenumber
10. Å - angstrom
11. NMR – Nuclear Magnetic Resonance Spectroscopy
12. FT-IR – Fourier Transform Infrared
13. XRD – X-ray Diffraction
14. HRMS – High Resolution Mass Spectrometry
15. J – coupling constant (in context of NMR spectra) or joules (unit of energy)
16. kJ/mol – kilojoule per mole
17. THF – tetrahydrofuran
18. TLC – thin layer chromatography
19. TBAF – tetrabutylammonium fluoride
20. SPhos - 2-Dicyclohexylphosphino-2',6'-dimethoxybiphenyl
21. PPh_3 – triphenylphosphine

22. $Pd(PPh_3)_4$ – tetrakis(triphenylphosphine)palladium(0)

23. Cs_2CO_3 – caesium carbonate

24. K_2CO_3 – potassium carbonate

25. $TiCl_4$ – titanium tetrachloride

26. $LiAlH_4$ or LAH – lithium aluminium hydride

INDEX

INTRODUCTION

a) Biphenyls and Atropisomerism:

Pattern recognition is essential to scientific inquiry, allowing not just the deduction of causal relationships but also the adaptation of natural trends for a select purpose. In the field of medicinal chemistry, pattern recognition has enabled the identification of privileged structures- widely applicable molecular scaffolds from which an array of useful compounds may be synthesized. Aryl rings constitute one such privileged class, providing for a range of favourable interactions with biologically relevant functional groups.[1] Interactions between proteins and drug molecules containing aryl groups have been shown to be dominated by hydrophobic interactions and π-stacking.[2] Aryl rings also exhibit favourable electrostatic interactions with amide groups[3], and favourable π-cation binding.[4] Not all aromatic structures, however, are equally valuable. A statistical analysis of NMR binding data conducted by Fesik *et al.* indicates that molecules containing a biphenyl substructure bind with greater selectivity and higher affinity to certain proteins than those with simple phenyl, napthyl or diphenylmethyl units, possibly owing to its shape and conformational flexibility.[5] As a result the biphenyl substructure is present in 4.3% of all marketed drugs, equating to 5,658 compounds which are active towards 311 different pharmacological targets.[6] Biphenyl moieties are also prevalent outside the realm of medicinal chemistry. Substituted biphenyls such as Buchwald's XPhos[7] and the derivatives of BIPHEP[8] have proven to be effective ligands in metal catalysed processes. Furthermore, biphenyl compounds have been the subject of much study for their semi-conductor properties[9] and are commonly encountered in liquid crystal technology.[10]

Given the ubiquity and utility of the biphenyl motif, a more detailed examination of its structure is necessary. The biphenyl core is composed of two phenyl rings linked by a sigma bond. Energetically favourable π overlap between the two aromatic rings is maximised when the phenyl rings are co-planar. However, such co-planarity leads to energetically unfavourable steric interactions between the flanking ortho substituents.[11] In an orthogonal conformation, the inverse is true, with the minimisation of steric repulsion being compensated by the loss of π overlap. The torsional angle between the planes containing the phenyl rings is therefore due to a compromise between steric and electronic factors, resulting in the phenyl rings being skewed at an angle with respect to each other in the ground state of the molecule.[12] It is important to note, however, that the torsional angle is dependent upon the environment and electronic state of the molecule.[11] In the crystal lattice of biphenyl the torsional angle tends to 0°[13], as opposed to 44° in the gas phase[14] and 32°[15] in solution. The torsional angle in biphenyl has also been shown to be affected by electronic excitation[11,16] and pressure.[17]

A non-zero torsional angle implies that substituted biphenyls are dissymmetric or asymmetric when the two sides of the molecule bridged by the sigma bond linker are not

identical.[18] Such molecules are chiral due to a rotational axis rather than a stereogenic atom. Unlike compounds with point chirality, where epimerisation requires the breaking of bonds, the stereochemistry of an axially chiral molecule can be inverted merely by rotation about the axis.[19] Compounds with a relatively low energy barrier to rotation about the stereogenic axis therefore exist as chiral rotamers that, at room temperature, rapidly undergo an inversion in stereochemistry.[20] However, if rotation about the chiral axis is sufficiently hindered, the isolation of optically pure stereoisomers is theoretically possible at ambient conditions. These configurationally stable (relatively), axially chiral stereoisomers are called atropisomers. The distinction between atropisomers and rotamers is arbitrary. In accordance with Oki's proposal, the rotational barrier about a chiral axis must be at least 23 kcal/mol – equivalent to a half-life of 1000 seconds at 298K- for the stereoisomer containing it to be considered an atropisomer.[18]

As with point-chiral molecules, convention exists for assignment of absolute stereodescriptors to atropisomers, illustrated below (Figure 1) using the example of 6,6'-dinitro-2,2'-biphenyldicarboxylic acid (the first enantiomerically pure atropisomer to be isolated[21]). A reference point is first chosen so as to obtain a Newman projection of the molecule about the chiral axis. The substituents immediately adjacent to the axis are then assigned priority in accordance with the Cahn-Ingold-Prelog rules[22], starting with the substituents of the proximate ring and assigning lower priority to substituents of the distal ring.[23] The sequential path from the substituent of second-highest priority to the substituent of third-highest priority then gives the stereodescriptor; a clockwise path corresponds to a R_a configuration while an anti-clockwise path corresponds to a S_a configuration.[23] The labels *M* (minus rotation) and *P* (plus rotation) may usually (with certain exceptions) be used in lieu of R_a and S_a respectively.[27]

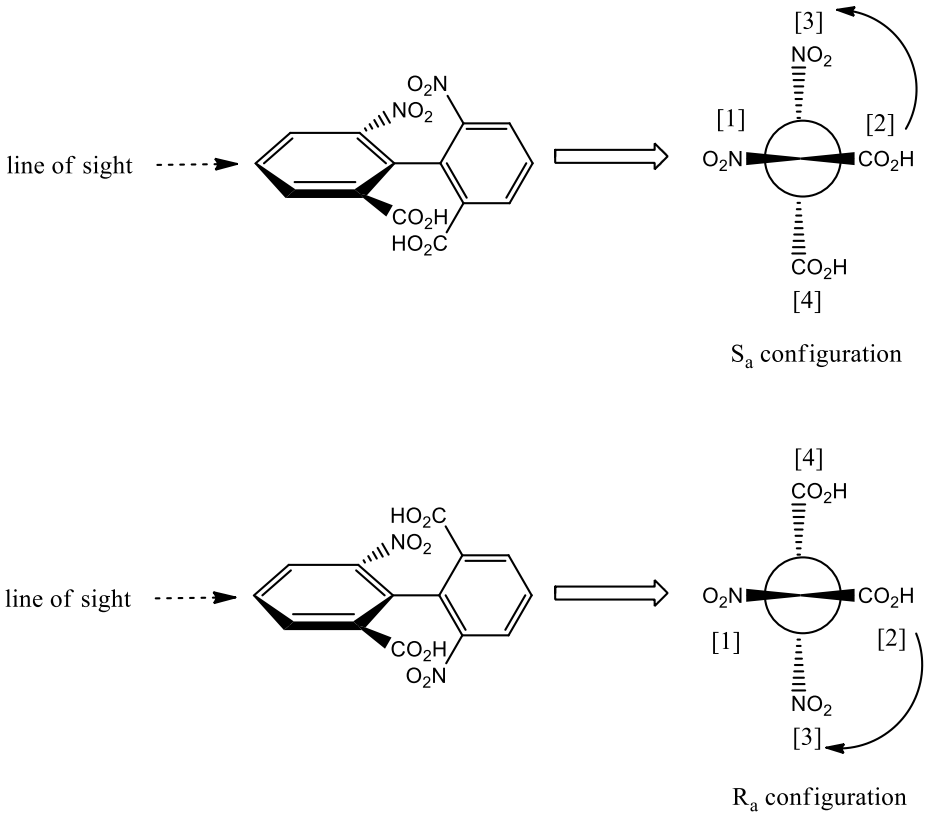

Figure 1 : *assignment of stereodescriptors to axially chiral compounds*

Atropisomerism is prevalent in both naturally occurring and synthetic compounds. Examples include the anti-plasmodial agent knipholone[24] (Figure 2) and gossypol (Figure 2), whose *M* enantiomer has been shown to possess potent anti-fertility and anti-cancer properties.[25] Both aforementioned compounds contain a chiral biaryl axis. However, since the criterion for atropisomerism is merely slow rotation about a stereogenic axis, compounds containing various types of chiral axes have been found. These include vancomycin (Figure 3), which possesses two chiral aryl-ether linkages within rotationally hindered macrocycles in addition to a chiral biaryl axis[12], telenzepine (Figure 3), which is chiral due to a hindered amide bond[26], and abyssomycin C (Figure 3), which has a rotationally hindered carbonyl-vinyl bond within an 11 membered ring.[27] Keller *et al.* have reviewed some biologically active atropisomeric compounds, representing a range of rotationally hindered chiral axes.[27]

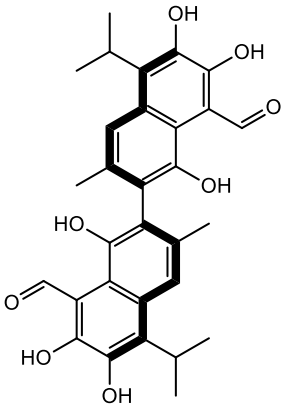

(R_a)-gossypol

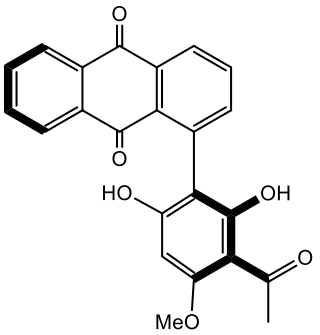

(R_a)-knipholone

Figure 2 : *naturally occurring atropisomeric compounds with chiral biaryl axes*

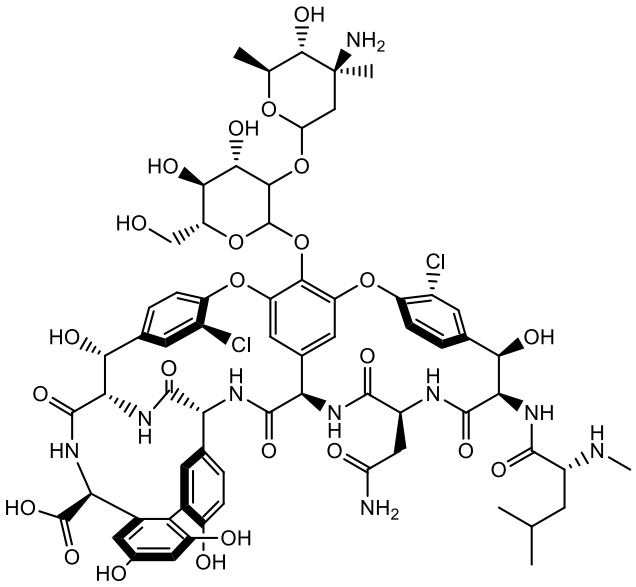

vancomycin

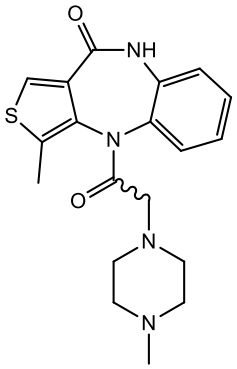

telenzepine

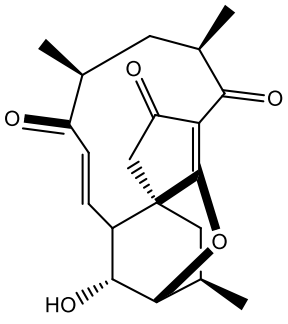

abyssomycin C

Figure 3: *examples of some types of chiral axes that can lead to atropisomerism*

b) Rotational Barriers/Atropisomerisation rates:

i) **In Biologically active compounds:**

Enantiomers are topologically equivalent and behave identically in achiral environments.[28] Biological systems, however, are inherently chiral. Consequently, the enantiomers of biologically active compounds frequently exhibit different pharmacodynamic and pharmacokinetic properties[29], as in the case of thalidomide.[30] Similar to point-chiral enantiomers, atrop-enantiomeric compounds can also differ in their biological activities. Zask *et al.* have reviewed some compounds whose atropisomers exhibit divergent pharmacological behaviour.[31]

The ability of atropisomers to undergo stereoinversion spontaneously via bond rotation adds a level of complexity to drug design. LaPlante *et al.* have categorized atropisomeric compounds according to their racemisation half-lives.[8] According to this categorisation, compounds with half-lives less than an hour are categorized as Class 1 atropisomers, those with half-lives ranging several hours to days have been classified as Class 2 atropisomers, and finally compounds with half-lives in the order of years have been classified as Class 3 atropisomers.[19] While Class 1 atropisomers can be developed as racemic mixtures and Class 3 atropisomers can be developed as either a single stereo-isomer or as racemic mixtures, Class 2 atropisomers pose a considerable challenge in drug design.[19] Thus, means of identifying Class 2 atropisomers and altering their structure to produce similarly efficacious compounds with significantly lower or higher half-lives of racemisation are crucial to the pharmaceutical industry.

Given the fact that biphenyls are a privileged scaffold in biologically active compounds, a qualitative understanding of factors influencing the barrier to rotation in biphenyl species would be useful and a predictive model even more so.

ii) **In Synthetic Chemistry:**

While stereolabile atropisomers pose a challenge in drug design, they are of considerable utility to the synthetic chemist. Configurationally unstable atrop-enantiomers exist as rapidly equilibrating racemic mixtures, making them ideal candidates for participation in dynamic kinetic resolutions. On the other *hand*, atrop-diastereomers can be thermally equilibrated to achieve, under the right conditions, a desired diastereomeric configuration. This latter strategy has been employed to great effect in Boger's total synthesis of the vancomycin aglycon. The vancomycin aglycon (Figure 4, stereogenic axes shown in bold) consists of three macrocycles. A key feature of Boger's synthesis is an analysis of the barrier to rotation about each chiral axis and subsequently, assembly of the macrocycles in descending order of the barrier to rotation about the chiral axis they contain.[32,33] The synthesis of each macrocycle is followed by diastereomeric enrichment via thermal equilibration.[33]

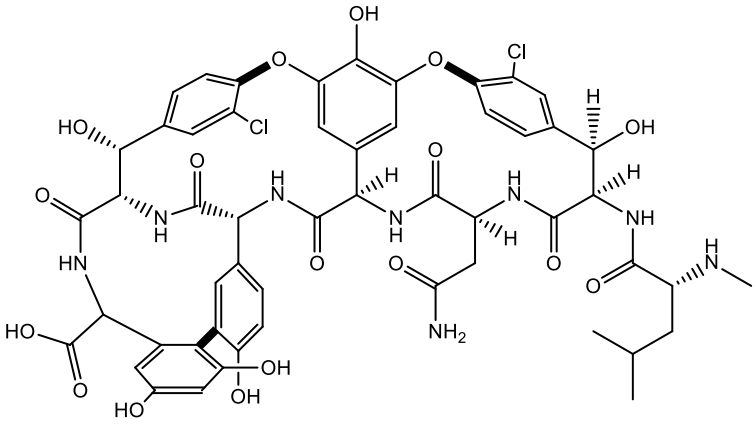

Figure 4: *Vancomycin aglycon*

Due to the order in which the macrocycles are synthesized, the configuration of each chiral axis is unperturbed by thermal equilibration of its successor macrocycle.[12,32] Furthermore, this approach allows recycling of undesired diastereomers, thereby improving overall efficiency of the synthesis.[12]

Clayden has synthesized enantiopure N,N-dialkyl benzamides by exploiting stereolabile aryl-amide bonds. Clayden's method involves introduction of a chiral centre *ortho* to the aryl-amide bond so as to enforce a large diastereomeric bias.[34] Consequently, this modified benzamide adopts the favoured diastereomeric configuration (made possible by ease of rotation about the stereogenic axis). Next, the aryl ring is further functionalized in order to raise the barrier to rotation about the aryl-amide bond.[34] Finally, the initially added chiral centre is removed to furnish an enantiopure, functionalized, configurationally stable benzamide.[34]

Bringmann's knipholone total synthesis relies on rapid and reversible epimerisation of an atrop-enantiomeric lactone. This so called "lactone approach" involves a Corey-Bakshi-Shibata (CBS) reduction on the stereolabile lactone precursor[35] (Figure 5). The stereochemistry of the biaryl axis in the product is therefore set up in a chiral reagent mediated dynamic kinetic resolution.

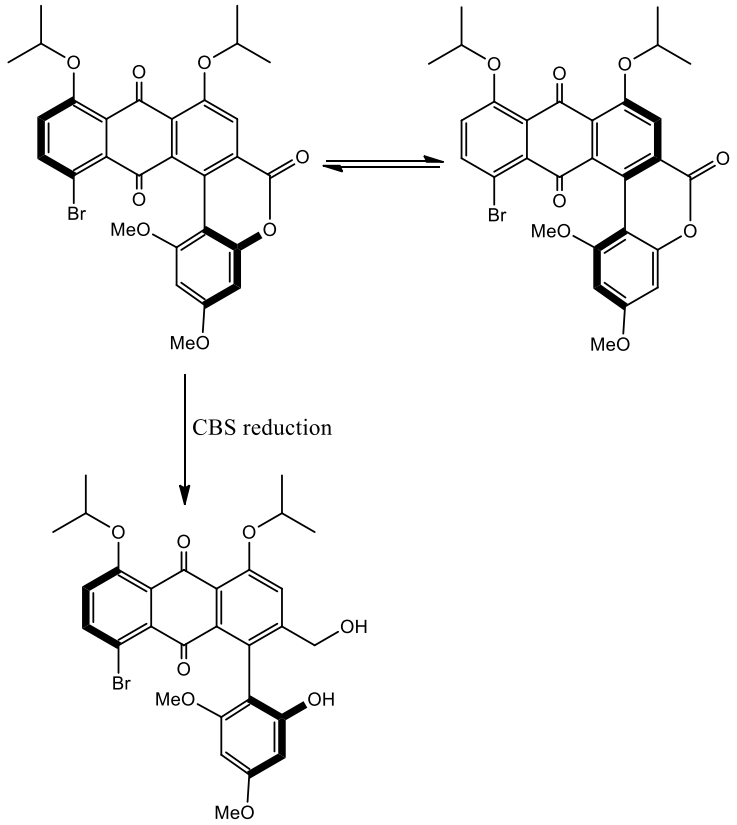

Figure 5: *Stereodetermining step in Bringmann's knipholone synthesis*

An organocatalytic, atropo-enantioselective tribromination of 3'-hydroxybiphenyl-3-carboxylic acid has been reported by Miller in which the stereodetermining step is a dynamic kinetic resolution of the substrate and possibly, the mono and di brominated intermediates.[36]

Asymmetric catalysis works by using a chiral catalyst to convert enantiomeric transition states into non-isoenergetic diastereomeric transition states. The pre-requisite for such a process to work is, of course, that the configuration of the catalyst remain constant over the catalytic cycles. The atropisomeric ligands BINAP and BINOL are a privileged set of asymmetric catalysts, having been effectively applied in a wide range of reactions.[37] Both BINOL and BINAP are configurationally stable, with extremely high barriers to rotation about the biaryl axis of 155 kJ/mol and 213 kJ/mol respectively.[38,39] This high stereochemical stability implies that when used as a source of chirality in asymmetric inductions, these compounds are useful only in an enantiomerically pure form, necessitating either a preparative resolution or atropo-enantioselective transformation to make them- which increases the cost of synthesising these ligands. Furthermore, when used in conjunction with chiral activators (i.e a second chiral ligand), such ligands form a diastereomeric mixture of catalytic species where one of the diastereomers possesses sub-optimal geometry.[40] Mikami *et al.* have used stereolabile, axially chiral ligands such as 2,2'-bis(diphenylphosphino)-1,1'-biphenyl (BIPHEP, shown in Figure 6) to overcome these problems.

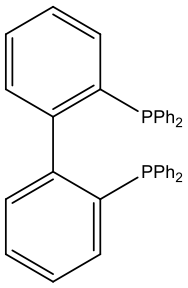

Figure 6: *BIPHEP*

Figure 7 depicts the use of a combination of BIPHEP and a chiral bidentate ligand to synthesize a diastereomerically pure metal complex.

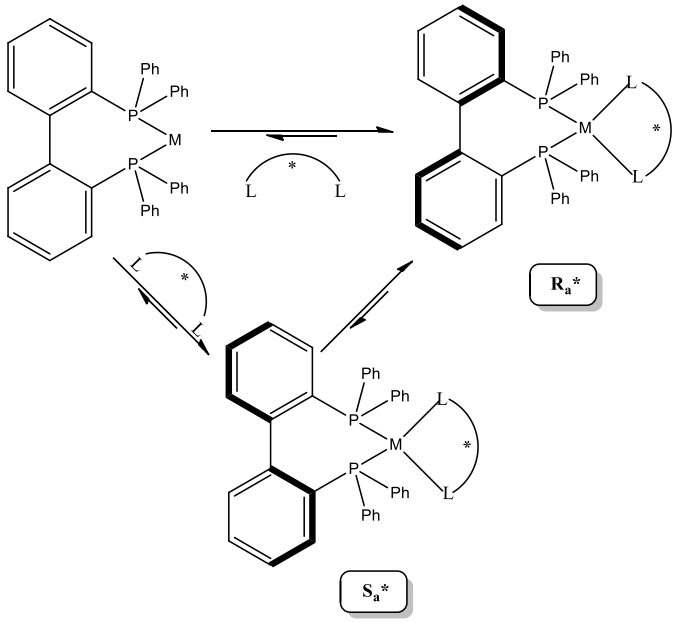

Figure 7: *Preparation of a diastereopure complex of BIPHEP using a chiral activator*

The chiral activator - in this example the chiral bidentate ligand - with configuration "*", on co-ordinating to the metal-BIPHEP complex, forms a mixture of diastereomeric complexes R_a* and S_a*, which through rotation about the biphenyl axis in BIPHEP undergo temperature controlled resolution to yield a diastereomerically enriched mixture of R_a* as the catalytic species.[40] A wide range of reactions catalysed by BIPHEP complexes of ruthenium, palladium, platinum and gold have been reported by Mikami, with BIPHEP complexes in certain cases delivering better enantioselectivities than analogous BINAP complexes.[41] Leitner *et al.* have recently used BIPHEP-rhodium complexes in conjunction with a proline derived chiral activator to achieve enantioselective hydrogenation of 2-acetamidoacrylates and hydroboration of styrene.[42]

A necessary condition for all the transformations described above is that the stereogenic axis in the substrate (or ligand) must undergo rapid inversion in stereochemistry and the same axis in the product must be stable enough to maintain its configuration under reaction

conditions. The ability to estimate the barrier to rotation in atropisomeric compounds would be therefore be valuable while planning synthetic routes- particularly in the case of biphenyls which appear in several utilitarian molecules.

c) Torsional angles:

The Eyring equation (Equation 1) specifies the barrier to rotation about a molecular axis as the difference between the free energy of the ground state molecule and free energy of the transition state the molecule must go through to complete one rotation.

$$k_{rate} = \frac{K k_B T e^{-(\Delta \ddot{G}/RT)}}{h} \qquad \textbf{(Equation 1)}$$

where: k_{rate} = rate of the process under consideration
k_B = Boltzmann's constant; T= temperature
h= Planck's constant; $\Delta \ddot{G}$ = free energy difference between ground state and transiton state
R= Gas Constant in $JK^{-1}mol^{-1}$ and K= transmission coefficient

The ground state energy of biphenyls is, as discussed above, an outcome of two opposing forces- steric repulsion and π overlap- which results in a torsional angle between the phenyl rings. All other geometric parameters of the biphenyl system remaining constant, this torsional angle gives a correlation between the geometry of the molecule and its free energy.[16] Besides being critical to calculating ground state energies, the torsional angle significantly affects electronic properties of biphenyls as well as the projection of substituents into space. The torsional angle is therefore in an important parameter in drug design, molecular electronics and synthetic chemistry.

Biologically active molecules interact with proteins that possess a specific shape and conformation.[27] Drug-receptor interactions therefore vary with the geometry of the drug molecule and the shape of such molecules needs to be optimized.[43] In the case of molecules containing the biphenyl moiety, this implies that the torsional angle can play an important role in the biological effects of the molecule. For instance, Lai *et al.* have found that the efficacy of ABCC2/MRP2 protein (responsible for drug resistance) inhibition by biphenyl substituted pyrazoles depends upon the torsional angle in the biphenyl substituent[44] and a study by Khim and Chang suggests the toxicity of polychlorinated biphenyls is affected by torsional angle dependant dipole moments.[45]

Biphenyls have also been extensively studied for molecular electronic applications due to the variation of several properties of biphenyl based junctions with torsional angles.[46] Examples include torsional angle dependant sensitivity of electric conductance to terahertz radiation in bipyridyl systems[46], conductance of 4,4'-disubstituted biphenyls[47], Seebeck effect of biphenyl junctions[48], and the rectifier characteristics of substituted biphenyl based devices[49].

With regard to synthetic methodology, it has been shown that biaryl torsional angles can influence reaction outcomes. Page and co-workers have developed a methodology for enantioselective epoxidations catalysed by N-substituted biaryl azepinium salts (Figure 8).[50] The enantioselectivities of epoxidations catalysed by these biaryl azepinium salts have been found to correlate to the torsional angle in the biaryl moiety present in the catalyst[50] (although no rationale for this correlation has presently been provided by the authors).

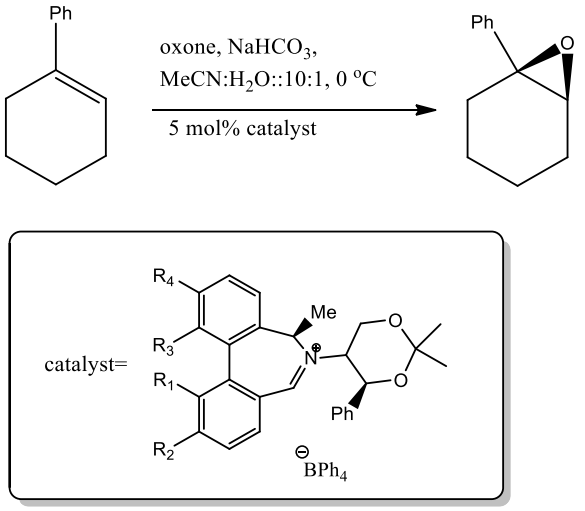

Figure 8: *Page's Biaryl azepinium salt catalysed stereoselective epoxidation*

Abboud *et al.* have reported an enantioselective hydroformylation of allyl nitrile and vinyl acetate catalysed by rhodium complexes of a biphenyl bridged bisphosphate ligand.[51] In this case, enantioselectivity and regioselectivity of the hydroformylation depend upon the torsional angle of the biphenyl bridge (circled in Figure 9) contained within the ligand which, as suggested by DFT calculations, is due to dependence of ligand bite angle on the torsional angle of the biphenyl bridge.[51]

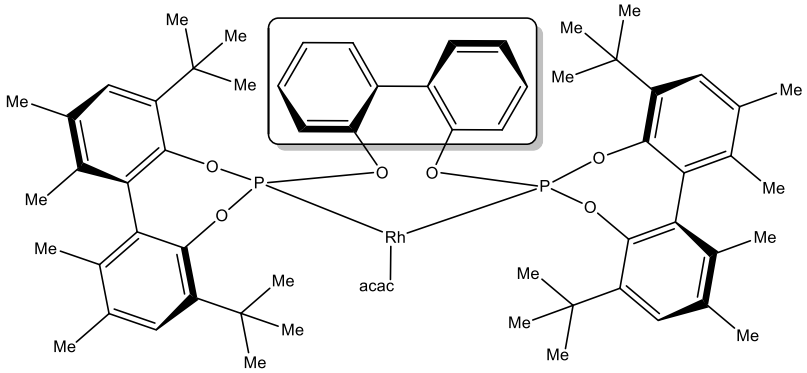

Figure 9: *Biphenyl bridged catalyst for asymmetric hydroformylation (Abboud et al.)*

d) Measuring rotational barriers, atropisomerisation rates, and torsional angles:

A survey of the chemical literature clearly indicates the value of being able to predict barriers to rotation and torsional angles in biphenyl compounds. In response to this need, several methods of determining rotational barriers have been reported. In principle, any analytical technique that can discriminate between atropisomers can be used to determine barriers to rotation, although the magnitude of this barrier dictates which technique is most suitable. For all the methods described below, it is assumed that the racemisation of biphenyl atropisomers is a first order reversible process.

Dynamic Nuclear Magnetic Resonance (D-NMR) methods have been applied to determine the barrier to rotation in atropisomeric biphenyls that racemise on the NMR timescale. A pre-requisite for such methods is that the molecule under study must contain a diastereotopic group such that the diastereotopic peaks appear at significantly different frequencies at accessible temperatures.[52] Several groups have used line shape analysis and the coalescence method to calculate the free energy of rotation about the stereogenic axis in atropisomeric biphenyls.[53-56] Notably, Sternhell *et al.* have examined the steric bulk of various functional groups using 1,1-dimethyl-5-substituted-6-(o-substituted phenyl) indanes (Figure 10a) as probes. The geminal dimethyl group incorporated into these probes provides the diastereotopic protons necessary for tracking atropisomerisation and rate constants are thus determinable through line shape analysis.[52] In a modification of Sternhell's approach, Mazanti, Ruzziconi and Schlosser have determined free energy of activation values for racemisation of various 3-isopropyldimethylsilyl-2'-substituted biphenyls (Figure 10b) using NMR line shape analysis and have proposed the use of these free energy values (designated "B values" by the authors) as a measure of a functional group's steric bulk.[57] While the B values reported by Ruzziconi *et al.* largely follow the same trends in steric bulk as those indicated by A values, the accuracy of B values as a measure of steric bulk depends upon the assumption that the electronic effect of a substituent on atropisomerisation barriers is insignificant compared to the steric effect of that substituent. Consequently, a few discrepancies arise in the case of substituents generally considered to have strong electronic effects. For instance, a comparison between the A values of the amino (NH_2) group and the dimethylamino ($N(CH_3)_2$) group suggests that the former, with an A value of 1.2 kcal/mol, is less "bulky" than the latter which has an A value of 2.1 kcal.mol. [57] In contradiction, the B values of the NH_2 group and $N(CH_3)_2$ group- 8.1 kcal/mol and 6.9 kcal/mol respectively- indicate the opposite. [57] Contradictions like these raise the possibility that electronic effects indeed play a significant role in determining atropisomerisation rates, as will be discussed in the proceeding section.

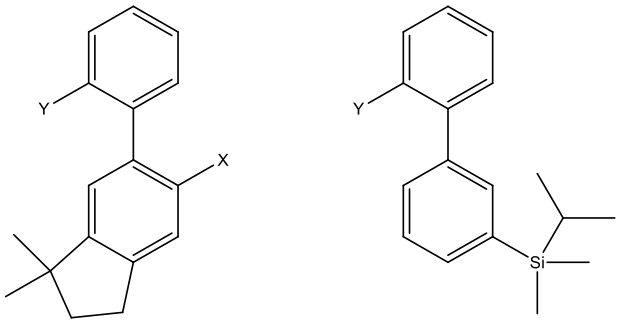

(a) (b)

Figure 10: *Biaryl probes containing diastereotopic groups*

For atropisomeric biphenyls with large racemisation barriers, dynamic chromatographic techniques can be employed for determination of rate constants and thermodynamic data. Dynamic High Performance Liquid Chromatography (D-HPLC) methods have been shown to be suitable for biphenyls with racemisation barriers of 65-105 kJ/mol while Dynamic Gas Chromatogaphy (D-GC) methods have been used for compounds with higher racemisation barriers falling in the 70-140 kJ/mol range.[58] The basic procedure for these techniques involves separation of a racemic mixture of atropisomers such that the combined effect of elution and racemisation yields elution profiles which, upon matching with computer simulated elution profiles, give rate constants for the racemisation process.[59,60] Activation parameters can then be obtained by determining rate constants at multiple temperatures. Koenig and co-workers have studied racemisation barriers in a number of substituted biphenyl compounds by D-GC and D-HPLC. From these experiments, Koenig *et al.* have reported an increase in racemisation barriers due to electron withdrawing groups and decrease in racemisation barriers due to electron donating groups in the case 4,4'-disusbstituted-2,2'-bis(trifluoromethyl)biphenyls (Figure 11a).[61] They have also observed a "buttressing effect" in 3-alkyl-2,2'-disubstituted biphenyls where the presence of the alkyl group prevents bending of the 2-substituent away from the opposite aryl ring(Figure 11c).[62] Interestingly, Koenig *et al.* have also found that the effect of electron withdrawing and electron donating substituents in 4,4'-disusbstituted-2,2'-diisopropylbiphenyls (Figure 11b) follows a trend opposite to the one observed in 2,2'-bis(trifluoromethyl) analogues.[62] The authors have postulated a favourable interaction between the benzylic protons and the π-electron cloud of the neighbouring phenyl ring to explain this observation.[62]

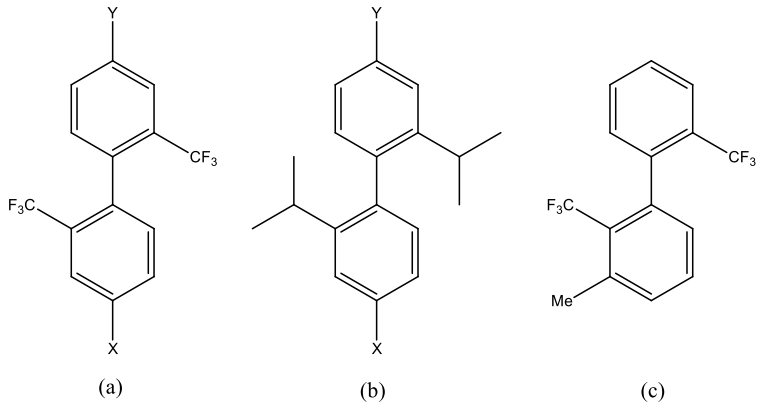

Figure 11: *Biaryl moieties investigated by Koenig et al.*

Other studies of biphenyl racemisation rates by chromatography include Bihlmeier, Mayor, and Klopper's determination of racemisation barriers, activation parameters and substituent effects in atropsiomeric 4,4'-disubstituted-2,2'-butyl bridged biphenyls (Figure 12) by D-HPLC which, like the findings of Koenig *et al*, indicate that electron withdrawing substituents increase atropisomerisation barriers while electron donating substituents decrease them.[63] Most recently, Wessig and Trapp have reported the use of D-HPLC for determination of racemisation barriers in various BIPHEP derivatives.[64]

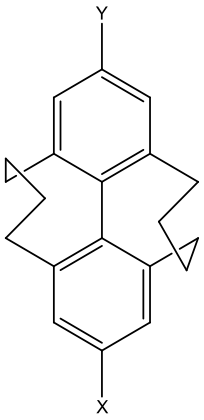

Figure 12: *Butyl bridged biphenyl moiety examined by Bihlmeier et al.*

In the case of charged biphenyls, capillary electrophoresis presents itself as a technique for studying atropisomerisation. Unlike the aforementioned chromatographic methods, no simulated elution profile is required for estimation of rate constants with capillary electrophoresis.[58] Instead, the electrophoretic method involves resolution of a racemic mixture of enantiomers, followed by selective heating of one enantiomer.[58] The rate constant for racemisation can then be calculated by tracking the racemisation profile of each enantiomer over time.[58] Koenig *et al.* have applied capillary electrophoresis for calculating the free energy of activation for the racemisation of water soluble 2,2'-bis-(trifluoromethyl)-4,4'-diammonium biphenyl and 2,2'-diisopropyl-4,4'-diammonium biphenyl .[58]

Vibrational Circular Dichroism (VCD) and Electronic Circular Dichroism (ECD) spectroscopy has proven very useful for detecting stereoisomerism and assigning configuration in pharmaceuticals[65,66] and natural products.[27] In CD spectroscopy the bands produced by a chiral molecule are opposite in sign to those produced by its enantiomer.[67] With the help of computational methods, absolute configuration can be correlated to CD spectra.[27] Pivonka and Wesolowski have used VCD spectroscopy for calculating the atropisomerisation rates in certain GABA modulators containing a rotationally hindered biphenyl motif. By tracking the intensity of CD bands of an initially enantiopure analyte over time, the racemisation rate can be calculated assuming first order kinetics for the process.[67]

Computational methods, and in particular high level DFT modelling, have also been applied extensively towards calculating racemisation rates of biphenyl species- either in combination with spectroscopic[57] or chromatographic techniques[64], or as stand-alone computational simulations.[68,69] Masson has calculated theoretical racemisation rates for 46 atropisomeric biphenyl compounds and has identified the hybrid functional approximations B3LYP-D, B97-D and TPSS-D3 as promising tools for estimating rotational barriers in biphenyl compounds.[70] DFT computations have also been widely used for calculating another important parameter in biphenyls: the torsional angle. Muchall *et al.* have, for instance, studied the effect of substituents on the torsional angle of biphenyl compounds and have suggested the use of electronic excitation potentials for predicting biphenyl geometry.[71] Sierra *et al.* have used DFT calculations to examine the variation of torsion angle with changing substituents in 4-amino-4'-substituted biphenyls and have suggested that steric factors are the dominant contribution to torsional angle, unless the substituents produce a strong "push-pull" effect between the two phenyl rings.[72]

Various spectroscopic methods provide an empirical alternative to torsional angle determination in biphenyls. By exploiting the correlation between spectral properties and degree of conjugation between the phenyl rings or the geometry of the biphenyl compound, torsional angles can be estimated using UV[73] and IR[74] spectroscopy. Based on a correlation between first and fourth ionisation potentials in biphenyls, photo-electron spectroscopy has also been employed for calculating torsional angles in polychlorinated biphenyls.[75] NMR spectroscopy, well known for its efficacy at elucidating structural features, has been applied towards calculating torsional angles in biphenyls- either on the basis of predictive equations[76], or by FIREMAT experiments using ^{13}C solid state spectra.[77] Additionally, X-Ray Diffraction (XRD) has been used to obtain solid state structures of several biphenyl compounds. Leroux has published an analysis of the crystal structures of mono and di-halogenated biphenyls, supplemented by DFT calculations, to identify the effects of fluorine substitution on biphenyl torsional angles.[78]

Using the methods described above, it is possible to study electronic and steric effects on atropisomerization barriers by calculating racemization rates in a range of substituted chiral biphenyls. We elected to explore 4-aryl pyridine moieties as probes, reasoning that changes in the electronic and steric nature of the 4-aryl substituent would affect the degree of conjugation between the aryl substituent and the pyridine ring, thereby influencing the basicity of the molecule. Under this assumption, the basicity constants of these pyridine

probes can be used for a qualitative study of substituent effects on the ground state geometry of the probe. We also hoped to use the data derived from these basicity constants to develop a semi-empirical, computationally aided model for predicting ground state geometry and barriers to rotation in biphenyls. The work presented in the following sections details the synthesis of a library of 4-aryl pyridines, 4-aryl-3-picolines and 4-aryl-3,5-lutidines, the measurement of the acid dissociation constants (K_a's) of the conjugate acids of these compounds, and a qualitative discussion of substituent effects based on the K_a's so obtained.

STRUCTURE-BASICITY RELATIONSHIPS OF 4-ARYL PYRIDINE MOIETIES

PREMISE

The aim of this project was to develop a computational model to predict ground state geometries and rotational barriers in substituted biphenyls. Previous simulations have shown that the effect of substituents on these two parameters tend to be dominated by steric repulsions between the flanking ortho substituents (indicated by R_1, R_2, R_3, and R_4 in Figure 13).[68,72] However, the electronic effect of substituents on the two rings has also been shown to be significant.[62,72] For instance, Grein has suggested that the geometry of 2,2'-dihalobiphenyls cannot be explained on the basis of steric effects alone.[68] Additionally, Gomez-Gallago's simulations have indicated that certain substituents significantly affect biphenyl geometry by exerting an electronic effect[72] and the empirical studies of Konig and others show that the electronic effects of substituents produce significant variation in biphenyl rotational barriers.[61,62]

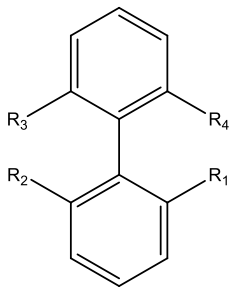

Figure 13: *Biphenyl compound with flanking ortho substituents*

It appears, therefore, that a model designed to estimate ground state geometries and rotational barriers in substituted biphenyls will need to account for the electronic effects of a substituent. Since there is a significant resonance interaction between the two aryl rings of a biphenyl molecule[79], we reasoned that the electronic effect of a substituent on one of the rings would also induce an effect on the second ring. Measuring the effect of a substituent on the ring to which it is not directly attached might therefore indicate the effect of substituents on the degree of π overlap between the two aryl rings and by extension, the torsional angle of the biphenyl molecule and the energy of its ground state.

Hammett constants have traditionally been used as a quantitative measure of the electronic effect of a substituent.[80] Furthermore, quantum chemical parameters have been previously calculated by using Hammett constants as an empirical guide[81], which could potentially be useful for our purpose. Hammett constants for a substituent are calculated from the effect of a substituent on the acid dissociation constant of a reference carboxylic acid.[82] Since we were interested in the biphenyl system, this would imply measuring the acid dissociation constants of 4-aryl benzoic acids (Figure 14, where "X" denotes the substituent). Byron *et al.* have previously reported the acid dissociation constants of these compounds.[83,84] However, the difference in acid dissociation constant produced by various substituents in the 4-aryl benzoic

acid probe is small (most substituents produced a difference in pK_a of less than 0.2 units).[83,84] Furthermore, in the case of 4-aryl benzoic acids, the reactive centre- the carboxylic acid functionality- is not a part of the biphenyl system but is instead conjugated to it.

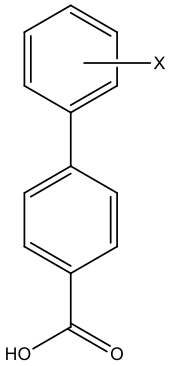

Figure 14: *Biphenyl carboxylic acid moiety examined by Byron et al.*

To study substituent effects on the biphenyl system, we chose to use 4-aryl pyridine moieties (Figure 15) as probes instead. These would have the advantage of having the reactive centre- the basic nitrogen in the pyridine ring- incorporated into the aromatic system, providing a closer match to the biphenyl species we intended to model.

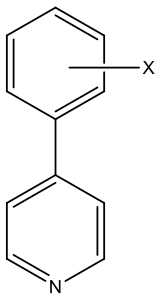

Figure 15: *4-aryl pyridine moiety selected for this study*

Accordingly, a series of 4-aryl pyridines was synthesized. The substituents on the aryl ring were chosen on the basis of their steric bulk (as quantified by A values[85]), on their electron donating or electron withdrawing capacity (as quantified on the basis of Hammett constants in both meta (σ_m) and para positions (σ_p)[82]), and on basis of the substituent possessing π-acceptor or π-donating orbitals. Table 1 lists the substituents chosen for study along with their A values and Hammett constants. In addition to the 4-aryl pyridine series, we also synthesized a library of 4-aryl-3-picolines and 4-aryl-3,5-lutidines in order to study the effect of increasing steric bulk in the flanking ortho positions on the effect of the various substituents. Where possible, we also obtained crystal structures of the compounds synthesized, since these have been used previously to guide torsional angle simulations.[68]

Substituent	A value (kJ/mol)	σ_m*	σ_p*
Methyl (CH_3)	7.1	-0.07	-0.17
Methoxy (OCH_3)	3.1	0.12	-0.27
Trifluoromethyl (CF_3)	8.8	0.43	0.54
Nitro (NO_2)	4.6	0.71	0.78
Cyano (CN)	0.9	0.56	0.66

***:** *a negative σ value indicates an electron withdrawing effect*

a positive σ value indicates an electron donating effect

Table 1: *A values and Hammett constants for substituents selected for this study*

SYNTHESIS

The functional group tolerance of the Suzuki-Miyaura coupling[86], in conjunction with the commercial availability of a wide range of boron nucleophiles, led us to the conclusion that this versatile reaction would be an efficient way of assembling the desired 4-aryl pyridine species. Furthermore, Marks *et al.* have previously reported the superiority of the Suzuki-Miyaura (SM) coupling over the Negishi and Stille couplings for the synthesis of sterically hindered 4-xylyl-3,5-lutidine-N-oxides.[87] Accordingly, a procedure for arylboronic acid-bromopyridine coupling was borrowed from the literature[88] and the reaction between phenylboronic acid and 4-bromopyridine hydrochloride (both commercially available) was used to test reaction conditions. Following purification by column chromatography, 4-phenyl pyridine, **1a**, was obtained in 93% yield using the literature procedure after 16 hours of refluxing the two coupling partners in a 4:1 mixture of glyme and water with 2 equivalents of caesium carbonate and 5mol% tetrakis(triphenylphosphine) palladium(0) ($Pd(PPh_3)_4$).

Heating the same reaction mixture to 100^oC in a microwave reactor significantly shortened reaction times, giving **1a** in 95% yield within an hour. In comparison, refluxing the reaction mixture over the same duration gave a 59% yield of **1a**. It was observed that significant amounts of a fine black powder were deposited on the walls of the reaction vial after microwave irradiation. Suspecting that this powder was elemental palladium and that this loss of palladium during the reaction was negatively affecting yields, we added a sub-stoichiometric amount of tetrabutylammonium fluoride (TBAF) solution to the reaction

mixture- reasoning that the added fluoride would form *in situ* a fluoro-palladium anionic species with a lipophilic counter-ion and therefore keep the palladium in solution. Gratifyingly, the addition of TBAF resulted in significant improvements in yield, particularly for boron nucleophiles containing strong electron withdrawing groups such as 2-nitrophenylboronic acid pinacol ester (Table 2). However, the precipitation of the black powder persisted even in the presence of TBAF and without further investigation an explanation for the increase in yield upon addition of fluoride cannot be provided.

Compound	Yield with 0mol% TBAF	Yield with 20mol% TBAF
4-(3-methoxyphenyl)-pyridine	59%	78%
4-(2-trifluoromethylphenyl)-pyridine	48%	75%
4-(2-nitrophenyl)-pyridine	15%	34%

Table 2: *Effect of added TBAF on SM coupling yields*

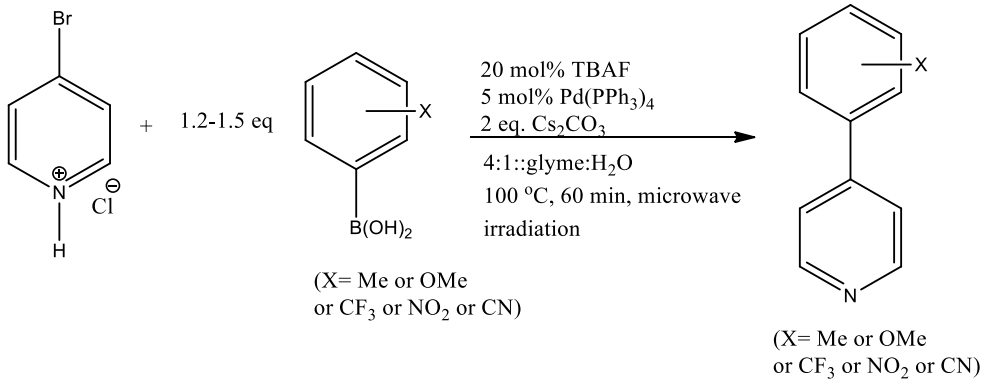

Scheme 1: *Synthesis of 4-aryl pyridines*

Eighteen 4-aryl pyridines- compounds **1a-r**- were synthesized using the reaction conditions described above (Scheme 1) followed by flash chromatography for purification. Yields of the isolated products are given below (Table 3), with the designation of the substituent on the aryl ring given alongside the compound name.

Compound	Substituent	Designation	Yield (in nearest whole number %)
4-phenyl pyridine	H	**1a**	95

4-(2-methylphenyl)-pyridine	$2CH_3$	**1b**	75
4-(3-methylphenyl)-pyridine	$3CH_3$	**1c**	95
4-(4-methylphenyl)-pyridine	$4CH_3$	**1d**	95
4-(2,4-dimethylphenyl)-pyridine	$2CH_3$+$4CH_3$	**1e**	83
4-(2-methoxyphenyl)-pyridine	$2OCH_3$	**1f**	91
4-(3-methoxyphenyl)-pyridine	$3OCH_3$	**1g**	78
4-(4-methoxyphenyl)-pyridine	$4OCH_3$	**1h**	80
4-(2,4-dimethoxyphenyl)-pyridine	$2OCH_3$+$4OCH_3$	**1i**	80
4-(2-trifluoromethylphenyl)-pyridine	$2CF_3$	**1j**	74
4-(3-trifluoromethylphenyl)-pyridine	$3CF_3$	**1k**	52
4-(4-trifluoromethylphenyl)-pyridine	$4CF_3$	**1l**	75
4-(2-nitrophenyl)-pyridine	$2NO_2$	**1m**	34
4-(3-nitrophenyl)-pyridine	$3NO_2$	**1n**	66
4-(4-nitrophenyl)-pyridine	$4NO_2$	**1o**	78
4-(2-cyanophenyl)-pyridine	2CN	**1p**	81
4-(3-cyanophenyl)-pyridine	3CN	**1q**	81
4-(4-cyanophenyl)-pyridine	4CN	**1r**	69

Table 3: *Isolated yields of 4-aryl pyridine compounds*

At a later stage, we also needed to synthesize compounds **1s-x** (Figure 16).

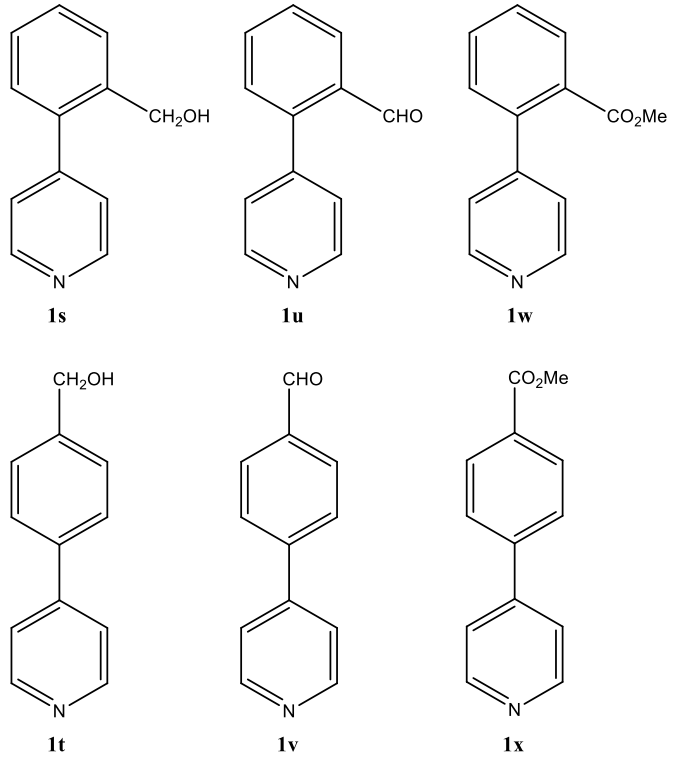

Figure 16: *Clockwise: 4-(2-hydroxymethyl)-pyridine, 4-(2-formyl)-pyridine, 4-(2-carbomethoxy)-pyridine, 4-(4-carbomethoxy)-pyridine, 4-(4-formyl)-pyridine, 4-(4-hydroxymethyl)-pyridine*

1u and **1v** were synthesized via the SM coupling of 4-pyridylboronic acid with 2-bromobenzaldehyde and 4-bromobenzaldehyde respectively under reaction conditions identical to those used for producing compounds **1a-r**. Similarly, the SM coupling of 4-pyridylboronic acid with methyl 2-iodobenzoate and methyl 4-bromobenzoate furnished **1w** and **1x** (Scheme 2).

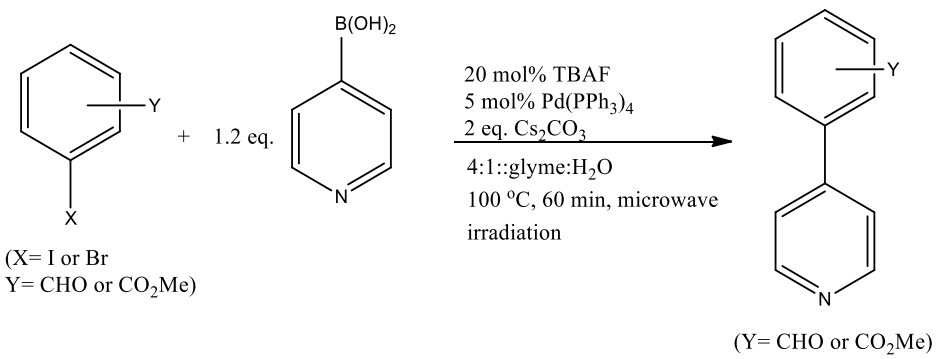

Scheme 2: *Synthesis of 1u-v and 1w-x*

The reduction of **1u** and **1v** using sodium borohydride ($NaBH_4$) (Scheme 3) gave compounds **1s** and **1t.**

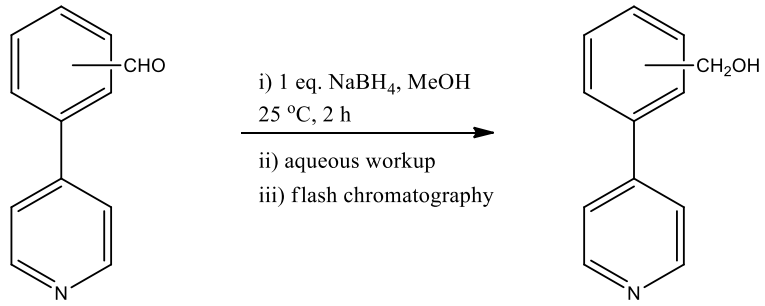

Scheme 3: *Reduction of 1u/v to 1s/t*

Compounds **1s-x** were thus isolated in yields shown in Table 4.

Compound	Substituent	Designation	Yield (in nearest whole number %)
4-(2-hydroxymethylphenyl)-pyridine	$2CH_2OH$	**1s**	76
4-(4-hydroxymethylphenyl)-pyridine	$4CH_2OH$	**1t**	74
4-(2-formylphenyl)-pyridine	2CHO	**1u**	62
4-(4-formylphenyl)-pyridine	4CHO	**1v**	75
4-(2-carbomethoxyphenyl)-pyridine	$2CO_2CH_3$	**1w**	47
4-(4-carbomethoxyphenyl)-pyridine	$4CO_2CH_3$	**1x**	56

Table 4: *Isolated yields of compounds **1s-x***

Synthesis of the picoline and lutidine libraries necessitated the preparation of suitable electrophiles. A previously reported procedure[89] (Scheme 5) was used to obtain 4-bromo-3-picoline and 4-bromo-3,5-lutidine starting from 3-picoline-N-oxide and 3,5-lutidine respectively. 3,5-lutidine was oxidised to its N-oxide using hydrogen peroxide and acetic acid. 3-picoline-N-oxide was obtained commercially. Both N-oxides were nitrated using a sodium nitrate-sulfuric acid mixture followed by bromination to furnish the two 4-bromo-N-oxides. These were then reduced by zero valent titanium, generated *in situ* from titanium tetrachloride and lithium aluminium hydride, to obtain the desired products.

Freshly purified 4-bromo-3-picoline appeared as a colourless viscous oil. Over the course of a few hours, however, this oil turned reddish-brown. Yields of SM couplings using this sample of 4-bromo-picoline were inconsistent and decreased with each subsequent reaction. Furthermore, addition of the discoloured sample to an aqueous alkaline solution produced bright red mixtures, indicating that 4-bromo-3-picoline was spontaneously suffering some form of chemical change. A literature search revealed that 4-halo pyridine moieties undergo oligomerisation, initiated by SN_{Ar} attack of the pyridine nitrogen on the 4 position of a second 4-halo pyridine.[90] This problem was overcome by storing 4-bromo-3-picoline and 4-bromo-3,5-lutidine as their hydrochloride salts which, on the basis of ^{1}H Nuclear Magnetic Resonance (NMR) spectra, were stable for at least five months at $0^{o}C$.

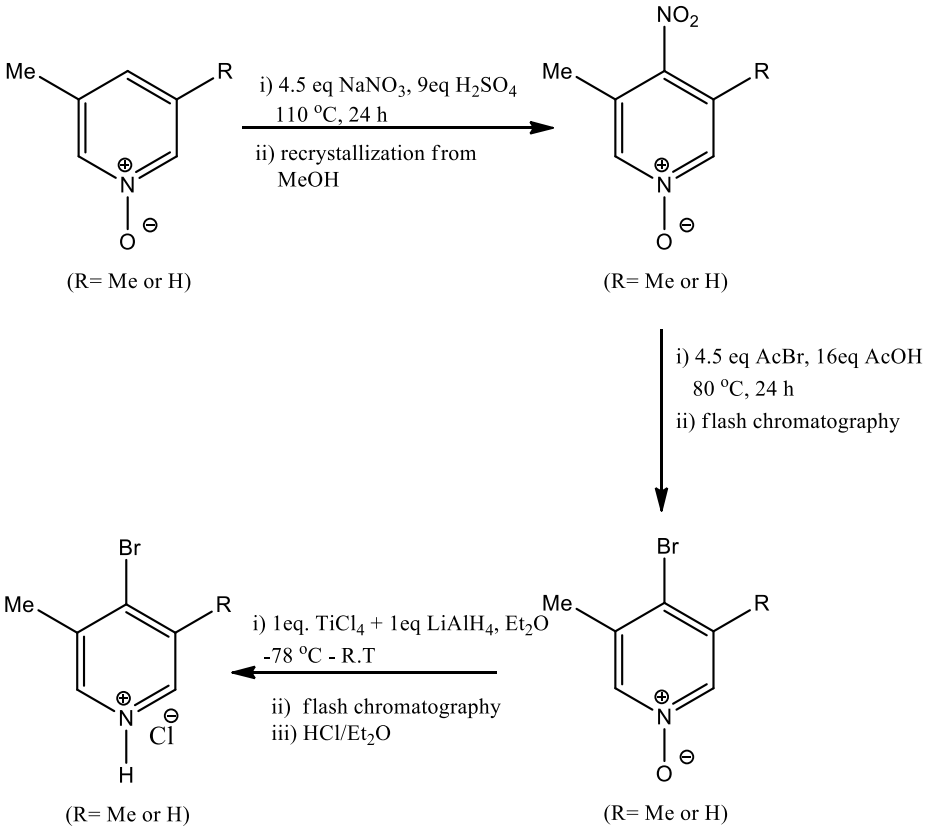

Scheme 5: *Synthesis of 4-bromo-3-picoline and 4-bromo-3,5-lutidine*

We also explored the possibility of using picoline and lutidine diazonium salts as electrophiles since the SM coupling of aryl diazonium salts is well documented.[91] The reduction of 4-nitro-3-picoline-N-oxide to 4-amino-3-picoline was achieved in moderate yield using 3 equivalents of Ti(0). However, the attempted diazotisation of 4-amino-3-picoline resulted in exothermic decomposition of the substrate. This is consistent with reports of 4-diazopyridinium salts being unstable.[92] While Filimonov *et al.* have exploited the inherent instability of 4-diazopyridinum salts for the conversion of 4-aminopyridines to pyridyl triflates[93], we decided not to apply this protocol since aryl bromides have been shown to be better electrophiles for the SM coupling than aryl triflates.[94]

Having prepared the 4-bromo-3-picoline and 4-bromo-3,5-lutidine salts, we turned our attention to their SM coupling. Anticipating a slower cross-coupling reaction for these electrophiles due to the increased steric hindrance about the 4 position, we changed our catalytic system from $Pd(PPh_3)_4$ to a combination of palladium (II) acetate as pre-catalyst and Buchwald's SPhos ligand.[95] Palladium-SPhos complexes have previously been shown to be effective catalysts for the SM coupling of sterically hindered diortho substituted arenes.[95]

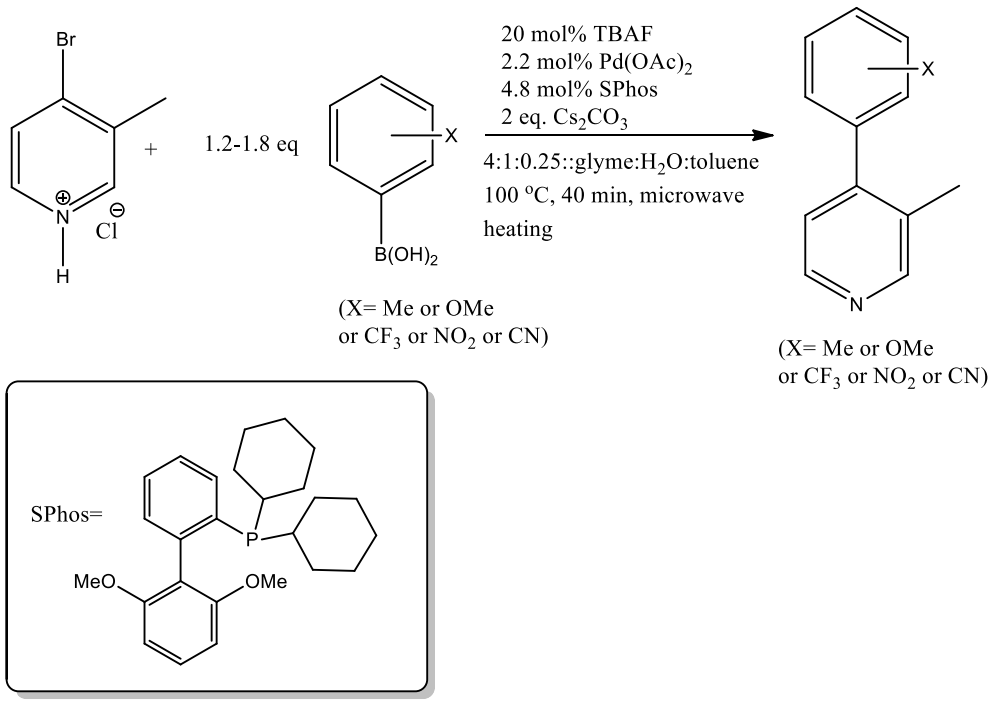

Scheme 6: *Synthesis of 4-aryl-3-picolines*

Using the reaction conditions shown in Scheme 6, moderate to good yields (Table 5) of the 4-aryl-3-picolines **7a-r** were obtained.

Compound	Substituent	Designation	Yield (in nearest whole number %)
4-phenyl-3-picoline	H	**7a**	83
4-(2-methylphenyl)-3-picoline	$2CH_3$	**7b**	57
4-(3-methylphenyl)-3-picoline	$3CH_3$	**7c**	87
4-(4-methylphenyl)-3-picoline	$4CH_3$	**7d**	72
4-(2,4-dimethylphenyl)-3-picoline	$2CH_3$+$4CH_3$	**7e**	51
4-(2-methoxyphenyl)-3-picoline	$2OCH_3$	**7f**	82
4-(3-methoxyphenyl)-3-picoline	$3OCH_3$	**7g**	67
4-(4-methoxyphenyl)-3-picoline	$4OCH_3$	**7h**	56

: *A values and Hammett constants for substituents selected for this study*

4-(2,4-dimethoxyphenyl)-3-picoline	$2OCH_3$+$4OCH_3$	**7i**	84
4-(2-trifluoromethylphenyl)-3-picoline	$2CF_3$	**7j**	49
4-(3-trifluoromethylphenyl)-3-picoline	$3CF_3$	**7k**	55
4-(4-trifluoromethylphenyl)-3-picoline	$4CF_3$	**7l**	64
4-(2-nitrophenyl)-3-picoline	$2NO_2$	**7m**	39
4-(3-nitrophenyl)-3-picoline	$3NO_2$	**7n**	70
4-(4-nitrophenyl)-3-picoline	$4NO_2$	**7o**	79
4-(2-cyanophenyl)-3-picoline	2CN	**7p**	42
4-(3-cyanophenyl)-3-picoline	3CN	**7q**	87
4-(4-cyanophenyl)-3-picoline	4CN	**7r**	68

Table 5: *Isolated yields of 4-aryl-3-picolines*

A higher temperature of 125^{o}C was required for the SM couplings of 4-bromo-3,5-lutidine. Low to moderate yields were obtained for most of the 4-aryl-3,5-lutidines (Table 6). **12p** was isolated with a poor 12% yield while reactions with 2-nitrophenylboronic acid pinacol ester and 2-trifluoromethylphenylboronic acid failed to return any product.

Compound	Substituent	Designation	Yield (in nearest whole number %)
4-phenyl-3,5-lutidine	H	**12a**	65
4-(2-methylphenyl)-3,5-lutidine	$2CH_3$	**12b**	49
4-(3-methylphenyl)-3,5-lutidine	$3CH_3$	**12c**	45

4-(4-methylphenyl)-3,5-lutidine	$4CH_3$	**12d**	36
4-(2,4-dimethylphenyl)-3,5-lutidine	$2CH_3$+$4CH_3$	**12e**	54
4-(2-methoxyphenyl)-3,5-lutidine	$2OCH_3$	**12f**	47
4-(3-methoxyphenyl)-3,5-lutidine	$3OCH_3$	**12g**	49
4-(4-methoxyphenyl)-3,5-lutidine	$4OCH_3$	**12h**	56
4-(2,4-dimethoxyphenyl)-3,5-lutidine	$2OCH_3$+$4OCH_3$	**12i**	54
4-(2-trifluoromethylphenyl)-3,5-lutidine	$2CF_3$	**12j**	0
4-(3-trifluoromethylphenyl)-3,5-lutidine	$3CF_3$	**12k**	45
4-(4-trifluoromethylphenyl)-3,5-lutidine	$4CF_3$	**12l**	58
4-(2-nitrophenyl)-3,5-lutidine	$2NO_2$	**12m**	0
4-(3-nitrophenyl)-3,5-lutidine	$3NO_2$	**12n**	53
4-(4-nitrophenyl)-3,5-lutidine	$4NO_2$	**12o**	42
4-(2-cyanophenyl)-3,5-lutidine	2CN	**12p**	12
4-(3-cyanophenyl)-3,5-lutidine	3CN	**12q**	60
4-(4-cyanophenyl)-3,5-lutidine	4CN	**12r**	60

Table 6: *Isolated yields of 4-aryl-3,5-lutidines*

Since **12j** and **12m** could not be obtained using the aforementioned SM coupling conditions, we decided to pursue an alternate synthetic route. As shown in Scheme 8, this route involved the aldol condensation of 2-trifluoromethyl or 2-nitro benzaldehyde with propanal followed by reaction of the resulting cinnamaldehyde product with propanal and an ammonium salt to generate a 1,4-dihydropyridine species which could be oxidised to furnish **12j** and **12m**.

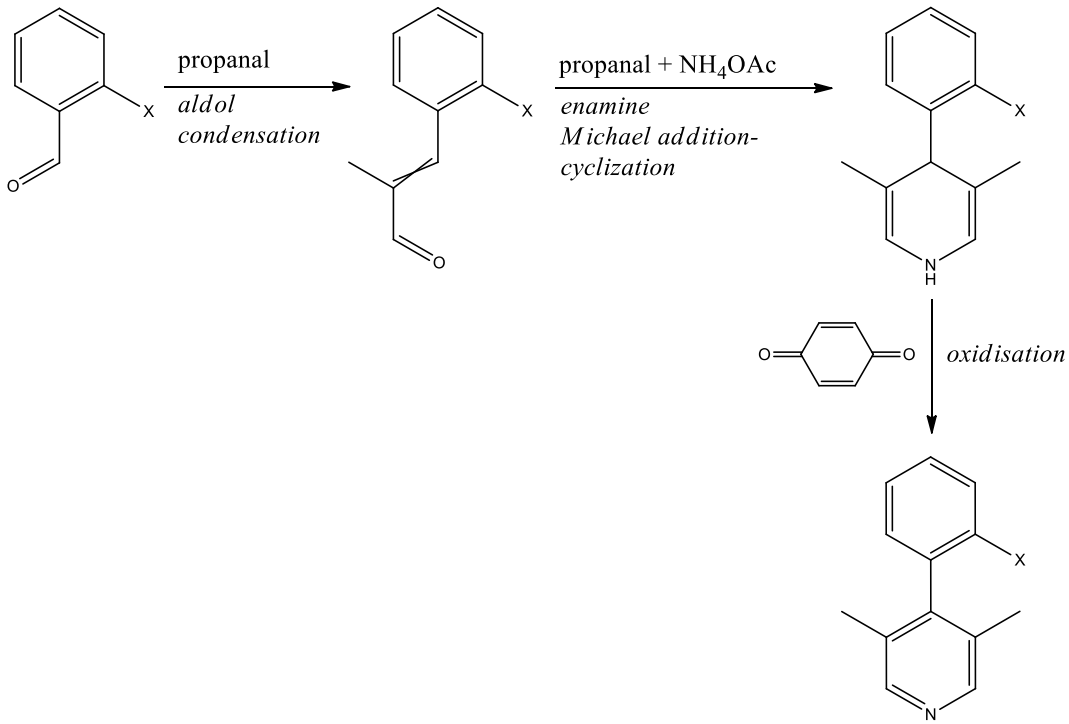

Scheme 8: *Proposed synthetic route to 12j and 12m*

The aldol condensation between propanal and both 2-trifluoromethylbenzaldehyde and 2-nitrobenzaldehyde produced, under various conditions, a thick gel from which no product could be isolated. We also attempted the addition of propanal enolate, generated by kinetic deprotonation of propanal, to the benzaldehyde moieties. Disappointingly, this reaction only gave a mixture of multiple products which could not be purified by chromatography. In both cases only significant amounts of the 2-substituted benzaldehyde substrate could be separated from the reaction mixture. Due to the failure of the first step of our proposed synthetic route, compounds **12j** and **12m** have thus far not been isolated.

The 58 4-aryl-pyridine moieties we obtained in the manner described above were characterized based on ^{1}H, ^{13}C, DEPT 135 and, where applicable, ^{19}F NMR spectra, High Resolution Mass Spectrometry (HRMS), and Infrared (IR) Spectra. Uncorrected melting points are reported for the solid compounds and where possible crystal structures have been collected.

MEASUREMENT OF ACID DISSOCIATION CONSTANTS

The acid dissociation constants (K_a's) of the conjugate acids of **1a-x**, **7a-r** and- with the exception of **12j** and **12m**- **12a-r** - were measured by UV-visible spectrophotometry. These compounds were all insoluble in water and a suitable solvent system first had to be chosen. Surmising that **12e** was likely to be the most lipophilic compound in our library, we attempted preparation of a 10^{-3} mol dm^{-3} solution of **12e** in various acetonitrile-water mixtures. A 50% solution of water in acetonitrile was found to be the most aqueous solvent system that could yield a 10^{-3} mol dm^{-3} solution of **12e** and all K_a's were therefore measured in a 1:1 mixture of acetonitrile and water.

With the solvent system established, UV-visible absorbances of the compounds in our library (analytes) were mapped within a 200-800 nanometre interval in both strongly acidic and strongly basic media at 25°C by mixing equal volumes of a $5X10^{-5}$ – $3X10^{-4}$ mol dm^{-3} solution of the analyte in acetonitrile with a 0.1 mol dm^{-3} aqueous solution of HCl or KOH. The absorbance in HCl solution corresponds to the absorbance of the protonated form of the analyte (A_{max}) occurring at wavelength λ_{max}, while the absorbance in KOH solution corresponds to absorbance of the neutral form of the analyte (A_{min}) at wavelength λ_{min}. For the *first few compounds tested in such a manner*, absorbances were additionally measured over a range of *p*H's to check for the appearance of an isosbestic point (Figure 17), which would indicate the presence of only two absorbing species (the base and its conjugate acid).

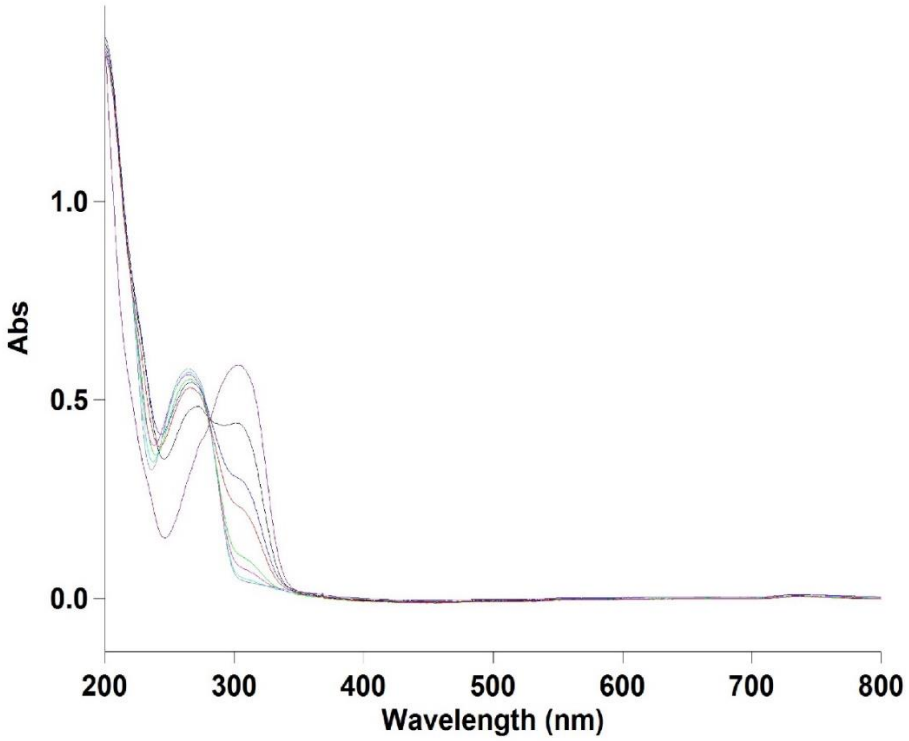

Figure 17: *Absorbance v Wavelength plot*

From these absorbance measurements, an analytical wavelength- λ_{obs}- was chosen such that the difference between A_{max} and A_{min} was maximum at this wavelength. The absorbance of the analyte at λ_{obs} (A_{obs}) was then measured over a pH range at 25^{o}C to obtain a plot of A_{obs} versus pH. (A_{obs} versus *p*H values can be found in the Compact Disk accompanying this manuscript)

λ_{max}, λ_{min}, λ_{obs}, and concentration of the analytes used for measurement of *p*K_a values are given below in Tables 7,8,9. All wavelengths are expressed in nanometres (nm), and concentrations are expressed in 10^{-6} moles dm^{-3} (µM).

<u>UV-vis Absorbance data for 4-Aryl pyridines:</u>

Compound	Substituent	λ_{max}	λ_{min}	λ_{obs}	Analyte Concentration
Pyridine	---	256	257	254	200
1a	H	288	255	300	100
1b	$2CH_3$	283	248	296	100
1c	$3CH_3$	290	258	293	50
1d	$4CH_3$	303	265	303	100
1e	$2CH_3$+$4CH_3$	299	257	303	100
1f	$2OCH_3$	333	295	333	200

1g	$3OCH_3$	285	258	291	100
1h	$4OCH_3$	328	280	328	50
1i	$2OCH_3$+$4OCH_3$	346	298	346	75
1j	$2CF_3$	258	260	258	150
1k	$3CF_3$	272	248	285	75
1l	$4CF_3$	271	249	282	75
1m	$2NO_2$	247	256	252	150
1n	$3NO_2$	266	245	283	50
1o	$4NO_2$	284	286	284	50
1p	2CN	268	245	273	100
1q	3CN	271	250	281	50
1r	4CN	276	261	296	100
1s	$2CH_2OH$	278	246	278	75
1t	$4CH_2OH$	297	261	297	100
1u	2CHO	243	255	244	100
1v	4CHO	286	275	305	100
1w	$2CO_2CH_3$	263	215	274	150
1x	$4CO_2CH_3$	281	265	293	50

Table 7: *Absorbance versus wavelength data for 4-aryl pyridines*

UV-vis Absorbance data for 4-Aryl-3-picolines:

Compound	**Substituent**	**λ_{max}**	**λ_{min}**	**λ_{max}**	**Analyte Concentration**
1a	H	271	242	286	100
1b	$2CH_3$	264	208	266	100
1c	$3CH_3$	272	245	286	200
1d	$4CH_3$	292	251	303	100
1e	$2CH_3$+$4CH_3$	290	251	290	50
1f	$2OCH_3$	314	271	313	200
1g	$3OCH_3$	270	246	273	50
1h	$4OCH_3$	314	266	314	100
1i	$2OCH_3$+$4OCH_3$	328	266	328	200
1j	$2CF_3$	263	263	263	100
1k	$3CF_3$	265	235	265	75
1l	$4CF_3$	264	236	264	100
1m	$2NO_2$	264	263	264	50
1n	$3NO_2$	262	232	263	50
1o	$4NO_2$	273	277	267	50
1p	2CN	266	268	267	200
1q	3CN	265	214	265	75
1r	4CN	266	246	272	75

Table 8: *Absorbance versus wavelength data for 4-aryl-3-picolines*

UV-vis Absorbance data for 4-Aryl-3,5-lutidines:

Compound	Substituent	λ_{max}	λ_{min}	λ_{max}	Analyte Concentration
1a	H	267	267	267	200
1b	$2CH_3$	267	265	268	200
1c	$3CH_3$	270	266	278	200
1d	$4CH_3$	271	243	280	200
1e	$2CH_3$+$4CH_3$	268	266	271	200
1f	$2OCH_3$	270	273	268	250
1g	$3OCH_3$	269	273	262	200
1h	$4OCH_3$	304	265	304	200
1i	$2OCH_3$+$4OCH_3$	324	274	321	300
1j	$2CF_3$	---	---	---	---
1k	$3CF_3$	267	267	267	200
1l	$4CF_3$	267	267	267	150
1m	$2NO_2$	---	---	---	---
1n	$3NO_2$	265	267	262	75
1o	$4NO_2$	270	270	270	50
1p	2CN	270	270	270	200
1q	3CN	267	267	266	200
1r	4CN	266	267	366	100

Table 9: *Absorbance versus wavelength data for 4-aryl-3,5-lutidines*

Least squares fitting of this plot to Equation 2 gave a value for K_a along with the associated error.

$$A_{obs} = \frac{A_{min}10^{-pH} + A_{max}K_a}{10^{-pH} + K_a} \qquad \textbf{Equation 2}$$

The negative logarithms of the K_a values (pK_a's) so obtained are given below in Tables 10-12. In addition to the pK_a values of the 58 compounds we had synthesized, we also measured the pK_a of the conjugate acid of pyridine in both water and 1:1 acetonitrile-water mixture to check the accuracy of our spectrophotometric method as well as the effect of solvent on the pK_a values.

pK_a values for 4-Aryl pyridines:

Compound	Substituent	pK_a
Pyridine (aqueous)	---	5.20±0.03
Pyridine (1:1::acetonitrile:water)	---	3.59±0.03
1a	H	3.51±0.05
1b	$2CH_3$	3.34±0.05
1c	$3CH_3$	3.54±0.05
1d	$4CH_3$	3.70±0.04
1e	$2CH_3$+$4CH_3$	3.46±0.04
1f	$2OCH_3$	3.62±0.06
1g	$3OCH_3$	3.41±0.04
1h	$4OCH_3$	3.84±0.04
1i	$2OCH_3$+$4OCH_3$	3.97±0.03
1j	$2CF_3$	2.71±0.03
1k	$3CF_3$	2.93±0.05
1l	$4CF_3$	2.94±0.04
1m	$2NO_2$	2.67±0.06
1n	$3NO_2$	2.78±0.03
1o	$4NO_2$	2.69±0.03
1p	2CN	2.48±0.04
1q	3CN	2.94±0.04
1r	4CN	2.87±0.04
1s	$2CH_2OH$	3.36±0.05
1t	$4CH_2OH$	3.53±0.04
1u	2CHO	3.43±0.15
1v	4CHO	3.02±0.05
1w	$2CO_2CH_3$	3.23±0.03
1x	$4CO_2CH_3$	3.09±0.05

Table 10: p*K_a values for 4-aryl pyridines*

pK_a values for 4-Aryl-3-picolines:

Compound	Substituent	pK_a
7a	H	3.57±0.04
7b	$2CH_3$	3.54±0.05
7c	$3CH_3$	3.60±0.04
7d	$4CH_3$	3.64±0.04
7e	$2CH_3$+$4CH_3$	3.58±0.04
7f	$2OCH_3$	3.64±0.04
7g	$3OCH_3$	3.62±0.06
7h	$4OCH_3$	3.73±0.03
7i	$2OCH_3$+$4OCH_3$	3.81±0.04
7j	$2CF_3$	3.00±0.04
7k	$3CF_3$	3.23±0.04

7l	$4CF_3$	3.22±0.05
7m	$2NO_2$	3.06±0.07
7n	$3NO_2$	3.09±0.05
7o	$4NO_2$	2.97±0.05
7p	2CN	2.76±0.04
7q	3CN	3.14±0.04
7r	4CN	3.16±0.05

Table 11: p*K$_a$ values for 4-aryl-3-picolines*

*p*K$_a$ values for 4-Aryl-3,5-lutidines:

Compound	**Substituent**	**pK$_a$**
12a	H	3.90
12b	$2CH_3$	3.89±0.03
12c	$3CH_3$	3.94±0.03
12d	$4CH_3$	3.99±0.03
12e	$2CH_3$+$4CH_3$	3.96±0.04
12f	$2OCH_3$	3.99±0.05
12g	$3OCH_3$	3.87±0.03
12h	$4OCH_3$	4.00±0.03
12i	$2OCH_3$+$4OCH_3$	4.01±0.03
12j	$2CF_3$	---
12k	$3CF_3$	3.49±0.04
12l	$4CF_3$	3.48±0.04
12m	$2NO_2$	---
12n	$3NO_2$	3.40±0.06
12o	$4NO_2$	3.24±0.18
12p	2CN	3.10±0.04
12q	3CN	3.14±0.04
12r	4CN	3.16±0.05

Table 12: p*K$_a$ values for 4-aryl-3,5-lutidines*

RESULTS AND DISCUSSION

A pK_a value of 5.20±0.03 was obtained for pyridine in water, which is in excellent agreement with literature values of 5.17 [98] and 5.22.[96] In a 1:1 mixture of acetonitrile (MeCN) and water, we calculated a pK_a of 3.59±0.03 for pyridine. This value lies between the previously measured 3.88 for pyridine in a 40:60::MeCN:water mixture and 3.00 for pyridine in a 60:40::MeCN:water mixture based on buffers which were calibrated in water.[97] As demonstrated by Bosch and Rosés, this decrease in pK_a is partly due to a difference between solvation effect of water and the MeCN-water mixture as well as change in buffer activity on moving from water to a mixed solvent system.[97] Since our procedure involves preparation and calibration of buffer solutions in water, the pK_a value of pyridine in 1:1 MeCN-water mixture reported herein will be lower than those reported by other authors who have calibrated buffers in MeCN-water mixtures.[98]

The pK_a obtained for 4-phenyl-pyridine- 3.51±0.05 -is marginally lower than that of pyridine in 1:1 MeCN-water mixture. Using Equation 4, we can deduce that the free energy change produced by deprotonating the conjugate acid of 4-phenyl-pyridine in 1:1 MeCN-water mixture at 25°C is, to the first decimal place, +20.0±0.3 kJ/mol. To facilitate a discussion of substituent effects on pK_a, this value can be used to introduce the parameter $d\Delta G$. Here, $d\Delta G$ is defined as the difference between the free energy change produced by deprotonation of the conjugate acid of a reference base in a 1:1 MeCN-water mixture at 25°C and the free energy change produced by deprotonation of the conjugate acid of a base containing a particular substituent under the same conditions.

$$\triangle G = -RT\ln(K_a)\ \text{J/mol} \qquad \textbf{(Equation 3)}$$

$$\text{and } \ln(K_a) = -2.303pK_a$$

$$\Longrightarrow \triangle G = +(2.303RTpK_a)/1000\ \text{kJ/mol} \quad \textbf{(Equation 4)}$$

where: $\triangle G$ = free energy change upon deprotonation of the conjugate acid of a base in a specific solvent at temperature "T"
K_a= acid dissociation constant of the conjugate acid of the base,
R= Universal Gas Constant in $JK^{-1}mol^{-1}$

Mathematically, $d\Delta G$ can be expressed using Equation 5. By definition, a negative value of $d\Delta G$ indicates an increase in basicity of the compound containing the relevant substituent relative to the reference base while a positive value of $d\Delta G$ implies a decrease in basicity relative to the reference base.

$$\triangle G^{H} = + (2.303RTpK^{H}_{a})/1000 \text{ kJ/mol}$$

where $\triangle G^{H}$ =free energy change produced on deprotonation of the conjugate acid of a reference base and pK^{H}_{a} = negative logarithm of the acid dissociation constant of the conjugate acid of reference base

and

$$\triangle G^{X} = + (2.303RTpK^{X}_{a})/1000 \text{ kJ/mol}$$

where $\triangle G^{X}$ =free energy change produced on deprotonation of the conjugate acid of a base containing substituent "X"
and pK^{X}_{a} = negative logarithm of the acid dissociation constant of the conjugate acid of the base containing the substituent "X"

$$\Longrightarrow \quad d\triangle G = (\triangle G^{H} - \triangle G^{X}) \text{ kJ/mol}$$

$$\Longrightarrow \quad d\triangle G = 5.70(pK^{H}_{a} - pK^{X}_{a}) \text{ kJ/mol at } 25^{o}C \quad (\textbf{Equation 5})$$

As mentioned in the previous section, the conventional indicator of substituent effects has been the Hammett constant σ. Mathematically, σ is expressed using Equation 6 [81]. As seen from Equation 6, σ is a dimensionless quantity that is related to *d*ΔG by Equation 7.

$$\sigma = \log(K_a^{X}) - \log(K_a^{H}) = pK_a^{H} - pK_a^{X} \quad (\textbf{Equation 6})$$

$$d\Delta G = 2.303RT\sigma \quad (\textbf{Equation 7})$$

Since both rotational barrier and ground state geometry of biphenyls are temperature dependant[85], we have elected here to quantify substituent effects using the temperature dependant quantity *d*ΔG. Furthermore, since pK_a's have been measured at 298K, the numerical value of σ is attenuated by a factor of 5.7 relative to *d*ΔG, which could lead to small substituent effects expressed in terms of σ values being overlooked.

For compounds **1a-x** 4-phenyl-pyridine (**1a**) is chosen as the reference base. For compounds **7a-r** the reference base is 4-phenyl-3-picoline (**7a**) and for compounds **12a-r**, 4-phenyl-3,5-lutidine (**12a**) is selected as the reference base. Thus, comparison of *d*ΔG values for a particular substituent across the pyridine, picoline and lutidine series can elucidate the effect of increasing steric bulk in the flanking ortho position (presumably leading to an increased torsional angle) on the effect of that substituent. Comparison of *d*ΔG values within a series provides the relative magnitude of a substituent effect based upon position and nature of the substituent. *d*ΔG values for the pyridine series (denoted $d\Delta G^{Py}$), picoline series (denoted $d\Delta G^{Pi}$) and lutidine series (denoted $d\Delta G^{Lu}$) are shown in Table 13. The substituents are designated by a numerical prefix which indicates the position of the substituent on the phenyl ring (Figure 12) along with the molecular formula of the substituent. The error in calculating *d*ΔG values

is derived from the standard error propagation formula shown in Equation 8. *d*ΔG values that are smaller than the associated error are considered negligible.

$$E(d\triangle G) = 5.70\sqrt{[E(pK_a^X)]^2 + [E(pK_a^H)]^2} \text{ kJ/mol} \quad \textbf{(Equation 8)}$$

where $E(d\triangle G)$ = error in calculating $d\triangle G$ values;
$E(pK_a^X)$ is the error in measuring pK_a^X
and $E(pK_a^H)$ is the error in measuring pK_a^H

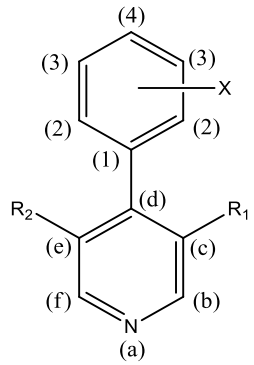

X= substituent
For pyridine series: $R_1 = R_2 = H$
For picoline series: $R_1 = CH_3$ and $R_2 = H$
For lutidine series: $R_1 = R_2 = CH_3$

Figure 18: *Labelled substituent positions*

Entry	Substituent (X)	$d\Delta G^{Py}$	$d\Delta G^{Pi}$	$d\Delta G^{Lu}$
1	H	0.0±0.0†	0.0±0.0†	0.0±0.0†
2	$2CH_3$	1.0±0.4	Negligible	Negligible
3	$3CH_3$	Negligible	Negligible	Negligible
4	$4CH_3$	-1.0±0.4	-0.4±0.3	Negligible
5	$2CH_3$+$4CH_3$	Negligible	Negligible	Negligible
6	$2OCH_3$	-0.6±0.4	-0.4±0.3	Negligible
7	$3OCH_3$	Negligible	Negligible	Negligible
8	$4OCH_3$	-1.9±0.3	-0.9±0.3	Negligible
9	$2OCH_3$+$4OCH_3$	-2.6±0.3	-1.4±0.3	-0.4±0.3
10	$2CF_3$	4.6±0.3	3.3±0.3	---
11	$3CF_3$	3.3±0.4	1.9±0.3	2.5±0.4
12	$4CF_3$	3.2±0.3	2.0±0.4	2.6±0.4
13	$2NO_2$	4.8±0.4	2.9±0.4	---

14	$3NO_2$	4.2±0.3	2.7±0.3	3.1±0.5
15	$4NO_2$	4.7±0.7	3.4±0.5	4.0±1.1
16	2CN	5.9±0.3	4.6±0.3	4.8±0.4
17	3CN	3.3±0.3	2.4±0.3	2.9±0.4
18	4CN	3.7±0.3	2.3±0.3	2.7±0.4
19	$2CH_2OH$	0.9±0.4	---	---
20	$4CH_2OH$	Negligible	---	---
23	2CHO	Negligible	---	---
24	4CHO	2.8±0.4	---	---
25	$2CO_2CH_3$	1.7	---	---
26	$4CO_2CH_3$	2.4±0.4	---	---

†: *by definition*

Table 13: *d*ΔG *values for compounds with measured* pK_a *values*

A discussion of substituent effects on *p*K_a must begin by examining the mode of transmission of substituent effects. Inductive effects, which are produced by substituent induced polarization of covalent sigma bonds, decay exponentially with each intervening bond.[99] A direct inductive effect by the substituent on the nitrogen atom of the 4-aryl-pyridine species is therefore likely to be insignificant since there are 6-8 intervening bonds.

Campanelli and Domenicano have conducted an *in-silico* investigation on the transmission of substituent effects in 4-substituted biphenyls.[100]

(a) *orthogonal conformation* (b) *coplanar conformation*

Figure 19: *Biphenyl conformations studied by Campanelli et al***.**

The salient points from this investigation are noteworthy here:

i) In an orthogonal conformation (Figure 19a), where the torsional angle between rings A and B is 90°, no resonance interactions between A and B are present. The substituent X polarizes the π cloud of ring A, producing different π charges at each position of ring A. This polarization of the π cloud in ring A causes a field effect upon ring B. In cases where X produces a mesomeric effect on ring A, the partial π charges at positions ortho and para to X are further modified due to resonance, in turn modifying the field effect upon ring B.

ii) In a coplanar configuration (Figure 19b), where the torsional angle between A and B is zero, both resonance and field effects influence ring B. Substituents that exert a mesomeric effect on ring A influence the distribution of electron density between A and B via resonance. Substituents that do not have a mesomeric effect on ring A still affect the resonance between A and B by polarizing the π cloud of A.

Additionally, a study of substituent effects on C13 NMR shifts in 4-substituted biphenyls by Schulman *et al.* suggests that the mesomeric effect of the substituent predominantly affects C13 NMR shifts.[101] Based on these reports and the fact that the torsional angle in the pyridine, picoline and lutidine probes is between 0° and 90°, it can be expected that substituent effects on the pK_a's of these probes will be due to a combination of resonance and field effects, with the relative importance of each effect depending upon the torsional angle between the phenyl and pyridyl ring. The calculations of Campanelli *et al.* suggest that in 4-substituted biphenyls (Figure 19a&b), π charges meta to the substituent X appear to have the largest effect on ring B, with the field effect on B due to π charges at the ortho and para positions (relative to X) being approximately equal.[100] Considering the fact that there are twice as many ortho positions as para, it would seem that partial π charges on ring A that are in greater proximity to ring B produce a greater field effect. While it is yet unknown whether a similar trend is valid for 2 and 3-substituted biphenyls, this assumption suggests that 2-substituents would exert a more powerful field effect than substituents in the 3 or 4 position.

A discussion of substituent effects based on the interpretation of *d*ΔG values is given below:

<u>Electron Withdrawing Substituents (*d*ΔG >0):</u>

9 crystal structures have been obtained which indicate that the torsional angles in compounds **1a-x**, **7a-r** and **12a-r** lie between 0° and 90°. While the torsional angles in these compounds may be different in solution, it is nevertheless likely that these compounds exist, in the ground state, in a conformation that is neither orthogonal nor coplanar. The effects of an electron withdrawing substituent are thus expected to be transmitted via:

i) Resonance interactions between the phenyl and pyridyl ring which is influenced by the lowering of π-electron density on the phenyl ring due to the substituent.
ii) Field effects on the pyridyl ring due to polarization of the phenyl ring's π-cloud by the substituent.
iii) Substituents with π-acceptor orbitals, such as the nitro group (NO_2) and the cyano group (CN), when in the 2 and/or 4 position, could possibly exert a mesomeric effect on the pyridyl ring. Figure 20 shows the dependence of the substituent's mesomeric effect on its position: for 3-substituents, electron withdrawal due to resonance (denoted by δ+) with the substituent is confined to the phenyl ring. 4-substituents on the other hand exert a mesomeric effect on both phenyl and pyridyl rings.

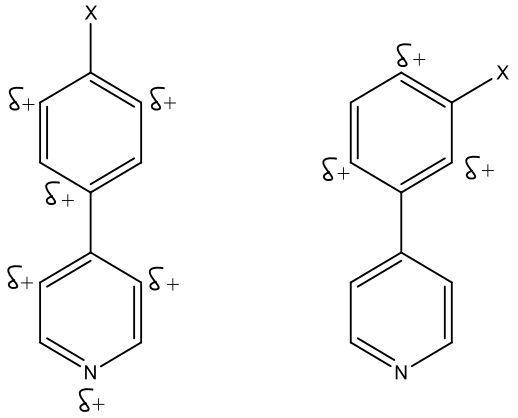

Figure 20: *Dichotomy between mesomeric effects of 3 substituents and 2/4 substituents*

From the *d*ΔG values for the trifluoromethyl (CF_3), CN and NO_2 substituted probes, it is evident that the total effect of these substituents is, in the 3 position, very similar to their effect in the 4-position. In the case of CN and NO_2 substituents, it is possible that the mesomeric interaction between the substituents in the 4 position is compensated for by a larger field effect in the 3-substituted compounds. However, the CF_3 group is not known to exert a mesomeric effect and the $d\Delta G^{Py}$, $d\Delta G^{Pi}$, and $d\Delta G^{Lu}$ values for 3-CF_3 and 4-CF_3 indicate that the field effects exerted by 3 and 4 substituents are similar in magnitude. This implies that the difference between resonance interactions in 3-substituted probes and 4-substituted probes is small and that mesomeric interactions between the substituent and the pyridyl ring (discussed above in Point iii) are not significant.

Overall, resonance between the phenyl and pyridyl rings appears to have a significant effect on pK_a, based on the decrease in *d*ΔG values for the CF_3, CN and NO_2 substituents on going from the pyridine series to the picoline and lutidine series.

The CF_3 and CN substituents have larger *d*ΔG values in the 2 positon than in the 3 or 4 positions. Since the CF_3 group does not exhibit a mesomeric effect, this trend must result from a field effect. Campanelli *et al.* have calculated the partial π-charges that result from polarization of the phenyl π-cloud due to a substituent. According to these calculations, CF_3, CN and NO_2 groups induce the largest positive π-charges at positions ortho to the substituent.[100] Based on this result, the largest charges induced by the 2-substituent should occur at positions 1 and 3 (numbering of positions shown in Figure 18) while the 3-substituent and 4-substituent should induce the largest π-charges in positions 2 and 4 and 3 and 3 respectively. The relatively large *d*ΔG values for 2-substituents therefore support the assumption that π-charges in greater proximity to the pyridyl ring produce a greater field effect.

Unlike the CF_3 and CN groups, the 2-NO_2 substituent has *d*ΔG values similar to the 3-NO_2 and 4-NO_2 substituents. The crystal structure of **1m** (Figure 21) provides a likely explanation for this trend.

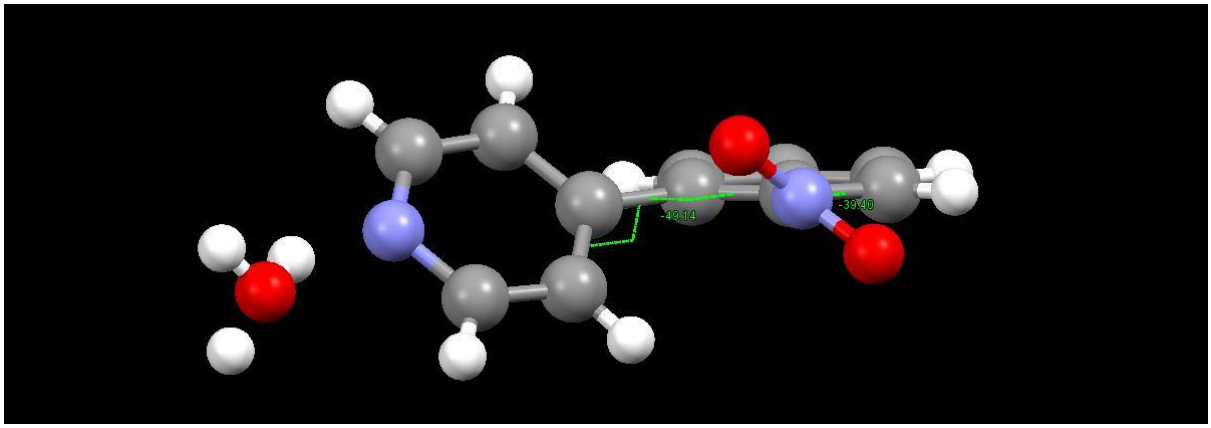

Figure 21: *4-(2-nitrophenyl)-pyridine crystal structure*

The NO_2 group in the crystal structure above is twisted approximately 40° out of the plane of the phenyl ring. This would lead to reduced conjugation with the phenyl ring, leading to smaller π-charges on the phenyl ring on account of the twisted NO_2 substituent exerting a decreased mesomeric effect. The smaller π-charges on the phenyl ring are likely to reduce both field and resonance interactions with the pyridyl ring. The smaller than expected *d*ΔG value for the 2-NO_2 substituent can thus be explained by the reduced electron withdrawing capability of the NO_2 group when twisted out of the plane of the phenyl ring. In support of this thesis, the crystal structures of compounds **1n** (Figure 22) and **12n** (Figure 23) show the 3-NO_2 group to be approximately in the plane of the phenyl ring.

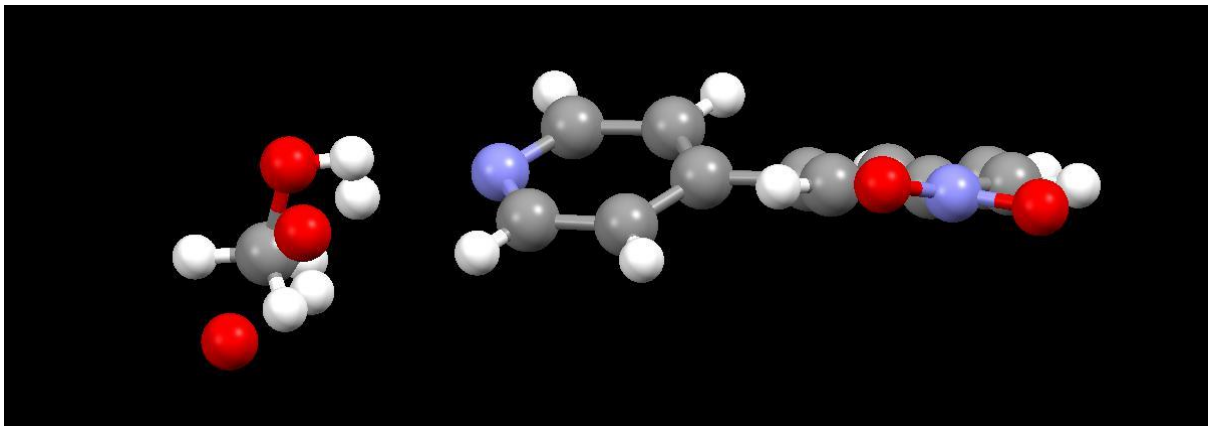

Figure 22: *4-(3-nitrophenyl)-pyridine crystal structure*

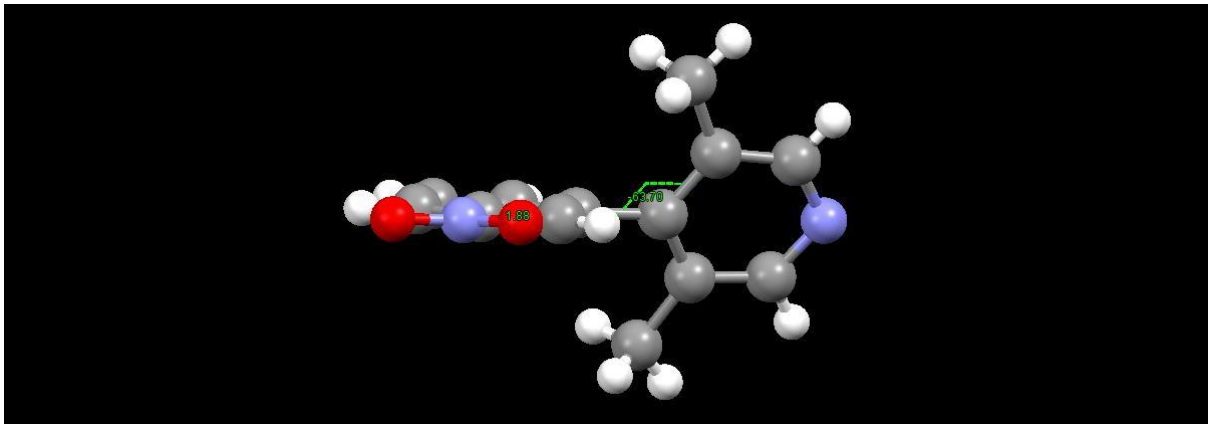

Figure 23: *4-(3-nitrophenyl)-3,5-lutidine crystal structure*

The cyano group in the 2 position produces the largest substituent effect amongst all the substituents tested. However, in the 3 and 4 position its effects are similar to those of the CF_3 group in the 3 and 4 position, implying the large *d*ΔG values for the 2-CN substituent do not stem from greater mesomeric or field effects. We hypothesized that the strong substituent effects for the CN group might be due to secondary electronic effects. The cyano group has two mutually perpendicular, vacant, anti-bonding π* orbitals. If one of these π* orbitals is assumed to overlap with the π system of the phenyl ring (by being perpendicular to the plane of the phenyl ring), the second π* orbital might be in a favourable orientation for overlap with the π system of the pyridyl ring. Figure 24 depicts the hypothesized interaction between the cyano group and the pyridyl ring: The shaded π* lobes are in the plane of the phenyl ring while the light π* lobes are perpendicular to the phenyl ring.

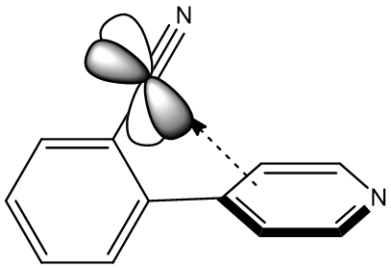

Figure 24: *Depiction of hypothesized interaction between pyridyl ring and cyano groups*

This π -π* interaction between the pyridyl ring and the cyano group, we reasoned, would decrease electron density over the pyridyl system, thereby contributing to a lower *p*K_a. Precedent for donation into the π* orbitals of the cyano group exists in the form of organometallic complexes of nitriles, which have been shown to exhibit electron donation by the metal into the π* orbital of the cyano group.[102] Furthermore, the crystal structure of **1p** (Figure 25), reveals the distance between the carbon atom of the cyano group and the nearest π-bond in the pyridyl ring to be in the 2.9-3 Å range - a range in which non-covalent interactions such as halogen bonding are known to occur.[103]

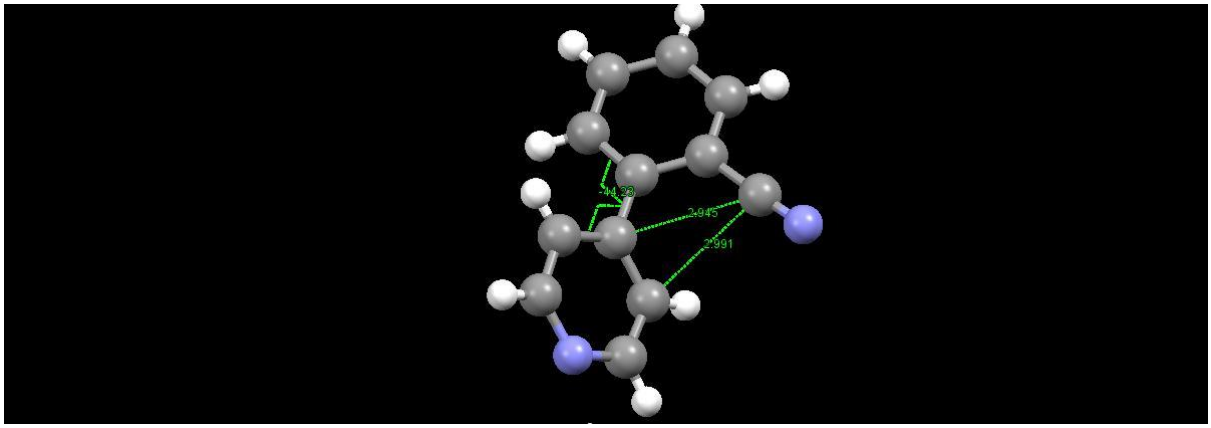

Figure 25: *4-(2-cyanophenyl)-pyridine crystal structure*

To test the presence of this secondary electronic effect, we synthesized compounds **1u-x**. These compounds contain the formyl or carbomethoxy functional group, both of which possess a single π* anti-bonding orbital. A significant pyridyl π-carbonyl π* interaction would require the carbonyl functionality of these two substituents to twist out of conjugation with the phenyl ring (Figure 26) and we reasoned that such twisting might be detectable from the IR specta, *p*K_a values and X-ray structures of these compounds.

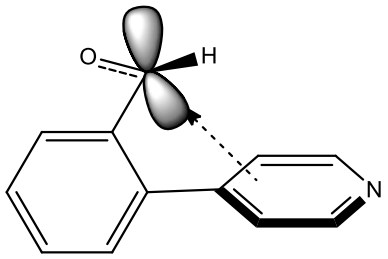

Figure 26: *Depiction of hypothesized interaction between pyridyl ring and carbonyl group*

The formyl group (CHO) was found to have negligible effect on *p*K_a in the 2 position. A large error was also associated with the measured *p*K_a of compound **1u**. This error is due to the deviation of A_{obs} from expected values at lower *p*H's, possibly due to the existence of an aldehyde-hydrate equilibrium which is shifted with change in *p*H. In the 4-position, the CHO group was found to have a relatively weak electron withdrawing effect. The carbomethoxy group (CO_2CH_3) was found to exert a stronger effect in the 4-position than in the 2-position, which is opposite to the trend followed by CF_3, CN and NO_2 substituents as well as the opposite of what would be expected in the case of significant carbomethoxy π*-pyridyl π interaction.

The IR spectra of compounds containing carbonyl groups show a strong absorption band in the 1600-1850 cm^{-1} range.[104] When attached to an electronic donating group, the carbonyl band is shifted to lower frequencies (or lower wave numbers).[105] Conjugation of the carbonyl functionality with an aryl ring thus results in the C=O stretch in aromatic carbonyl compounds

occurring at lower wave numbers than aliphatic carbonyl compounds.[104] It would therefore be expected that twisting of the carbonyl group in compounds **1u** and **1w** out of conjugation with the phenyl ring would result in shifting of the C=O band to a higher frequency. The C=O bands in the IR spectra of **1u** occur at 1692 cm^{-1}. The IR spectrum of **1v** contains closely overlapping bands at 1694 and 1680 cm^{-1}. In compounds **1w** and **1x**, the C=O bands occur at 1721 and 1717 cm^{-1} respectively. The appearance of the C=O band at a marginally higher frequency in **1w** than in **1u** rules out significant twisting of the formyl group out of conjugation with the phenyl ring, as supported by the crystal structure of **1u** (Figure 27). As seen below, the formyl group in the crystal structure of **1u** is twisted out of plane by a very small 8° angle

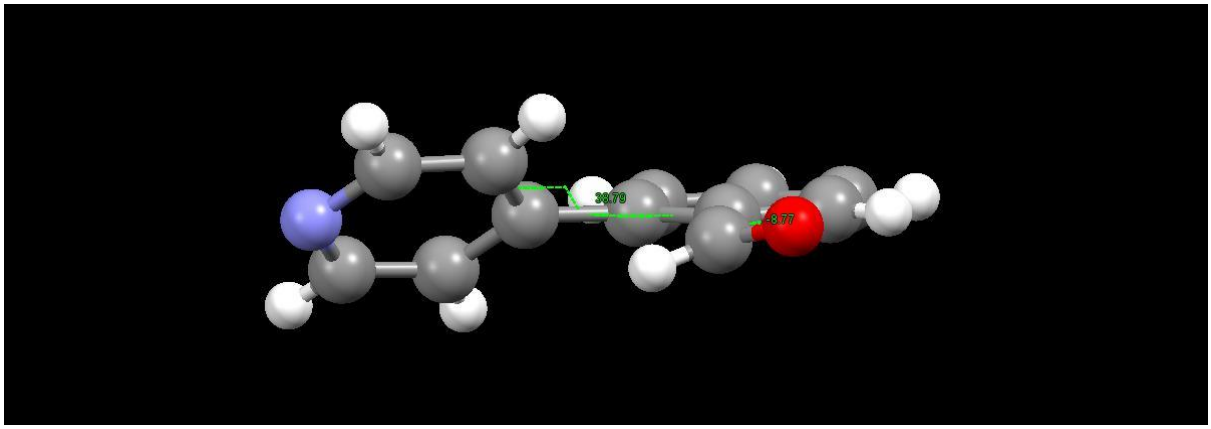

Figure 27: *4-(2-carbomethoxyphenyl)-pyridine crystal structure*

While the C=O band in **1w** does appear at a slightly higher frequency than in **1x**, the $d\Delta G^{Py}$ values for the CO_2CH_3 substituent are not consistent with the carbomethoxy π*-pyridyl π interaction hypothesis. Based on the trend in $d\Delta G^{Py}$ values for the CO_2CH_3 substituent and the NO_2 substituent, it appears that the steric hindrance imposed by the CO_2CH_3 substituent in the 2 position either forces a larger torsional angle or causes the carbomethoxy to be twisted slightly out of conjugation with the phenyl ring. In both cases, electron withdrawal from the pyridyl ring due to resonance is reduced, leading to smaller $d\Delta G^{Py}$ values for the CO_2CH_3 substituent in the 2 position than in the 4 position. By the same rationale, the small size of the cyano group allows a smaller torsional angle, which should enhance the resonance between the phenyl and pyridyl rings. It therefore is possible that the larger $d\Delta G$ values for the 2-CN substituent compared to the 2-CF_3 substituent is due to the different sizes of the two substituents. This is corroborated by the crystal structure of **1p** (Figure 25), that shows the torsional angle to be approximately 42°, which is smaller than the 45° torsional angle for biphenyl and the 60° torsional angle for compound **1f** (See Figure 28 below).

It is also possible, however that the orientation of the π* orbital in the C=O groups of **1u**, **1v**, **1w** and **1x** precludes interaction with the π orbital of the pyridyl ring, which is not the case with the CN group which possesses two mutually perpendicular π* orbitals. Further examination of the unexpectedly large $d\Delta G$ values for the 2-CN substituent is therefore required. A functionalised alkyne group, which also possesses mutually perpendicular π* orbitals, might serve as a useful probe in this context.

Electron Donating Substituents ($d\Delta G<0$):

The $d\Delta G^{py}$ value for the 2-CH_3 substituent (Entry 2, Table 13) indicates a lower basicity for **1b** relative to the reference compound **1a**. This effect is contradictory to the generally accepted assumption that methyl groups have a net electron donating effect, as deduced from the Hammett sigma constants for example.[81] According to the calculations of Campanelli *et al.*, the phenyl ring has a net electron donating effect when it is coplanar to the aryl system to which it is attached.[100] The methyl group in the 2 position is likely to increase the torsional angle between the phenyl and pyridyl ring on account of its greater steric bulk (relative to hydrogen)[106], which would decrease or eliminate any resonance generated net electron transfer from the phenyl ring to the pyridyl ring. The disappearance of the 2-methyl substituent effect in the picoline and lutidine series supports this thesis, since any electron donation by the phenyl ring in reference compounds **7a** and **12a** would already be weakened or eliminated by the increase in torsional angle caused by the methyl substituent(s) on the pyridine ring.

A comparison of $d\Delta G^{py}$ values for the 3-CH_3 and 4-CH_3 substituent shows a net electron donating effect for the 4-CH_3 substituent but a negligible effect for the 3-CH_3 substituent. The same trend is observed for the 3-OCH_3 and 4-OCH_3 substituents. This is contrary to the substituent effects seen in the case of electron withdrawing groups. As discussed previously, electron withdrawing groups did not appear to exert a direct mesomeric effect on the pyridyl ring. However, the methyl and the methoxy groups only seem to affect the pyridyl ring when in the 2 and/or 4 position, which indicates a mesomeric interaction between the pyridyl ring and the substituent. It is currently unclear as to why this dichotomy between electron donating and electron withdrawing substituents exists.

If a mesomeric interaction between electron donating substituents and the pyridyl ring is assumed, the $d\Delta G^{py}$ values of the methyl group can be explained by hyperconjugation. Electron donation by hyperconjugation is consistent with the disappearance of the substituent effect in the picoline and lutidine series (due to the increased torsional angle and reduced resonance in the picoline and lutidine compounds) as well as the negligible $d\Delta G^{py}$ value for the 3-CH_3 substituent. The lack of a significant difference between the ^{13}C chemical shifts of the benzylic carbon in **1c** and **1d**- as would be expected in the case of mesomeric interaction between the benzylic carbon and phenyl ring[107] - does not rule out a hyperconjugative effect given the small magnitude of $d\Delta G^{py}$ for the 4-CH_3 substituent. For comparison, the protonation of 4-bromo-3-picoline- which would presumably produce a free energy change an order of magnitude larger than $d\Delta G^{py}$ for the 4-methyl substituent- causes the ^{13}C chemical shift of the benzylic proton to vary by only 0.78 ppm.

The lack of an observable substituent effect in the case of 2,4-dimethyl substitution (Entry 5, Table 13) can again be explained by increase in torsional angle between the pyridyl and

phenyl rings due to the 2-CH_3 group which would reduce hyperconjugation induced electron donation.

Substituent effects due to the methoxy group follow the same pattern seen for the methyl group with the exception that the 2-OCH_3 substituent has a small electron donating effect and the 3-OCH_3 substituent has a weak electron withdrawing effect. Again, a mesomeric interaction between the methoxy group and the pyridyl ring can be invoked to explain the observed *d*ΔG values. While the mesomeric effect of the 3-OCH_3 substituent will be confined to the phenyl ring, the electron withdrawing field effect of the methoxy group – as indicated by the positive Hammett constant for the methoxy group in the meta position – will lead to a slight decrease in electron density on the pyridyl ring. Although the 2-OCH_3 and 4-OCH_3 substituent both exert a mesomeric effect on the pyridyl ring, the crystal structure of compound **1f** (Figure 28) reveals the torsional angle to be 60°- which is larger than that observed in biphenyl or in the case of **1p**. The mesomeric effect of the methoxy group on the pyridyl ring is presumably weakened in **1f** due to a larger torsional angle, leading to a greater $d\Delta G^{py}$ value for the 4-OCH_3 substituent. As expected from a resonance transmitted effect, the substituent effects of the methoxy group decrease on going from to pyridine series to the picoline and lutidine series. The relation between $d\Delta G^{Py}$ values for the 2,4-dimethoxy substituent and the 2-OCH_3 and 4-OCH_3 substituents appears to be approximately additive. The small, negative $d\Delta G^{Lu}$ value for the 2,4-dimethoxy substituent possibly stems from the combined mesomeric effect of 2 methoxy groups, while the effect of a single methoxy group in the lutidine is below detection limits.

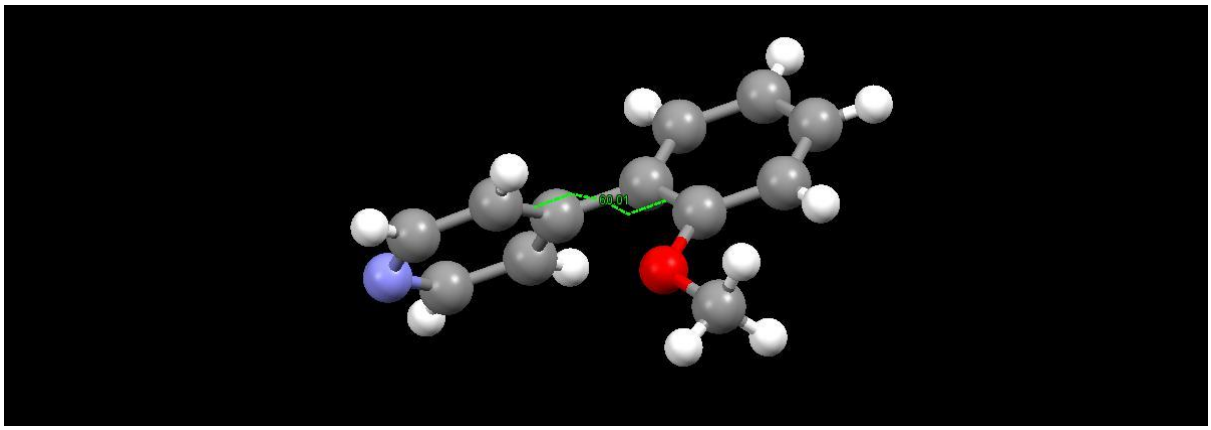

Figure 28: *4-(2-methoxyphenyl)-pyridine crystal structure*

The chalcogen elements oxygen and sulphur have been observed to preferentially interact with the edges of aromatic rings.[108] Hypothesizing that such interactions might affect the torsional angles in the 4-aryl-pyridine species, we synthesized compounds **1s** and **1t**. We reasoned that interaction between the oxygen atom and the edge of the pyridinyl ring might lead to interaction between the π* anti-bonding orbitals of the pyridine and the lone pair of electrons on the oxygen atom (Figure 29), causing an increase in pK_a.

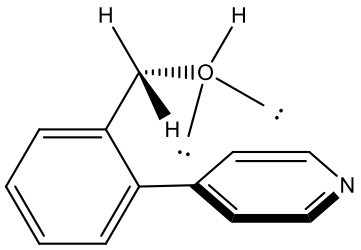

Figure 29: *Depiction of hypothesized interaction between hydroxyl group and pyridyl ring in 4-(2-hydroxymethylphenyl)-pyridine*

The $d\Delta G^{py}$ value for the hydroxymethyl (CH_2OH) substituent in the 2-position is close to that observed for the 2-CH_3 substituent, indicating a similar steric effect that reduces electron donation from the phenyl ring to the pyridyl ring. The $d\Delta G^{py}$ value for the 4-CH_2OH substituent is negligible, as opposed to the small negative value for the 4-CH_3 substituent. This is possibly due to the lack of a significant hyperconjugative effect caused by the electronegative oxygen atom. Accordingly, we can conclude that in the case of the hydroxymethyl group, no secondary electronic effects are detectable.

Substituent effects on rotational barriers:

The barrier to rotation in biphenyl species depends upon the difference between the energy of the molecule in the ground state and the energy of the transition state (TS) the molecule must go through in order to complete one rotation. Multiple computational studies[57,63,70] suggest that the TS involved in rotation about the sigma bond linker in biphenyl compounds possesses a near-planar or planar geometry (i.e a geometry in which the torsional angle between the two aryl rings is 0^o, as shown in Figure 19b). According to the calculations of Campanelli *et al.*, in a planar geometry, both electron withdrawing and electron donating groups enhance resonance interactions between the two aryl rings.[100] While non-resonant substituents affect resonance between the aryl rings through the induction of partial π-charges, substituents with π-acceptor or π-donating orbitals affect resonance through mesomeric effects as well as π-charge generation.[100] The substituent induced enhanced exchange of electron density between the two rings also leads to shortening of the sigma bond linker, which increases steric repulsions between the ortho substituents.[100] Thus, in the planar TS, the stabilization brought about by the substituent via enhanced resonance between the aryl rings is offset by an increase in steric repulsions between the ortho substituents.

According to the model described above, a biphenyl compound with an electron donating group on one of the rings and an electron withdrawing group on the other ring (i.e push-pull substitution) could lower the energy of the planar TS due to enhanced resonance stabilization.[62] Provided the groups in the ortho positions do not enforce a steric barrier large enough to preclude significant resonance stabilization of the TS, such push-pull substitution could result in lowering of the rotational barrier. Data published by Konig *et al.* on the

atropisomerization barriers ($\Delta_{rac}G$) of various 4,4'-disubstituted-2,2'-bis(trifluoromethyl)-biphenyl compounds (Figure 30) shows that this is indeed the case for certain compounds. As shown in Entry 10, Table 14, the push-pull substitution pattern in 4-methoxy-4'-nitro-2,2'-bis(trifluoromethyl)-biphenyl leads to a lower atropisomerisation barrier relative to 2,2'-bis(trifluoromethyl)-biphenyl (Entry 1, Table 14).

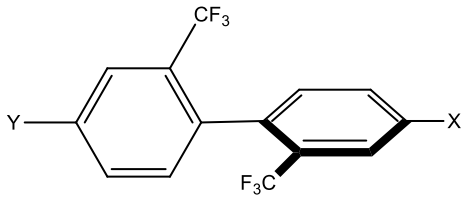

Figure 23: *4,4'-disubstituted-2,2'-bis(trifluoromethyl)-biphenyl moiety studied by Konig et al.*

Entry	Designation	Y	X	$\Delta_{rac}G$ (kJ/mol)
1	**13a**	H	H	107.0
2	**13b**	H	OCH_3	104.2
3	**13c**	H	NH_2	101.7
4	**13d**	OCH_3	OCH_3	102.4
5	**13e**	NH_2	NH_2	99.7
6	**13f**	H	CF_3	106.7
7	**13g**	H	NO_2	107.7
8	**13h**	CF_3	CF_3	107.6
9	**13i**	NO_2	NO_2	109.7
10	**13j**	OCH_3	NO_2	103.7

Table 14: *Atropisomerisation barriers of certain 4,4'-disubstituted-2,2'-bis(trifluoromethyl)-biphenyl moieties (Konig et al.)*

While the model based on Campanelli and Domenicano's calculations correctly predicts the lowering of $\Delta_{rac}G$ for **13j** relative to **13a**, it does not readily provide a rationalization for the lowering of $\Delta_{rac}G$ due to electron donating substituents and the increase in $\Delta_{rac}G$ due to electron withdrawing substituents.

Based on *ab-initio* calculations of the biphenyl structure, Wu and Mo have postulated that a σ-π* interaction between the sigma bonds connecting the ortho hydrogens to the phenyl ring (shown in bold in Figure 31) and the π* orbital of the adjacent phenyl ring (depicted as a vacant pair of lobes in Figure 31) stabilizes non planar biphenyl conformations.[79]

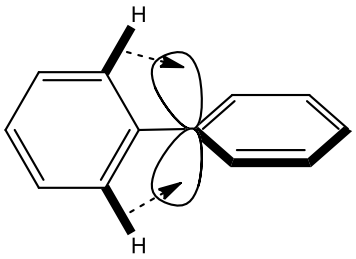

Figure 31: *Depiction of σ-π* interaction proposed by Wu and Mo*

Since this σ-π* interaction stabilizes non-planar ground state structures, the strengthening of this interaction should result in decreasing the energy of the ground state structure and consequently increasing the barrier to rotation. Furthermore, since the σ-π* interaction involves donation of electron density into the π systems, the interaction will presumably be strengthened by electron withdrawing substituents that lower electron density of the π system. By the same rationale, electron donating substituents should decrease the strength of the σ-π* interaction, thereby decreasing the barrier to rotation.

Konig *et al.* have postulated a different theory for explaining the effect of substituents on rotational barrier. According to their hypothesis, electron donating groups increase the electron density at positions 1 and d (refer to Figure 18), which causes the aryl rings to bend out of plane, thereby reducing steric repulsion between the flanking ortho substituents and leading to a decrease in energy of the planar conformation. This causes electron donating substituents to reduce the rotational barrier.[61] Electron withdrawing substituents have the opposite effect on the electron density at positions 1 and d and thus lead to an increase in the rotational barrier.[61]

The atropisomerisation rates shown in Table 14 are consist with both of the aforementioned hypotheses - the electron donating NH_2 and OCH_3 substituents are found to reduce $\Delta_{rac}G$ values while the electron withdrawing NO_2 and CF_3 groups are observed to have the opposite effect. The non-resonant CF_3 is also found to have a considerably weaker effect on $\Delta_{rac}G$ than the resonant NO_2 group. This may either be due to the NO_2 group being a stronger electron withdrawing agent (as indicated by the relevant *d*ΔG values in Table 13), or the ability of the NO_2 group to better stabilize the planar TS by increasing resonance interactions between the aryl rings, or a combination of both.

The $\Delta_{rac}G$ values for 4,4'-disubstituted-2,2'-diisopropyl-biphenyl compounds (Figure 32) determined by Konig *et al.* follow a trend opposite to the one seen in the case 4,4'-disubstituted-2,2'-bis(trifluoromethyl)-biphenyls.[62]

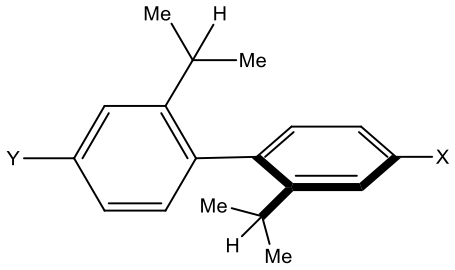

Figure 32: *4,4'-disubstituted-2,2'-diisopropyl-biphenyl moiety*

Entry	Designation	Y	X	$\Delta_{rac}G$ (kJ/mol)
1	**14a**	NH_2	NH_2	115.3
2	**14b**	NO_2	NO_2	105.4

Table 15: *Atropisomerisation barriers for certain 4,4'-disubstituted-2,2'-diisopropyl-biphenyl moieties (Konig et al.)*

Konig *et al.* have rationalized this result by postulating an attractive interaction between the π electrons of the aryl rings and the benzylic proton of the isopropyl group (circled in Figure 33), which stabilizes the non-planar ground state molecule (Figure 33).[62] In this case, the π-H interaction is strengthened by increased π electron density in the aryl rings. The electron donating NH_2 group thus stabilizes the ground state of **14a**, increasing its racemisation barrier while the NO_2 group, which leads to a weaker π-H interaction, results in a lower racemization barrier in the case of **14b**.

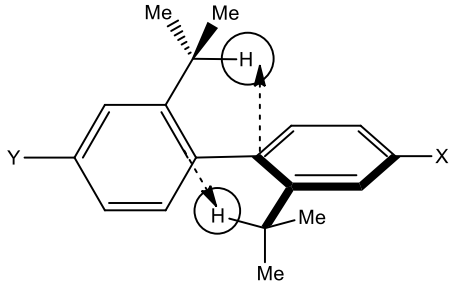

Figure 33: *Depiction of benzylic proton-π electron interaction proposed by Konig et al.*

Based on the computational studies of Campanelli *et al.*, Wu *et al.*, and the empirical data published by Konig *et al.*, it appears that the rotational barrier in biphenyl compounds is governed by a combination of several factors, which are subject to substituent effects in varying magnitudes. These include resonance stabilization of the TS, steric repulsion between groups in the ortho positions which destabilizes the TS, possible out-of-plane bending of the aryl groups, a possible σ-π* interaction, and where applicable, a possible π-H interaction (of which the latter two are expected to stabilize the non-planar ground state).

Given the multiple factors affecting rotational barriers, it is difficult to predict a precise trend in rotational barriers based solely upon the data obtained from pK_a measurements. However, based on data from previous studies, it may be possible to outline a speculative substituent-rotational barrier relationship.

From the $d\Delta G^{py}$ values in Table 13, it is clear that in the 3 and 4 position, the effect of the CN, CF_3 substituents are similar in magnitude, while the NO_2 group exerts a stronger effect in the same positions. The effect of the 4-CHO substituent is similar in magnitude to the effects of the 4-CN and 4-CF_3 substituents. Under the assumption that, in the absence of benzylic hydrogens (to preclude a π-H interaction), electron withdrawing substituents increase the rotational barrier in biphenyl type compounds, the $d\Delta G^{py}$ values suggest that the 3-CN, 4-CN 3-CF_3, 4-CF_3 and 4-CHO substituents will raise the rotational barrier, but to a lesser extent than the NO_2 substituent in the 3 or 4 position. By the same rationale, the 4-CO_2CH_3 substituent should lead to a smaller increase in the rotational barrier compared to the electron withdrawing groups mentioned above. Since the resonant groups CN and NO_2 reduce the electron density at the 1 and d positions (refer to Figure 18), a larger rotational barrier for biphenyl compounds with the 4-CN or 4-NO_2 substituent than the analogous biphenyl compounds with the 3-CN or 4-NO_2 substituent might corroborate the hypothesis of Konig *et al.* regarding out-of-plane bending.

The negligible $d\Delta G^{py}$ value for the 3-CH_3 and 4-CH_2OH substituents suggests these substituents will not have a significant impact on rotational barriers. The more strongly electron donating 4CH_3 and 4-OCH_3 substituents, on the other hand, should lead to decrease in the rotational barrier with a greater decrease expected for the methoxy substituent. The 3-OCH_3 substituent exerts a small electron withdrawing effect on the pyridyl ring and, given the nature of the mesomeric effect, should not lead to an increase in electron density at the 1 position (refer to Figure 18). Thus, the lack of a decrease in the rotational barrier due to the 3-OCH_3 substituent should further corroborate Konig's hypothesis.

Substitution in the 2 position will include an added steric factor. The relatively bulky CF_3 (A value = 8.8 kJ/mol[85]) can be expected to raise the rotational barrier to a greater extent in the 2 position than in the 3 or 4 positions. This increase may be due to both the steric effect as well as the greater electron withdrawing effect, as indicated by the larger $d\Delta G^{py}$ value for the 2-CF_3 substituent. While the steric bulk of the CN group is not significantly greater than that of hydrogen (A value = 0.9 kJ/mol[85]), the 2-CN substituent has the largest $d\Delta G^{py}$ value amongst all substituents tested and this greater electronic effect might therefore lead to a larger increase in rotational barrier by the CN substituent in the 2 position than in the 3 or 4 positions. In the 2 position the NO_2 substituent, as mentioned before, is twisted out of the plane of the phenyl ring, which is likely to reduce steric repulsion with the flanking ortho hydrogen- as indicated by the torsional angle comparable to the torsional angle observed in compound **1p**. Given the similarity of $d\Delta G^{py}$ value for the NO_2 group in all three positions and the fact that it is twisted out of plane in the 2 position, it is possible that the expected increase in rotational barrier due to the NO_2 group is similar regardless of its position. The $d\Delta G^{py}$ values for the CHO and CO_2CH_3 substituents are both lower in the 2 position than in the 4 position. However, the increased steric repulsion between the flanking ortho hydrogen and the 2-CHO (A value = 3.3 kJ/mol[85]) or 2-CO_2CH_3 substituent (A value = 5.4 kJ/mol[85]) may be expected to compensate for the weaker electronic effect. By this rationale, the CHO and CO_2CH_3 substituents should increase the rotational barrier to a similar or greater extent in the 2 position than in the 4 position. A similar steric argument is applicable for the 2-CH_3 (A value = 7.1 kJ/mol[85]) and 2-CH_2OH (A value *ca.* 7.1 kJ/mol, based on the A value for the CH_3 group and

CH_2OTs group[85]) substituents, and these can also be expected to lead to an increase in rotational barrier, particularly given their weak electronic effect. The 2-OCH_3 substituent exerts a relatively weak electron donating effect. However, the expected decrease in rotational barrier to the electronic effect of the 2-OCH_3 substituent is likely to be compensated by the steric repulsion between the flanking ortho hydrogen and the methoxy group, as is indicated by the relatively large torsional angle in compound **1f**. Thus, the OCH_3 group may lead to a decrease in rotational barrier in the 4-position and either a smaller decrease or an increase in rotational barrier in the 2 position.

The presence of benzylic protons in the picoline and lutidine compounds makes it difficult to predict substituent effects on rotational barrier since it is currently not feasible to predict the existence or magnitude of π-H or σ- π* interactions in these compounds. Another possibility is that the increased steric bulk introduced in the flanking ortho positions by the presence of the methyl groups dominates the contribution to the rotational barrier, thereby weakening the electronic effect of all substituents.

In conclusion, we have synthesized and characterised 58 4-aryl pyridine type compounds, determined the acid dissociation constants of their conjugate acids in a 1:1 MeCN-water solution at 298 K, and obtained crystal structures for compounds **1f**, **1m**, **1n**, **1p**, **1u**, **7r**, **12l**, **12n**, **12q** and **12r**. Using the parameter *d*ΔG to quantify substituent effects, we have observed a large substituent effect for the cyano group in the 2 position and a smaller than expected substituent effect for the nitro group in the 2 position- which we attribute to the substituent being twisted out of the plane of the ring to which it is attached. We now aim to use the data produced in this study to guide a computational study aimed at modelling and predicting ground state geometries and rotational barriers of substituted biphenyl compounds.

SUPPORTING INFORMATION

a) General Information:

Propanal was twice distilled over anhydrous sodium sulfate and stored under a nitrogen atmosphere. Diisopropylamine was distilled over KOH pellets and stored a nitrogen atmosphere. Unless specified, all other reagents were obtained from commercial sources and used without further purification. Solvents were obtained from Fisher scientific, and H2O was deionised before use. HPLC grade acetonitrile from Fischer scientific was used for spectrophotometric measurements.

All 58 aryl-pyridine type compounds were characterised on the basis of NMR, MS, IR, and where applicable, XRD experiments. Previously reported compounds were characterised by comparison of ^{1}H NMR spectra with those reported in the literature and on the basis of subsequent reactions.

NMR spectra were recorded on a Bruker Avance-400, calibrated to the residual solvent. Assignments are based on ^{1}H, ^{13}C, and DEPT-135 spectra. Liquid chromatography-mass spectrometry (LCMS) was performed on an Agilent HP 1100 series chromatograph (Mercury Luna 3µ C18 (2) column) attached to a Waters ZQ2000 mass spectrometer with ESCi ionisation source in ESI mode. Elution was carried out at a flow rate of 0.6 mL/min using a reverse phase gradient of MeOH–water or MeCN-water, both containing 0.1% formic acid. High resolution mass spectra (HRMS) were recorded on a Waters Micromass LCT Premier spectrometer using time of flight with positive electrospray ionisation (ESI+), an ABI/MDS Sciex Q-STAR Pulsar with ESI+ and an ASAP (atmospheric pressure solids analysis probe ionisation), or a Bruker BioApex II 4.7e FTICR utilising either ESI+ or a positive electron ionisation (EI+) source equipped with a direct insertion probe. The mass reported is that containing the most abundant isotopes (35Cl and 79Br).

IR spectra were recorded neat on a Perkin-Elmer Spectrum Two FT-IR spectrometer using Universal ATR sampling accessories. Letters in parentheses refer to the relative absorbency of the peak: w – weak (30% of the most intense peak), m- medium (30-75% of the most intense peak), s- strong (%absorbance greater than 75%).

Melting points were obtained using an Optimelt automated melting point system at a heating rate of 1 ^{o}C/min. All melting points are uncorrected.

X-ray diffraction experiment was carried out on a D8 Venture 3-circle Bruker AXS diffractometer with a PHOTON 100 CMOS area detector, using graphite-monochromated Mo Kα radiation (λ = 0.71073 Å) from IμS microsource and a Cryostream (Oxford Cryosystems) open-flow N2 cryostat. The structure was solved by direct methods (SHELXS 2013/1 software2) and refined by full-matrix least squares against F2 of all reflections, using OLEX23 and SHELXL 2014/7 software.

Elemental analysis of 4-phenyl-pyridine, **1a**, was performed by ion chromatography and inductively coupled plasma optical emission spectroscopy. (ICP/OES)

UV-visible spectra were recorded on a Cary-100 spectrophotometer thermostated to 25 ^{o}C.

b) Procedure for Measurement of Acid Dissociation Constants:

A series of acetic acid- potassium acetate and formic acid – potassium formate buffers with 0.1 M ionic strength were prepared by adding the required amount of 0.5 M HCl solution to 981 mg (10 mmol) of potassium acetate or 840 mg (10 mmol) potassium formate in a 100 ml volumetric flask. The volumes of HCl added are given below in Table 16. The *p*H of the buffer solutions thus prepared was measured using a *p*H probe calibrated in the range 1.79 – 4 or 4 - 7. The measured *p*H's of the buffer solutions are shown in Table 16 and 17.

Acetic acid – potassium acetate buffers:

Volume of 0.5 M HCl (mL)	Calculated *p*H	Measured *p*H
18	3.80	3.46
17	4.00	3.89
15	4.28	4.14
10	4.76	4.63
7	5.03	4.91
5	5.23	5.29
2	5.71	5.68

Table 16: *pH values of acetate buffers prepared for* pK_a *measurement*

Formic acid – potassium formate buffers:

Volume of 0.5 M HCl (mL)	Calculated *p*H	Measured *p*H
18	2.80	2.69
17	3.00	2.98
15	3.27	3.22

Table 17: *pH values of formate buffers prepared for* pK_a *measurement*

The procedure following preparation and calibration of the buffer solutions is described below using the determination of the *p*K_a of the conjugate acid of pyridine in a 1:1 acetonitrile:water solution as an illustrative example:

A 200 µM solution of pyridine was prepared in the chosen solvent system. 0.5 ml of this pyridine solution was then pipetted into a 1ml quartz cuvette along with 0.5 ml of a 0.1 M HCl solution. The cuvette was then placed into the cell of the spectrophotometer, the temperature of which was maintained at 25^{o}C, and the absorbance of the solution was mapped in the 200-800 nanometer interval to obtain λ_{max} (Table 7). This process was then repeated using 0.5 ml of the pyridine solution and 0.5 ml of a 0.1 M KOH solution to obtain λ_{min} (Table 7). The difference between the absorbance of pyridine (absorbance mapped in KOH solution) and that of its conjugate acid (absorbance mapped in HCl solution) appeared to be maximum at a wavelength of 254 nm (Table 7). The analytical wavelength, λ_{obs}, was

therefore chosen as 254 nm. Since the absorbance of the 200 µM pyridine solution in HCl solution lay between 0.8 and 1.2 Absorbance Units, 200 µM was chosen as the analyte concentration (Table 7).

Having defined the above parameters A_{obs} was measured at 254 nm at different *p*H levels in the following manner.

The absorbance of a 200 µM pyridine solution was measured at the analytical wavelength at different *p*H values by pipetting 0.5 ml of the analyte into the quartz cuvette along with 0.5 ml of the relevant buffer solution (concentration of all buffer solutions used was 0.1 M). The data shown in Table 18 was thus generated. A plot of A_{obs} versus *p*H was graphed using Kaleidagraph v4.5 (Figure 34). Curve fitting of this plot using Equation 2 furnished the pK_a for pyridine in a 1:1 MeCN:water solvent system, based on buffers calibrated in water.

In Figure 34: $m_1 = A_{max}$, $-\log(m_2) = pK_a$, and $m_3 = A_{min}$.

***p*H**	**A_{obs}**
1	1.012
2.69	0.942
2.98	0.899
3.22	0.843
3.46	0.609
4.14	0.590
4.63	0.476
13	0.436

Table 18: *pH vs. A_{obs} values for pyridine in 1:1::MeCN:water mixture*

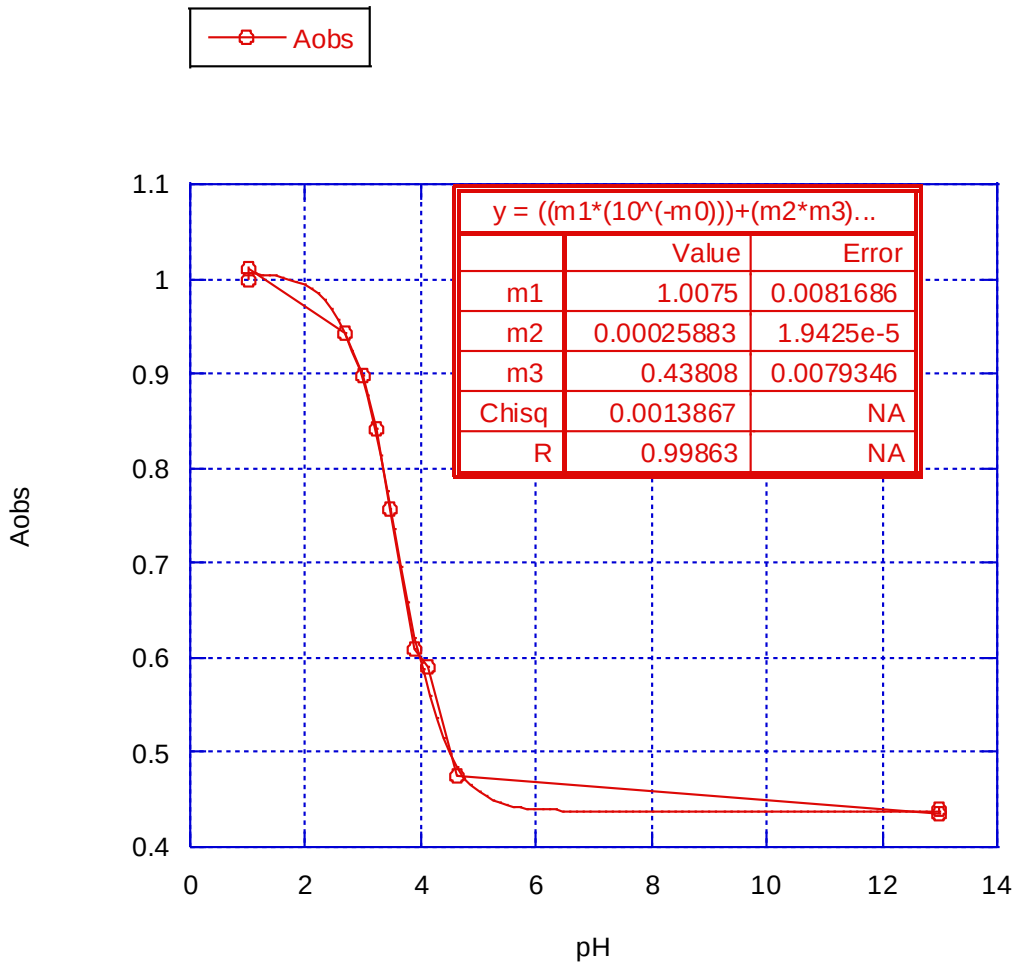

Figure 34: *curve fit to A_{obs} v pH plot for pyridine*

c) Synthetic Procedures:

Representative procedure for synthesis of 4-aryl pyridines **1a-r**: To a 20ml microwave vial equipped with a magnetic stir bar were added 8 ml 1,2-dimethoxyethane, 2 ml deionized water, 650 mg (2 mmol) caesium carbonate, 0.2 ml of a 1M TBAF solution in THF, 58 mg (0.05 mmol) tetrakis(triphenylphosphine)palladium(0), and 1.2 or 1.5 or 1.8 equivalents of the relevant boronic acid/pinacol ester. Finally, 195 mg (1.0 mmol) 4-bromopyridine hydrochloride were added to the vial following which it was capped and the temperature of the reaction mixture raised to 100 ^{o}C in a microwave reactor. After 60 minutes, the reaction mixture was allowed to cool to room temperature, filtered under vacuum through a silica gel plug, concentrated *in-vacuo*, and purified by flash chromatography eluting with an ethyl acetate-hexane mixture to yield the corresponding 4-aryl pyridine.

4-nitro-3-picoline-N-oxide, **2**: To a 1000 ml flask equipped with a magnetic stir bar were added 21.82 g (200 mmol) of 3-picoline-N-oxide, 76.5 g (900 mmol) sodium nitrate and 96 ml (1,802 mmol) of concentrated sulfuric acid. The flask was then fitted with a reflux condenser and the reaction mixture kept stirring at 100 ^{o}C for 24 hours. The mixture was then allowed to cool to room temperature after which 50 ml deionized water and 200 ml dichloromethane were added and neutralization carried out with a K_2CO_3 solution, taking care not to let the pH of the aqueous layer increase above approximately 8. The organic layer was then separated and further extractions from the aqueous layer carried out with dichloromethane. The combined dichloromethane extracts were dried over sodium sulfate, concentrated *in-vacuo*, and purified by recrystallization from methanol to give **2** in 69% yield.

3,5-lutidine-N-oxide, **8**: 34.28 ml (600 mmol) glacial acetic acid and 48.96 ml (600 mmol) of a 50% w/w aqueous hydrogen peroxide solution were taken in a flask and stirred for 10 minutes. 68.37 ml (600 mmol) of 3,5-lutidine was then added to the flask, and the reaction mixture was kept stirring for 30 hours at 85 ^{o}C. The reaction mixture was then cooled gradually to 0^{o}C, the residual peroxide reduced using sodium thiosulfate and sodium iodide as indicator, and neutralization carried out with K_2CO_3 solution. 3,5-lutidine-N-oxide was then extracted from the aqueous solution using a 15% solution of isopropanol in dichoromethane after which it was purified by recrystallization from ethyl acetate to give the product as white needle shaped crystals with 56% yield.

4-nitro-3,5-lutidine-N-oxide,**9**: To a 1000 ml flask equipped with a magnetic stir bar were added 21.82g (200 mmol) of 3,5-lutidine-N-oxide, 76.5 g (900 mmol) sodium nitrate and 96 ml (1,802 mmol) of concentrated sulfuric acid. The flask was then fitted with a reflux condenser and the reaction mixture kept stirring at 115 ^{o}C for 30 hours. The mixture was then allowed to cool to room temperature after which 50 ml deionized water and 200 ml dichloromethane were added and neutralization carried out with a K_2CO_3 solution, taking care not to let the pH of the aqueous layer increase above approximately 8. The organic layer was then separated and further extractions from the aqueous layer carried out with dichloromethane. The combined dichloromethane extracts were dried over sodium sulfate, concentrated *in-vacuo*, and purified by recrystallization from methanol to give **9** in 63% yield.

Procedure for bromination of **2** or **9**: To a 500 ml oven dried flask equipped with a magnetic stir bar were added 100 mmol of **2** or **9** and 91.4 ml (1600 mmol) of glacial acetic acid. The mixture was stirred till homogenous followed by dropwise addition of 33.28 ml (450 mmol) of acetyl bromide. After addition of acetyl bromide, the flask was fitted with a reflux condenser and stirred for 24 hours at 85 ^{o}C. The reaction mixture was then allowed to cool to room temperature, slowly poured onto crushed ice and neutralised using a K_2CO_3 solution, taking care not to let the *p*H of the resulting solution exceed 8. The neutralised solution was then extracted thrice with a 10% solution of isopropanol in dichloromethane, the organic layer dried over sodium sulfate and then concentrated *in vacuo* to furnish a brown powder.

This crude product was purified by flash chromatography eluting with 4% methanol in dichloromethane to furnish 4-bromo-3-picoline-N-oxide, **3** in 66% yield and 4-bromo-3,5-lutidine-N-oxide, **10** in 58% yield.

Procedure for reduction of **3** or **10**: To an oven dried flask under a nitrogen atmosphere was added 50 ml dry THF. The flask was then cooled to -78 ^{o}C using a dry ice-acetone bath. To the chilled THF was added 5.49 ml (50 mmol) of $TiCl_4$ and the resulting yellow suspension was allowed to stir for ten minutes. To this suspension were slowly added 1.9 g of $LiAlH_4$ to furnish a black suspension. The reaction mixture was allowed to warm up to room temperature and then stirred for 1 hour after which it was again cooled to -78 ^{o}C. 50 mmol of **3** or **10** were then added to the flask and the resulting reaction mixture was then allowed to gradually warm up to room temperature and then left stirring for 90 minutes. After this period of time, the reaction mixture was quenched with a cold 5M solution of NH_4OH and extracted 4 times with dichloromethane. The organic extract was dried over sodium sulfate, rapidly concentrated *in vacuo*, and the crude oil thus obtained purified by flash chromatography eluting with 20% ethyl acetate in hexane to furnish a solution of 4-bromo-3-picoline, **4**, or 4-bromo-3,5-lutidine, **11a**. An excess of ethereal solution of HCl was then added to the solution of **4** or **11a** in ethyl acetate-hexane to obtain 4-bromo-3-picoline hydrochloride, **5**, or 4-bromo-3,5-lutidine-hydrochloride, **11b** in 60-66% yield.

4-amino-3-picoline, **6**: 10mmol of **2** were reduced using the same procedure as that used for the reduction of **3** or **10**, but with three equivalents each of $TiCl_4$ and $LiAlH_4$. The crude product obtained after extraction and concentration *in vacuo* was purified by flash chromatography eluting with methanol to obtain **6** in 5-% yield.

Representative procedure for synthesis of 4-aryl-3-picolines **7a-r**: To a 20ml microwave vial equipped with a magnetic stir bar were added 8 ml 1,2-dimethoxyethane, 2 ml deionized water, 0.2 ml of a 1M TBAF solution in THF and 5 mg (**0.022 mmol**) palladium(II) acetate. 20 mg (**0.048 mmol**) SPhos was dissolved in 0.5 ml toluene and then added to the vial after which the mixture was stirred till the solution turned dark red in colour. Then 650 mg (**2 mmol**) caesium carbonate was added followed by 1.2 or 1.5 or 1.8 mmol of the relevant boronic acid/pinacol ester and finally, 207 mg (**1.0 mmol**) of 4-bromo-3-picoline hydrochloride. The vial was then capped and the temperature of the reaction mixture raised to 100^{o}C in a microwave reactor. After 40 minutes, the reaction mixture was allowed to cool to room temperature, filtered under vaccum through a silica gel plug, concentrated *in-vacuo*, and purified by flash chromatography eluting with an ethyl acetate-hexane mixture to yield the corresponding 4-aryl-3- picoline.

Representative procedure for synthesis of 4-aryl-3,5-lutidines **12a-r**: To a 20ml microwave vial equipped with a magnetic stir bar were added 8 ml 1,2-dimethoxyethane, 2 ml deionized

water, 0.2 ml of a 1M TBAF solution in THF and 5 mg (**0.022 mmol**) palladium(II) acetate. 20 mg (**0.048 mmol**) SPhos was then dissolved in 0.5 ml toluene and then added to the vial after which the mixture was stirred till the solution turned dark red in color. Then 650 mg (**2 mmol**) caesium carbonate was added followed by 1.2 or 1.5 or 1.8 mmol of the relevant boronic acid/pinacol ester and finally, 221 mg (**1.0 mmol**) of 4-bromo-3,5-lutidine hydrochloride. The vial was then capped and the temperature of the reaction mixture raised to 125 ^{o}C in a microwave reactor. After 40 minutes, the reaction mixture was allowed to cool to room temperature, filtered under vaccum through a silica gel plug, concentrated *in-vacuo*, and purified by flash chromatography eluting with an ethyl acetate-hexane mixture to yield the corresponding 4-aryl-3,5-lutidine.

Aldol condensation between propanal and 2-trifluoromethylbenzaldehyde/2-nitrobenzaldehyde:

Procedure A: To 5 ml of absolute ethanol were added 672 mg (12 mmol) of finely powdered KOH and the mixture was stirred till homogenous. 12 mmol of the relevant aldehyde and 0.72 ml (10 mmol) of propanal were dissolved in 5 ml of absolute ethanol and added dropwise through an addition funnel to the ethanolic KOH solution over 30 minutes at ambient temperature. The reaction was monitored by TLC, and after two hours was quenched with acetic acid and extracted using dichloromethane. The organic layer was dried over sodium sulfate and concentrated *in vacuo* to furnish a viscous orange gel. The same procedure was repeated at 0 and -10 ^{o}C .

Procedure B: To an oven dried flask under an atmosphere of nitrogen was added 10 ml of dry THF and the flask was chilled to -78 ^{o}C. 1.4 ml (10 mmol) of diisopropylamine was then added to the flask followed by 4 ml of a 2.5 M solution of n-butyllithium in hexane. The mixture was stirred for 10 minutes at -78 ^{o}C followed by addition of 0.72 ml of propanal. After stirring for another hour at -78 ^{o}C, the mixture thus obtained was added in portions through a syringe to a second flask containing 12 mmol of the relevant aldehyde dissolved in 10 ml of THF, kept at 0 ^{o}C. After addition of the propanal – diisopropylamine – butyllithium mixture, the reaction was monitored by TLC and quenched after 2 hours with acetic acid and extracted with dichloromethane. The organic layer was dried over sodium sulfate and concentrated *in vacuo* to furnish a yellow oil.

Spectroscopic Data

4-phenylpyridine, **1a**:

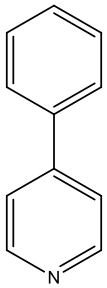

Chemical Formula: $C_{11}H_9N$
Exact Mass: 155.07

Isolated yield: 95%

^{1}H NMR (400 MHz, Chloroform-*d*) δ 8.69 – 8.62 (m, 2H), 7.66 – 7.60 (m, 2H), 7.53 – 7.40 (m, 5H).

^{13}C NMR (101 MHz, Chloroform-*d*) δ 150.21 (2CH), 148.35 (C), 138.11 (C), 129.12 (2CH), 129.07 (CH), 126.99(2CH), 121.64 (2CH).

IR (neat) ν = 3037.4 (w), 1584.9 (m), 1544.6 (m), 1480.5 (m), 1410.4 (m), 1232.9 (m), 1190.2 (m), 829.2 (m), 758.3 (s), 687.0 (m), 667.7 (m)

Elemental Analysis: Calculated for $C_{11}H_9N$- C, 85.13%; H, 5.84%, N, 9.03%; found- C, 84.63% (Δ= -0.5%); H, 5.83% (Δ= -0.01%); N, 8.98% (Δ= -0.03%)

Melting point: 74.6 – 76.8 ^{o}C (1:9::AcOEt:Hexanes)

4-(2-methylphenyl)pyridine, **1b**:

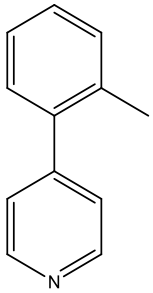

Chemical Formula: $C_{12}H_{11}N$
Exact Mass: 169.09

Isolated yield: 75%

^{1}H NMR (400 MHz, Chloroform-*d*) δ 8.72 – 8.59 (m, 2H), 7.38 – 7.17 (m, 6H), 2.30 (s, 3H).

^{13}C NMR (101 MHz, Chloroform-*d*) δ 149.77 (C) , 149.65 (2CH) , 139.09 (C) , 135.00 (C) , 130.67 (CH), 129.26 (CH) , 128.39 (CH) , 126.12 (CH) , 124.26 (2CH) , 20.28 (CH_3) .

LCMS(in MeCN): R_t=1.38min, m/z=170.3$[M+H]^+$; HR-MS: calculated for $C_{12}H_{12}N$- 170.0970, found- 170.0968 (Δ= -1.2ppm)

IR (neat) ν = 3022.3 (w), 1594.0 (m), 1541.4 (m), 1479.5 (m), 1408.5 (m), 1217.0 (w), 828.4 (m), 759.4 (s), 745.5 (m), 725.1 (m), 617.1 (m), 575.1 (m)

4-(3-methylphenyl)pyridine, **1c**:

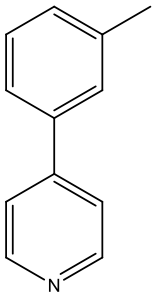

Chemical Formula: $C_{12}H_{11}N$
Exact Mass: 169.09

Isolated yield: 95%

^{1}H NMR (400 MHz, Chloroform-*d*) δ 8.69 – 8.63 (m, 2H), 7.52 – 7.48 (m, 2H), 7.46 – 7.42 (m, 2H), 7.38 (t, *J* = 7.4, 1H), 7.26 (d, *J* = 7.4 Hz, 1H), 2.44 (s, 3H).

^{13}C NMR (101 MHz, Chloroform-*d*) δ 150.19 (2CH) , 148.19 (C) , 139.19 (C) , 135.14 (C) , 129.85 (2CH) , 126.81 (2CH) , 121.38 (2CH) , 21.24 (CH_3) .

LCMS(in MeCN): R_t=1.49min, m/z=170.3$[M+H]^+$; HR-MS: calculated for $C_{12}H_{12}N$- 170.0970, found- 170.0974 (Δ= 2.4 ppm)

IR (neat) ν = 3025.8 (w), 1592.8 (m), 1547.3 (m), 1480.7 (m), 1404.2 (m), 1408.5 (m), 1220.5 (w), 827.0 (m), 778.6 (s), 717.5 (m), 696.9 (m), 615.7 (m), 582.8 (m)

4-(4-methylphenyl)pyridine, **1d**:

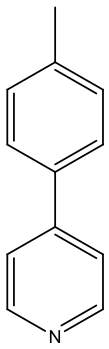

Chemical Formula: $C_{12}H_{11}N$
Exact Mass: 169.09

Isolated yield: 95%

^{1}H NMR (400 MHz, Chloroform-*d*) δ 8.67 – 8.62 (m, 2H), 7.54 (d, *J* = 8.4 Hz, 2H), 7.51 - 7.47 (m, 2H), 7.29 (d, *J* = 8.4 Hz, 2H), 2.42 (s, 3H).

^{13}C NMR (101 MHz, Chloroform-*d*) δ 150.19 (2CH) , 148.19 (C) , 139.19 (C) , 135.14 (C) , 129.85 (2CH) , 126.81 (2CH) , 121.38 (2CH) , 21.24 (CH_3) .

LCMS(in MeCN): R_t=1.44min, m/z=170.3$[M+H]^+$; HR-MS: calculated for $C_{12}H_{12}N$- 170.0970, found- 170.0966 (Δ= -2.4 ppm)

IR (neat) ν = 3035.4 (w), 1596.0 (m), 1487.0 (m), 1234.4 (m), 1212.3 (m), 1028.4 (m), 990.8 (m), 798.8 (s), 708.0 (m), 556.1 (m)

Melting point: 97.0 – 97.8 ºC (1:9::AcOEt:Hexanes)

4-(2,4-dimethylphenyl)pyridine, **1e**:

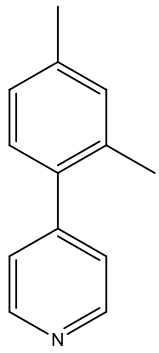

Chemical Formula: $C_{13}H_{13}N$
Exact Mass: 183.10

Isolated yield: 82.5%

^{1}H NMR (400 MHz, Chloroform-*d*) δ 8.63 – 8.54 (m, 2H), 7.49 – 7.41 (m, 2H), 7.29 (d, *J* = 8.3 Hz, 1H), 6.61 – 6.55 (m, 2H), 3.85 (s, 3H), 3.81 (s, 3H).

^{13}C NMR (101 MHz, Chloroform-*d*) δ 161.48 (C), 157.77 (C), 149.45 (2CH), 146.09 (C), 131.12 (CH), 124.05 (2CH), 120.38 (C), 105.06 (CH), 99.06 (CH), 55.53 (CH_3), 55.47 (CH_3).

LCMS(in MeOH): R_t = 2.27 min, m/z = 184.0$[M+H]^+$; HR-MS: calculated for $C_{13}H_{14}N$- 184.1126, found- 184.1130 (Δ= 2.2 ppm)

IR (neat) ν = 2940.4 (w), 2837.6 (w), 1610.3 (m), 1593.9 (m), 1207.3 (s), 1158.0 (s), 1070.1 (s), 990.9 (m), 821.6 (m), 721.7 (m), 560.4 (s)

4-(2-methoxyphenyl)pyridine, **1f**:

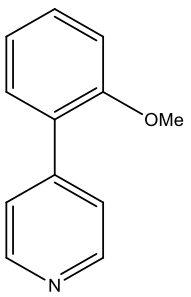

Chemical Formula: $C_{12}H_{11}NO$
Exact Mass: 185.08

Isolated yield: 91%

^{1}H NMR (400 MHz, Chloroform-*d*) δ 8.63 – 8.59 (m, 2H), 7.47 – 7.43 (m, 2H), 7.38 – 7.35 (m, 1H), 7.34 – 7.29 (td, *J* = 7.5, 1.1 Hz, 1H), 7.03 (td, *J* = 7.5, 1.1 Hz, 1H), 6.97 (dd, *J* = 8.3, 1.0 Hz, 1H), 3.78 (s, 3H).

^{13}C NMR (101 MHz, Chloroform-*d*) δ 156.52 (C) , 149.49 (2CH) , 146.27 (C) , 130.44 (CH) , 130.14 (CH) , 127.59 (C) , 124.29 (2CH) , 121.06 (CH) , 111.42 (CH) , 55.48 (CH_3) .

LCMS(in MeCN): R_t=1.33min, m/z=186.3$[M+H]^+$; HR-MS: calculated for $C_{12}H_{12}NO$- 186.0919, found- 186.0921 (Δ=1.1ppm)

IR (neat) ν = 3016.9 (w), 2966.4 (w), 1606.7 (m), 1590.5 (m), 1483.2 (m), 1457.1 (m), 1409.7 (m), 1215.4 (m), 801.7 (m), 759.5 (s), 609.8 (m), 580.5 (m), 552.5 (m)

Melting point: 76.6 – 79.5 ^{o}C (1:9::AcOEt:Hexanes)

4-(3-methoxyphenyl)pyridine, **1g**:

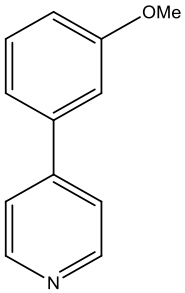

Chemical Formula: $C_{12}H_{11}NO$
Exact Mass: 185.08

Isolated yield: 78%

^{1}H NMR (400 MHz, Chloroform-*d*) δ 8.71 – 8.63 (m, 2H), 7.52 – 7.48 (m, 2H), 7.41 (t, *J* = 7.9 Hz, 1H), 7.22 (ddd, *J* = 7.7, 1.7, 0.9 Hz, 1H), 7.16 (dd, *J* = 2.5, 1.7 Hz, 1H), 6.99 (ddd, *J* = 8.3, 2.6, 1.0 Hz, 1H), 3.88 (s, 3H).

^{13}C NMR (101 MHz, Chloroform-*d*) δ 160.15 (C) , 150.19 (2CH) , 148.23 (C) , 139.59 (C) , 130.17 (CH) , 121.69 (2CH) , 119.39 (CH) , 114.32 (CH) , 112.79 (CH) , 55.36 (CH_3) .

LCMS(in MeCN): R_t=1.69min, m/z=186.1$[M+H]^+$; HR-MS: calculated for $C_{12}H_{12}NO$- 186.0919, found- 186.0928 (Δ= 4.8ppm)

IR (neat) ν = 2938.5 (w), 2835.0 (w), 1592.5 (m), 1548.0 (m), 1477.8 (m), 1406.9 (m), 1215.4 (s), 1172.8 (m), 1030.9 (m), 822.0 (m), 776.1 (s), 713.7 (m), 652.7 (m), 611.7 (m)

4-(4-methoxyphenyl)pyridine, **1h**:

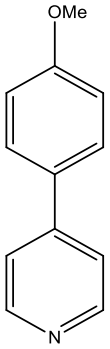

Chemical Formula: $C_{12}H_{11}NO$
Exact Mass: 185.08

Isolated yield: 80%

Melting point: 97.0 – 97.8°C

^{1}H NMR (400 MHz, Chloroform-*d*) δ 8.62 – 8.56 (m, 2H), 7.61 – 7.55 (m, 2H), 7.48 – 7.41 (m, 2H), 7.02 – 6.96 (m, 2H), 3.84 (s, 3H).

^{13}C NMR (101 MHz, Chloroform-*d*) δ 160.53 (C), 150.15 (2CH), 147.79 (C), 130.30 (C), 128.13 (2CH), 121.03 (2CH), 114.54 (2CH), 55.38 (CH_3).

LCMS(in MeOH): R_t = 1.52 min, m/z = 186.1$[M+H]^+$; HR-MS: calculated for $C_{12}H_{12}NO$- 186.0919, found- 186.0921 (Δ= 1.1 ppm)

IR (neat) ν = 3022.0 (w), 1604.4 (m), 1592.6 (m), 1578.3 (m), 1462.2 (m), 1409.7 (m), 1284.6 (m), 1253.9 (m), 1223.7 (m), 1182.3 (m), 1033.8 (m), 1014.9 (m), 806.0 (s), 567.9 (m), 498.7 (m)

4-(2,4-dimethoxyphenyl)pyridine, **1i**:

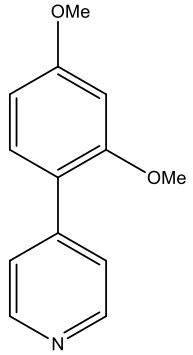

Chemical Formula: $C_{13}H_{13}NO_2$
Exact Mass: 215.09

Isolated yield: 80%

Melting point: 69.0 – 70.8°C

^{1}H NMR (400 MHz, Chloroform-*d*) δ 8.62 – 8.56 (m, 2H), 7.61 – 7.55 (m, 2H), 7.48 – 7.41 (m, 2H), 7.02 – 6.96 (m, 2H), 3.84 (s, 3H).

^{13}C NMR (101 MHz, Chloroform-*d*) δ 161.48 (C), 157.77 (C), 149.44 (2CH), 146.11 (C), 131.13 (CH), 124.07 (2CH), 120.43 (C), 105.05 (CH), 99.08 (CH), 55.56 (CH_3), 55.49 (CH_3).

LCMS(in MeCN): R_t=1.42min, m/z=216.4$[M+H]^+$; HR-MS: calculated for $C_{13}H_{14}NO_2$- 216.1025, found- 216.1035 (Δ= 4.6 ppm)

IR (neat) ν = 3016.9 (w), 2966.5 (w), 1606.7 (m), 1590.5 (m), 1483.2 (m), 1457.1 (m), 1409.7 (m), 1215.4 (m), 1121.9 (m), 1024.19 (m), 1016.6 (m), 828.17 (m), 759.5 (s), 609.8 (m), 580.5 (m)

4-(2-trifluoromethylphenyl)pyridine, **1j**:

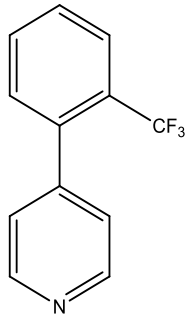

Chemical Formula: $C_{12}H_8F_3N$
Exact Mass: 223.06

Isolated yield: 74%

^{1}H NMR (400 MHz, Chloroform-*d*) δ 8.68 – 8.61 (m, 2H), 7.76 (d, *J* = 7.6 Hz, 1H), 7.59 (t, *J* = 7.6, 1H), 7.52 (t, *J* = 7.6 Hz, 1H), 7.29 (d, *J* = 7.6 Hz, 1H), 7.27 – 7.24 (m, 2H).

^{13}C NMR (101 MHz, Chloroform-*d*) δ 149.28 (2CH), 147.74 (C), 138.36 (q, *J* = 2.1 Hz, C), 131.66 (CH), 131.21 (CH), 128.38 (CH), 128.13 (q, *J* = 30.3 Hz, C), 125.20 (q, *J* = 274.7 Hz, CF_3), 126.27 (q, *J* = 5.3 Hz, CH), 123.91 (q, *J* = 1.6 Hz, 2CH).

^{19}F NMR (376 MHz, Chloroform-*d*) δ -56.72 (3F)

LCMS(in MeCN): R_t=2.85min, m/z=224.4$[M+H]^+$; HR-MS: calculated for $C_{12}H_9NF_3$- 224.0687, found- 224.0693 (Δ=2.7ppm)

IR (neat) ν = 3037.2 (w), 1596.3 (m), 1482.5 (w), 1448.8 (m), 1408.9 (w), 1312.5 (s), 1264.2 (m), 1171.3 (m), 1108.3 (s), 1075.1 (m), 1034.0 (m), 826.1 (m), 767.9 (s), 615.4 (m)

4-(3-trifluoromethylphenyl)pyridine, **1k**:

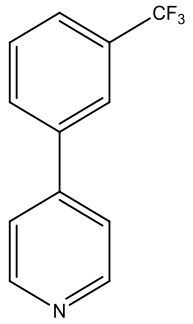

Chemical Formula: $C_{12}H_8F_3N$
Exact Mass: 223.06

Isolated yield: 52%

^{1}H NMR (400 MHz, Chloroform-*d*) δ 8.29 – 8.20 (m, 2H), 7.71 (td, *J* = 7.5, 1.4 Hz, 2H), 7.65 – 7.60 (m, 2H), 7.37 – 7.29 (m, 2H).

^{13}C NMR (101 MHz, Chloroform-*d*) δ 150.52 (2CH), 146.88 (C), 139.05 (C), 131.63 (q, *J* = 32.6 Hz C), 130.32 (q, *J* = 1.5 Hz, CH), 129.70 (CH), 125.70 (q, *J* = 3.8 Hz, CH), 123.91 (q, *J* = 273.71 Hz, CF_3), 123.86 (q, *J* = 3.8 Hz, CH), 121.63 (2CH).

^{19}F NMR (376 MHz, Chloroform-*d*) δ -62.71 (3F)

LCMS(in MeCN): R_t=2.06min, m/z=224.4$[M+H]^+$; HR-MS: calculated for $C_{12}H_9NF_3$- 224.0687, found- 224.0694 (Δ=3.1ppm)

IR (neat) ν = 1592.7 (m), 1552.7 (w), 1483.4 (w), 1439.6 (w), 1407.0 (w), 1333.9 (s), 1264.6 (m), 1164.4 (m), 1119.8 (s), 1097.0 (m), 1077.6 (m), 1042.7 (m), 794.4 (s), 698.06 (m), 636.6 (m), 613.0 (m)

4-(4-trifluoromethylphenyl)pyridine, **1l**:

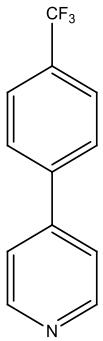

Chemical Formula: $C_{12}H_8F_3N$
Exact Mass: 223.06

Isolated yield: 75%

^{1}H NMR (400 MHz, Chloroform-*d*) δ 8.77 – 8.70 (m, 2H), 7.76 (s, 4H), 7.55 – 7.49 (m, 2H).

^{13}C NMR (101 MHz, Chloroform-*d*) δ 150.45 (2CH), 146.77 (C), 141.65 (q, *J* = 1.4 Hz, C), 130.95 (q, *J* = 32.7 Hz, C), 127.36 (2CH), 126.01 (q, *J* = 3.8 Hz, 2CH), 126.01 (q, *J* = 272.7 Hz, CF_3), 121.63 (2CH).

^{19}F NMR (376 MHz, Chloroform-*d*) δ -62.70 (3F).

LCMS(in MeCN): R_t=2.51min, m/z=224.4$[M+H]^+$; HR-MS: calculated for $C_{12}H_9NF_3$- 224.0687, found- 224.0696 (Δ=4.0ppm)

IR (neat) ν = 1596.9 (m), 1548.3 (w), 1401.1 (m), 1322.3 (s), 1121.3 (m), 1110.6 (m), 1070.0 (m), 1025.9 (m), 1015.3 (m), 811.0 (s), 730.0 (s), 645.5 (w), 604.1 (m)

4-(2-nitrophenyl)pyridine, **1m**:

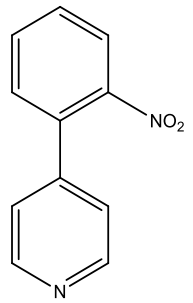

Chemical Formula: $C_{11}H_8N_2O_2$
Exact Mass: 200.06

Isolated yield: 34%

^{1}H NMR (400 MHz, Chloroform-*d*) δ 8.71 – 8.61 (m, 2H), 7.97 (dd, *J* = 8.1, 1.3 Hz, 1H), 7.68 (td, *J* = 7.6, 1.3 Hz, 1H), 7.57 (dd, *J* = 8.1, 7.5, 1.5 Hz, 1H), 7.41 (dd, *J* = 7.6, 1.5 Hz, 1H), 7.27 – 7.20 (m, 2H).

^{13}C NMR (101 MHz, Chloroform-*d*) δ 149.97 (2CH), 148.46 (C), 145.77 (C), 133.96 (C), 132.99 (CH), 131.52 (CH), 129.51 (CH), 124.59 (CH), 122.76 (2CH).

LCMS(in MeCN): R_t=1.27 min, m/z=201.8$[M+H]^+$; HR-MS: calculated for $C_{11}H_9N_2O_2$- 201.0664, found- 201.0672 (Δ=4.0ppm)

IR (neat) ν = 3023.9 (w), 1592.8 (m), 1520.3 (s), 1410.3 (m), 1350.8 (s), 1314.9 (m), 854.6 (s), 824.8 (m), 783.7 (s), 704.9 (s), 666.9 (m), 524.7 (m)

4-(3-nitrophenyl)pyridine, **1n**:

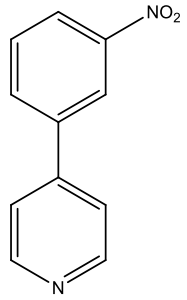

Chemical Formula: $C_{11}H_8N_2O_2$
Exact Mass: 200.06

Isolated yield: 66%

^{1}H NMR (400 MHz, Chloroform-*d*) δ 8.74 – 8.68 (m, 2H), 8.47 (t, *J* = 2.0 Hz, 1H), 8.27 (ddd, *J* = 8.2, 2.3, 1.0 Hz, 1H), 7.96 (ddd, *J* = 7.7, 1.8, 1.0 Hz, 1H), 7.68 (t, *J* = 8.0 Hz, 1H), 7.56 – 7.51 (m, 2H).

^{13}C NMR (101 MHz, Chloroform-*d*) δ 150.67 (2CH), 148.81 (C), 145.76 (C), 139.84 (C), 132.90 (CH), 130.25 (CH), 123.70 (CH), 121.92 (CH), 121.52 (2CH).

LCMS(in MeCN): R_t=1.30 min, m/z=201.4$[M+H]^+$; HR-MS: calculated for $C_{11}H_9N_2O_2$- 201.0664, found- 201.0671 (Δ=3.5ppm)

IR (neat) ν = 3088.6 (w), 1596.0 (w), 1525.0 (m), 1475.7 (m), 1412.5 (m), 1346.9 (s), 880.6 (m), 803.1 (s), 730.7 (s), 682.2 (s), 610.0 (m), 538.0 (m)

Melting point: 111.2 – 111.9 ºC (1:4::AcOEt:Hexanes)

4-(4-nitrophenyl)pyridine, **1o**:

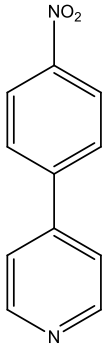

Chemical Formula: $C_{11}H_8N_2O_2$
Exact Mass: 200.06

Isolated yield: 78%

Melting point: 123.6 – 125.1ºC

^{1}H NMR (400 MHz, Chloroform-*d*) δ 8.73 – 8.67 (m, 2H), 8.31 (d, *J* = 8.8 Hz, 2H), 7.78 (d, *J* = 8.8 Hz, 2H), 7.56 – 7.51 (m, 2H).

^{13}C NMR (101 MHz, Chloroform-*d*) δ 150.44 (2CH), 148.16 (C), 146.10 (C), 144.35 (C), 128.03 (2CH), 124.32 (2CH), 121.82 (2CH).

LCMS(in MeCN): R_t=1.37 min, m/z=201.9$[M+H]^+$; HR-MS: calculated for $C_{11}H_9N_2O_2$- 201.0664, found- 201.0667 (Δ=1.5ppm)

IR (neat) ν = 3016.2 (w), 1592.1 (m), 1513.2 (m), 1342.5 (s), 1220.9 (m), 1071.9 (m), 854.6 (m), 812.7 (m), 752.4 (m), 732.3 (m), 693.2 (m), 553.4 (m)

Melting point: 123.6 – 125.1 ºC (1:4::AcOEt:Hexanes)

4-(2-cyanophenyl)pyridine, **1p**:

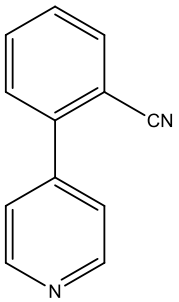

Chemical Formula: $C_{12}H_8N_2$
Exact Mass: 180.07

Isolated yield: 81%

^{1}H NMR (400 MHz, Chloroform-*d*) δ 8.77 – 8.70 (m, 2H), 7.81 (dd, *J* = 8.1, 1.4 Hz, 1H), 7.71 (td, *J* = 8.0, 1.2 Hz, 1H), 7.57 – 7.52 (m, 2H), 7.51 – 7.47 (m, 2H).

^{13}C NMR (101 MHz, Chloroform-*d*) δ 150.24 (2CH), 145.58 (C), 142.39 (C), 134.05 (CH), 133.25 (CH), 129.81 (CH), 129.00 (CH), 123.32 (2CH), 117.94 (C), 111.09 (C).

LCMS(in MeCN): R_t=1.26 min, m/z=181.3$[M+H]^+$; HR-MS: calculated for $C_{12}H_9N_2$- 181.0766, found- 181.0770 (Δ=2.2ppm)

IR (neat) ν = 3247.8 (w), 2225.6 (m, CN), 1602.7 (m), 1595.8 (m), 1545.2 (m), 1479.7 (m), 1412.7 (m), 997.3 (m), 832.2 (m), 766.7 (s)

4-(3-cyanophenyl)pyridine, **1q**:

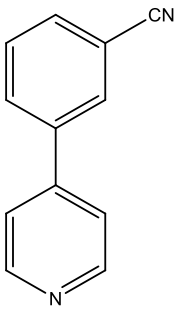

Chemical Formula: $C_{12}H_8N_2$
Exact Mass: 180.07

Isolated yield: 81%

^{1}H NMR (400 MHz, Chloroform-*d*) δ 8.65 – 8.58 (m, 2H), 7.81 (s, 1H), 7.78 (d, *J* = 7.8, 1H), 7.62 (d, *J* = 7.8, 1H), 7.52 (t, *J* = 7.8 Hz, 1H), 7.41 – 7.38 (m, 2H).

^{13}C NMR (101 MHz, Chloroform-*d*) δ 150.55 (2CH), 145.81 (C), 139.28 (C), 132.32 (CH), 131.28 (CH), 130.51 (CH), 130.04 (CH), 121.40 (2CH), 118.30 (C), 113.30 (C).

LCMS(in MeOH): R_t = 1.31 min, m/z = 181.1$[M+H]^+$; HR-MS: calculated for $C_{12}H_9N_2$- 181.0766, found- 181.0770 (Δ= 2.2 ppm)

IR (neat) ν = 3045.6 (w), 2226.7 (m, CN), 1595.2 (m), 1477.9 (m), 1396.3 (m), 787.3 (s), 821.8 (m), 689.5 (s), 615.1 (s), 526.4 (m)

Melting point: 111.0 – 113.3 ºC (3:7::AcOEt:Hexanes)

4-(4-cyanophenyl)pyridine, **1p**:

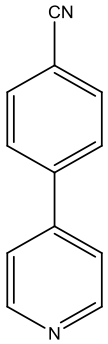

Chemical Formula: $C_{12}H_8N_2$
Exact Mass: 180.07

Isolated yield: 69%

^{1}H NMR (400 MHz, Chloroform-*d*) δ 8.75 – 8.70 (m, 2H), 7.81 – 7.71 (m, 4H), 7.53 – 7.48 (m, 2H).

^{13}C NMR (101 MHz, Chloroform-*d*) δ 150.62 (2CH), 146.30 (C), 142.59 (C), 132.90 (2CH), 127.77 (2CH), 121.60 (2CH), 118.40 (C), 112.78 (C).

LCMS(in MeCN): R_t=1.16 min, m/z=181.3$[M+H]^+$; HR-MS: calculated for $C_{12}H_9N_2$- 181.0766, found- 181.0770 (Δ=2.2ppm)

IR (neat) ν = 3034.2 (w), 2228.2 (m, CN), 1597.5 (m), 1399.5 (m), 850.1 (m), 801.7 (s), 689.8 (m), 527.0 (s), 515.7 (m)

Melting point: 79.4 – 81.1 ºC (3:7::AcOEt:Hexanes)

4-(2-hydroxymethylphenyl)-pyridine:

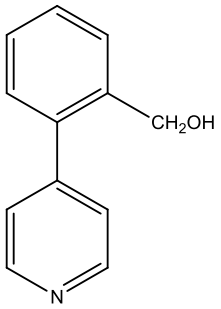

Chemical Formula: $C_{12}H_{11}NO$
Exact Mass: 185.08

Isolated yield: 76%

^{1}H NMR (400 MHz, Chloroform-*d*) δ 8.63 – 8.54 (m, 2H), 7.63 (dd, *J* = 7.5, 1.5 Hz, 1H), 7.47 (td, *J* = 7.5, 1.6 Hz, 1H), 7.41 (td, *J* = 7.5, 1.5 Hz, 1H), 7.38 – 7.34 (m, 2H), 7.31 – 7.26 (m, 1H), 4.61 (s, 2H).

^{13}C NMR (101 MHz, Chloroform-*d*) δ 149.41(2CH), 148.87(C), 138.54(C), 138.00(C), 129.52(CH), 129.09(CH), 128.88(CH), 127.97(CH), 124.34(2CH), 62.54(CH_2).

LCMS(in MeCN): R_t= 0.97 min, m/z=186.0$[M+H]^+$; HR-MS: calculated for $C_{12}H_{12}NO$- 186.0919, found- 184.00924 (Δ= 2.7 ppm)

IR (neat) ν = 3142.3 (m, OH), 2871.0 (w), 2821.0 (w), 1598.9 (m), 1409.8 (m), 1321.3 (m), 1047.1 (m), 998.6 (m), 840.9 (s), 761.0 (s), 748.7 (s), 619.9 (m)

4-(4-hydroxymethylphenyl)-pyridine:

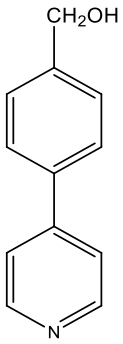

Chemical Formula: $C_{12}H_{11}NO$
Exact Mass: 185.08

Isolated yield: 74%

^{1}H NMR (400 MHz, Chloroform-*d*) δ 8.63 – 8.54 (m, 2H), 7.63 (dd, *J* = 7.5, 1.5 Hz, 1H), 7.47 (td, *J* = 7.5, 1.6 Hz, 1H), 7.41 (td, *J* = 7.5, 1.5 Hz, 1H), 7.38 – 7.34 (m, 2H), 7.31 – 7.26 (m, 1H), 4.61 (s, 2H).

^{13}C NMR (101 MHz, Chloroform-*d*) δ 150.17 (2CH), 148.09 (C), 142.21 (C), 137.24 (C), 127.58 (2CH), 127.13 (2CH), 121.58 (2CH), 64.68 (CH_2).

LCMS(in MeCN): R_t=1.11 min, m/z=186.0$[M+H]^+$; HR-MS: calculated for $C_{12}H_{12}NO$- 186.0919, found- 186.0924 (Δ= 2.7 ppm)

IR (neat) ν = 3154.1 (m, OH), 2819.5 (w), 1598.1 (m), 1400.1 (m), 1056.6 (m), 1000.3 (m), 802.8 (s), 720.1 (m)

4-(2-formylphenyl)pyridine, **1p**:

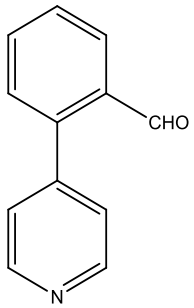

Chemical Formula: $C_{12}H_9NO$
Exact Mass: 183.07

Isolated yield: 62%

^{1}H NMR (400 MHz, Chloroform-*d*) δ 9.97 (s, 1H), 8.84 – 8.57 (m, 2H), 8.05 (dd, *J* = 7.8, 1.4 Hz, 1H), 7.69 (td, *J* = 7.5, 1.5 Hz, 1H), 7.58 (t, *J* = 7.5 Hz, 1H), 7.42 (dd, *J* = 7.7, 1.3 Hz, 1H), 7.37 – 7.21 (m, 2H).

^{13}C NMR (101 MHz, Chloroform-*d*) δ 191.13 (CHO), 149.76 (2CH), 145.90 (C), 142.68 (C), 133.90 (CH), 133.43 (C), 130.36 (CH), 129.04 (CH), 128.38 (CH), 124.75 (2CH).

LCMS(in MeCN): R_t=1.16 min, m/z=181.3$[M+H]^+$; HR-MS: calculated for $C_{12}H_{10}NO$- 184.0762, found- 184.0762 (Δ= 0.0 ppm)

IR (neat) ν = 3043.8 (w), 1692.9 (m, CHO), 1594.5 (m), 1405.2 (m), 1256.8 (m), 1196.5 (m), 836.7 (s), 771.9 (s), 761.8 (s), 642.3 (m), 614.3 (m)

4-(4-formylphenyl)pyridine, **1p**:

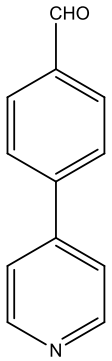

Chemical Formula: $C_{12}H_9NO$
Exact Mass: 183.07

Isolated yield: 75%

^{1}H NMR (400 MHz, Chloroform-*d*) δ 10.08 (s, 1H), 8.79 – 8.61 (m, 2H), 8.00 (d, *J* = 8.1 Hz, 2H), 7.80 (d, *J* = 8.2 Hz, 2H), 7.60 – 7.50 (m, 2H).

^{13}C NMR (101 MHz, Chloroform-*d*) δ 191.61 (C=O), 150.52 (2CH), 146.90 (CH), 143.96 (CH), 136.47 (CH), 130.42 (2CH), 127.73 (2CH), 121.75 (2CH).

LCMS(in MeCN): R_t=1.01 min, m/z=184.0[M+H]$^+$; HR-MS: calculated for $C_{12}H_{10}NO$- 184.0762, found- 184.0768 (Δ= 3.3 ppm)

IR (neat) ν = 3057.2 (w), 1694.5 (m, C=O), 1680.8 (m), 1594.7 (m), 1213.2 (m), 1167.9 (m), 843.7 (m), 799.4 (s), 735.2 (s), 720.2 (m), 694.9 (m)

4-(2-carbomethoxyphenyl)pyridine, **1p**:

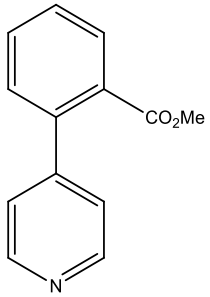

Chemical Formula: $C_{13}H_{11}NO_2$
Exact Mass: 213.08

Isolated yield: 47%

^{1}H NMR (400 MHz, Chloroform-*d*) δ 8.72 – 8.56 (m, 2H), 7.93 (dd, *J* = 1.5, 7.9 Hz, 1H), 7.59 (td, *J* = 7.5, 1.5 Hz, 1H), 7.50 (td, *J* = 7.6, 1.3 Hz, 1H), 7.33 (dd, *J* = 1.3, 7.7 Hz, 1H), 7.26 – 7.20 (m, 2H), 3.67 (s, 3H).

^{13}C NMR (101 MHz, Chloroform-*d*) δ 168.05 (C), 149.42 (2CH), 140.04 (C), 131.77 (CH), 130.37 (CH), 130.33 (CH), 130.18 (C), 128.40 (CH), 123.35 (2CH), 52.06 (CH_3).

LCMS(in MeCN): R_t=1.59 min, m/z=214.0[M+H]$^+$; HR-MS: calculated for $C_{13}H_{12}NO_2$- 214.0868, found- 214.0874 (Δ= 2.8 ppm)

IR (neat) ν = 2951.0 (w), 1721.3 (s, C=O), 1594.4 (m), 1409.2 (m), 1287.5 (s), 1256.8 (s), 1127.2 (m), 1092.4 (m), 911.5 (m), 761.4 (s), 728.0 (s), 614.9 (m)

4-(4-carbomethoxyphenyl)pyridine, **1p**:

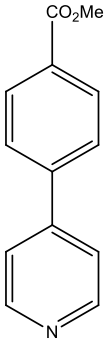

Chemical Formula: $C_{13}H_{11}NO_2$
Exact Mass: 213.08

Isolated yield: 56%

^{1}H NMR (400 MHz, Chloroform-*d*) δ 8.80 – 8.54 (m, 2H), 8.12 (d, *J* = 8.4 Hz, 2H), 7.67 (d, *J* = 8.4 Hz, 2H), 7.56 – 7.42 (m, 2H), 3.92 (s, 3H).

^{13}C NMR (101 MHz, Chloroform-*d*) δ 166.51 (C), 150.42 (2CH), 147.06 (C), 142.40 (C), 130.55 (C), 130.32 (2CH), 126.99 (2CH), 121.65 (2CH), 52.27 (CH_3).

LCMS(in MeCN): R_t=1.76 min, m/z=214.0$[M+H]^+$; HR-MS: calculated for $C_{13}H_{12}NO_2$- 214.0868, found- 214.0874 (Δ= 2.8 ppm)

IR (neat) ν = 1717.2 (s, C=O), 1595.6 (m), 1421.3 (m), 1278.0 (s), 1180.1 (m), 1101.1 (s), 816.4 (s), 954.1 (m), 764.7 (s), 700.3 (m), 647.3 (m)

Melting point: 103.2 – 104.2 °C (2:8::AcOEt:Hexanes)

3-methyl-4-nitropyridine-N-oxide, **2**:

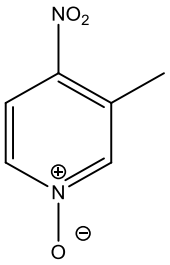

Chemical Formula: $C_6H_6N_2O_3$
Exact Mass: 154.04

Isolated yield: 69%

^{1}H NMR (400 MHz, Chloroform-*d*) δ 8.14 – 8.12 (m, 1H), 8.12 – 8.08 (m, 1H), 8.01 (d, *J* = 7.1 Hz, 1H), 2.62 (s, 3H).

4-bromo-3-methylpyridine-N-oxide, **3**:

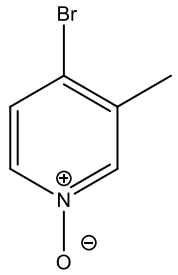

Chemical Formula: C_6H_6BrNO
Exact Mass: 186.96

Isolated yield: 66%

^{1}H NMR (400 MHz, Chloroform-*d*) δ 8.12 – 8.06 (m, 1H), 7.95 – 7.90 (m, 1H), 7.41 (d, *J* = 6.8 Hz, 1H), 2.33 (s, 3H).

4-bromo-3-methylpyridine, **4**:

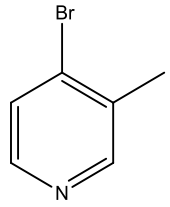

Chemical Formula: C_6H_6BrN
Exact Mass: 170.97

Isolated yield: 63%

^{1}H NMR (400 MHz, Chloroform-*d*) δ 8.39 (s, 1H), 8.20 (d, *J* = 7 Hz, 1H), 7.44 (d, *J* = 5.2 Hz, 1H), 2.35 (s, 3H).

4-bromo-3-methylpyridine hydrochloride, **5**:

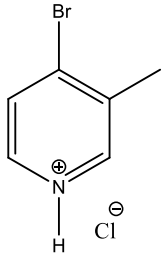

Chemical Formula: C_6H_7BrNCl
Exact Mass: 206.95

Isolated yield: 66%

^{1}H NMR (400 MHz, Methanol-d_4) δ 8.88 (s, 1H), 8.66 (d, J = 6.4 Hz, 1H), 8.31 (d, J = 6.0 Hz, 1H), 2.60 (s, 3H).

^{1}H NMR (400 MHz, Chloroform-d) δ 15.40 (s, 1H), 8.83 (s, 1H), 8.63 (d, J = 6.1 Hz, 1H), 8.10 (d, J = 6.1 Hz, 1H), 2.55 (s, 3H).

4-amino-3-methylpyridine **6**:

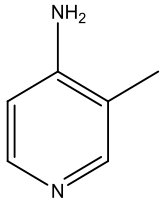

Chemical Formula: $C_6H_8N_2$
Exact Mass: 108.07

Isolated yield: 50%

^{1}H NMR (400 MHz, Chloroform-d) δ 8.06 – 7.99 (m, 2H), 6.46 (d, J = 5.5 Hz, 1H), 4.47 (s, 2H), 2.04 (s, 3H).

4-phenyl-3-methylpyridine, **7a**:

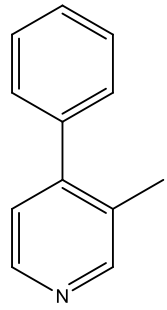

Chemical Formula: $C_{12}H_{11}N$
Exact Mass: 169.09

Isolated yield: 83%

^{1}H NMR (400 MHz, Chloroform-d) δ 8.50 (s, 1H), 8.46 (d, J = 5.0 Hz, 1H), 7.48 – 7.37 (m, 3H), 7.34 – 7.30 (m, 2H), 7.14 (d, J = 5.0 Hz, 1H), 2.27 (s, 3H).

^{13}C NMR (101 MHz, Chloroform-d) δ 151.31 (CH), 149.15 (C), 147.39 (CH), 139.09 (C), 130.59 (C), 128.54 (2CH), 128.44 (2CH), 127.95 (CH), 123.99 (CH), 17.25 (CH).

LCMS(in MeOH): R_t = 1.72 min, m/z = 170.3 $[M+H]^+$; HR-MS: calculated for $C_{12}H_{12}N$ - 170.0970, found- 170.0963 (Δ= -4.1 ppm)

IR (neat) ν = 3028.3 (w), 1590.3 (m), 1477.7 (m), 1403.9 (m), 835.4 (m), 769.7 (m), 741.9 (m), 700.4 (s), 628.0 (m), 578.7 (m), 570.9 (m), 513.3 (m)

4-(2-methylphenyl)-3-methylpyridine, **7b**:

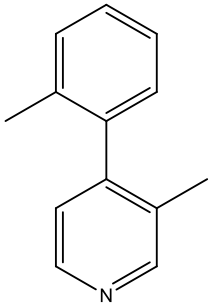

Chemical Formula: $C_{13}H_{13}N$
Exact Mass: 183.10

Isolated yield: 57%

^{1}H NMR (400 MHz, Chloroform-*d*) δ 8.51 (s, 1H), 8.46 (d, *J* = 4.9 Hz, 1H), 7.33 – 7.21 (m, 3H), 7.07 – 7.02 (m, 2H), 2.06 – 2.04 (m, 6H).

^{13}C NMR (101 MHz, Chloroform-*d*) δ 150.89 (CH), 149.46 (C), 147.16 (CH), 138.69 (C), 134.96 (C), 131.43 (C), 130.16 (CH), 128.34 (CH), 128.02 (CH), 125.83 (CH), 123.98 (CH), 19.65 (CH_3), 16.62 (CH_3).

LCMS(in MeOH): R_t = 2.10 min, m/z = 184.0 $[M+H]^+$; HR-MS: calculated for $C_{13}H_{14}N$ - 184.1126, found- 184.1127 (Δ= 0.5 ppm)

IR (neat) ν = 2900 (w), 1530 (m), 1460 (m), 1390 (m), 820 (m), 760 (s), 720 (s), 690 (s), 630 (m), 600 (m)

4-(3-methylphenyl)-3-methylpyridine, **7c**:

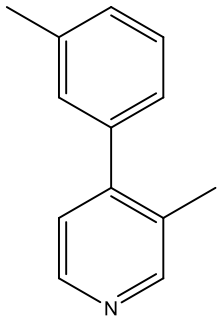

Chemical Formula: $C_{13}H_{13}N$
Exact Mass: 183.10

Isolated yield: 87%

^{1}H NMR (400 MHz, Chloroform-*d*) δ 8.49 (s, 1H), 8.45 (d, *J* = 5.0 Hz, 1H), 7.33 (t, *J* = 7.5 Hz, 1H), 7.21 (d, *J* = 7.6 Hz, 1H), 7.15 – 7.09 (m, 3H), 2.41 (s, 3H), 2.27 (s, 3H).

^{13}C NMR (101 MHz, Chloroform-*d*) δ 151.17 (CH), 149.39 (C), 147.24 (CH), 139.04 (C), 138.11 (C), 130.64 (C), 129.20 (CH), 128.67 (CH), 128.30 (CH), 125.60 (CH), 124.01 (CH), 21.45 (CH_3), 17.24 (CH_3).

LCMS(in MeOH): R_t = 2.06 min, m/z = 184.0 $[M+H]^+$; HR-MS: calculated for $C_{13}H_{14}N$ - 184.1126, found- 184.1131 (Δ= 2.7 ppm)

IR (neat) ν = 2922.8 (m), 1589.1 (m), 1548.1 (w), 1476.2 (m), 834.1 (m), 785.8 (s), 749.9 (m), 705.6 (s), 632.3 (m), 597.8 (m), 576.5 (m)

4-(4-methylphenyl)-3-methylpyridine, **7d**:

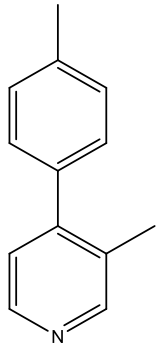

Chemical Formula: $C_{13}H_{13}N$
Exact Mass: 183.10

Isolated yield: 72%

^{1}H NMR (400 MHz, Chloroform-*d*) δ 8.51 (s, 1H), 8.47 (d, *J* = 5.0 Hz, 1H), 7.28 (d, *J* = 8.1 Hz, 2H), 7.24 (d, *J* = 8.2 Hz, 2H), 7.15 (d, *J* = 5.0 Hz, 1H), 2.43 (s, 3H), 2.30 (s, 3H)

^{13}C NMR (101 MHz, Chloroform-*d*) δ 151.27 (CH), 149.17 (C), 147.34 (CH), 137.82 (C), 136.16 (C), 130.64 (C), 129.14 (2CH), 128.48 (2CH), 124.05 (CH), 21.24 (CH_3), 17.31 (CH_3).

LCMS(in MeOH): R_t = 2.06 min, m/z = 184.1 $[M+H]^+$; HR-MS: calculated for $C_{13}H_{14}N$ - 184.1126, found- 184.1126 (Δ= 0.0 ppm)

IR (neat) ν = 2921.3 (w), 1591.3 (m), 1516.1 (m), 1481.9 (m), 812.8 (s), 752.4 (m), 697.1 (m), 577.4 (m), 552.9 (m), 514.5 (m)

4-(2,4-dimethylphenyl)-3-methylpyridine, **7e**:

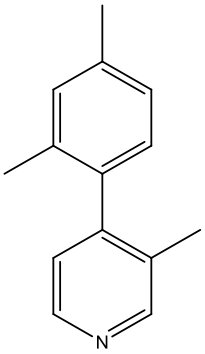

Chemical Formula: $C_{14}H_{15}N$
Exact Mass: 197.12

Isolated yield: 51%

^{1}H NMR (400 MHz, Chloroform-*d*) δ 8.49 (s, 1H), 8.43 (d, *J* = 4.9, 1H), 7.10 (app. s, 1H), 7.05 (d, *J* = 7.8 Hz, 1H), 7.02 (d, *J* = 4.9 Hz, 1H), 6.93 (d, *J* = 7.7 Hz, 1H), 2.36 (s, 3H), 2.05 (s, 3H), 2.01 (s, 3H).

^{13}C NMR (101 MHz, Chloroform-*d*) δ 150.85(CH), 149.50(C), 147.13(CH), 137.65(C), 135.81(C), 134.76(C), 131.59(C), 130.90(CH), 128.28(CH), 126.51(CH), 124.22(CH), 21.14(CH_3), 19.56(CH_3), 16.65(CH_3).

LCMS(in MeOH): R_t = 2.13 min, m/z = 198.1 $[M+H]^+$; HR-MS: calculated for $C_{14}H_{16}N$ – 198.1276, found- 198.1285 (Δ= 1.0 ppm)

IR (neat) ν = 2920.9 (w), 1615.4 (m), 1519.3 (m), 1480.6 (m), 1404,2 (m), 820.2 (s), 697.8 (m), 598.9 (m), 569.0 (m), 527.3 (m)

4-(2-methoxyphenyl)-3-methylpyridine, **7g**:

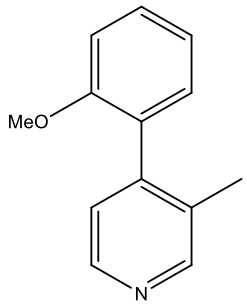

Chemical Formula: $C_{13}H_{13}NO$
Exact Mass: 199.10

Isolated yield: 82%

^{1}H NMR (400 MHz, Chloroform-*d*) δ 8.54 – 8.38 (m, 2H), 7.38 (ddd, *J* = 8.3, 7.4, 1.9 Hz, 1H), 7.10 (m, 2H), 7.03 (td, *J* = 7.4, 1.1 Hz, 1H), 6.98 (dd, *J* = 8.3, 1.0 Hz, 1H), 3.76 (s, 3H), 2.13 (s, 3H).

^{13}C NMR (101 MHz, Chloroform-*d*) δ 156.13 (C), 150.50 (CH), 146.96 (CH), 146.65 (C), 132.33 (C), 130.24 (CH), 129.60 (CH), 128.02 (C), 124.64 (CH), 120.66 (CH), 110.83 (CH), 55.37 (CH_3), 16.79 (CH_3).

LCMS(in MeOH): R_t = 1.83 min, m/z = 200.1$[M+H]^+$; HR-MS: calculated for $C_{13}H_{14}NO$- 200.1075, found- 200.1076 (Δ= 0.5 ppm)

IR (neat) ν = 2959.4 (w), 2836.0 (w), 1602.7 (m), 1480.0 (m), 1433.9 (m), 1268.7 (m), 1237.7 (m), 1119.3 (m), 1053.4 (m), 1026.3 (m), 834.5 (m), 821.3 (m), 790.4 (m), 752.5 (s), 625.7 (m)

4-(3-methoxyphenyl)-3-methylpyridine, **7h**:

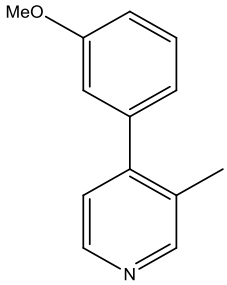

Chemical Formula: $C_{13}H_{13}NO$
Exact Mass: 199.10

Isolated yield: 67%

^{1}H NMR (400 MHz, Chloroform-*d*) δ 8.49 (s, 1H), 8.45 (d, *J* = 5.2 Hz, 1H), 7.35 (t, *J* = 8 Hz, 1H), 7.14 (d, *J* = 5.0 Hz, 1H), 6.94 (ddd, *J* = 8.3, 2.6, 1.0 Hz, 1H), 6.89 (ddd, *J* = 7.6, 1.6, 1.0 Hz, 1H), 6.84 (dd, *J* = 2.6, 1.5 Hz, 1H), 3.83 (s, 3H), 2.27 (s, 3H).

^{13}C NMR (101 MHz, Chloroform-*d*) δ 159.52 (C), 151.25 (CH), 149.09 (C), 147.30 (CH), 140.44 (C), 130.62 (C), 129.51 (CH), 123.89 (CH), 120.93 (CH), 114.34 (CH), 113.29 (CH), 55.31 (CH_3), 17.23 (CH_3).

LCMS(in MeOH): R_t = 1.86 min, m/z = 200.1$[M+H]^+$; HR-MS: calculated for $C_{13}H_{14}NO$- 200.1075, found- 200.1085 (Δ= 5.0 ppm)

IR (neat) ν = 2957.7 (s), 1588.2 (s), 1477.2 (m), 1427.6 (m), 1292.3 (m), 1218.6 (s), 1167.3 (m), 1052.9 (m), 1030.9 (m), 833.2 (m), 783.1 (m), 701.4 (s), 625.5 (m)

4-(4-methoxyphenyl)-3-methylpyridine, **7i**:

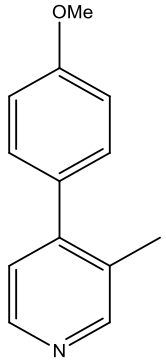

Chemical Formula: $C_{13}H_{13}NO$
Exact Mass: 199.10

Isolated yield: 56%

^{1}H NMR (400 MHz, Chloroform-*d*) δ 8.46 (s, 1H), 8.42 (d, *J* = 5.0 Hz, 1H), 7.28 – 7.23 (m, 2H), 7.12 (d, *J* = 5.0 Hz, 1H), 6.99 – 6.94 (m, 2H), 3.84 (s, 3H), 2.27 (s, 3H).

^{13}C NMR (101 MHz, Chloroform-*d*) δ 159.41 (C), 151.26 (CH), 148.82 (C), 147.31 (CH), 131.34 (C), 130.65 (C), 129.83 (2CH), 124.05 (CH), 113.87 (2CH), 55.31 (CH_3), 17.37 (CH_3).

LCMS(in MeOH): R_t = 1.79 min, m/z = 200.5$[M+H]^+$; HR-MS: calculated for $C_{13}H_{14}NO$- 200.1075, found- 200.1078 (Δ= 1.5 ppm)

IR (neat) ν = 2957.2 (w), 2836.8 (w), 1609.2 (m), 1515.1 (m), 1464.1 (m), 1286.2 (m), 1244.7 (s), 1175.1 (m), 1041.8 (m), 1022.6 (m), 824.7 (s), 554.1 (m), 528.3 (m)

4-(2,4-dimethoxyphenyl)-3-methylpyridine, **7j**:

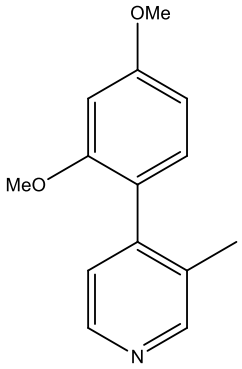

Chemical Formula: $C_{14}H_{15}NO_2$
Exact Mass: 229.11

Isolated yield: 84%

^{1}H NMR (400 MHz, Chloroform-*d*) δ 8.44 (s, 1H), 8.40 (d, *J* = 5.0 Hz, 1H), 7.07 (d, *J* = 4.9 Hz, 1H), 7.03 – 6.98 (m, 1H), 6.58 – 6.51 (m, 2H), 3.84 (s, 3H), 3.73 (s, 3H), 2.11 (s, 3H).

^{13}C NMR (101 MHz, Chloroform-*d*) δ 161.05 (C), 157.24 (C), 150.50 (CH), 146.91 (CH), 146.48 (C), 132.61 (C), 130.78 (CH), 124.98 (CH), 120.78 (C), 104.48 (CH), 98.64 (CH), 55.44 (CH_3), 55.38 (CH_3), 16.86 (CH_3).

LCMS(in MeOH): R_t = 1.86 min, m/z = 230.5$[M+H]^+$; HR-MS: calculated for $C_{14}H_{16}NO_2$- 230.1181, found- 230.1185 (Δ= 1.7 ppm)

IR (neat) ν = 2936.4 (w), 1610.3 (m), 1577.6 (m), 1464.6 (m), 1207.3 (s), 1154.5 (m), 1050.5 (s), 1033.2 (m), 833.9 (s), 798.0 (m), 550.4 (m)

4-(2-trifluoromethylphenyl)-3-methylpyridine, **7k**:

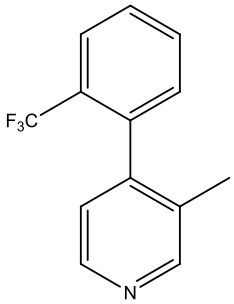

Chemical Formula: $C_{13}H_{10}F_3N$
Exact Mass: 237.08

Isolated yield: 49%

^{1}H NMR (400 MHz, Chloroform-*d*) δ 8.51 (s, 1H), 8.45 (d, *J* = 5.0 Hz, 1H), 7.80 (d, *J* = 8 Hz, 1H), 7.60 (t, *J* = 7.7 Hz, 1H), 7.52 (t, *J* = 8 Hz, 1H), 7.18 (d, *J* = 8 Hz, 1H), 7.07 (d, *J* = 4.9 Hz, 1H), 2.03 (s, 3H).

^{13}C NMR (101 MHz, Chloroform-*d*) δ 150.66 (CH), 146.96 (C), 146.52 (CH), 137.56 (q, *J* = 2.1 Hz, C), 131.68 (CH), 131.43 (C), 130.45 (CH), 128.23 (q, *J* = 30.3 Hz, C) , 128.19 (CH), 126.27 (q, *J* = 5.1 Hz, CH), 123.92 (app. d, *J* = 1.7 Hz, CH), 123.72 (q, *J* = 274.7 Hz, CF_3) , 16.78 (CH_3).

^{19}F NMR (376 MHz, Chloroform-*d*) δ -59.05 (3F).

LCMS(in MeOH): R_t = 2.00 min, m/z = 238.1$[M+H]^+$; HR-MS: calculated for $C_{13}H_{11}F_3N$- 238.0844, found- 238.0847 (Δ= 1.3 ppm)

IR (neat) ν = 3034.5 (w), 1593.1 (w), 1479.6 (w), 1448.8 (w), 1405.1 (w), 1314.0 (s), 1169.8 (m), 1108.6 (s), 1071.4 (m), 1034.3 (m), 835.6 (m), 769.3 (m), 654.2 (m), 601.7 (m)

4-(3-trifluoromethylphenyl)-3-methylpyridine, **7l**:

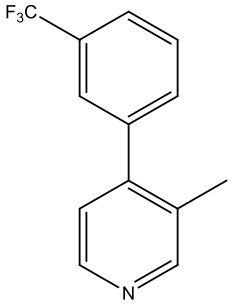

Chemical Formula: $C_{13}H_{10}F_3N$
Exact Mass: 237.08

Isolated yield: 55%

^{1}H NMR (400 MHz, Chloroform-*d*) δ 8.55 (s, 1H), 8.52 (d, *J* = 5.0 Hz, 1H), 7.69 (d, *J* = 7.9 Hz, 1H), 7.63 – 7.57 (m, 2H), 7.53 (d, *J* = 7.6 Hz, 1H), 7.16 (d, *J* = 5.0 Hz, 1H), 2.28 (s, 3H).

^{13}C NMR (101 MHz, Chloroform-*d*) δ 151.53 (CH), 147.60 (CH), 139.81 (C), 131.89 (CH), 131.01 (q, *J* = 32.6 Hz, C), 130.50 (C), 129.03 (CH), 125.34 (q, *J* = 3.8 Hz, CH), 124.81 (q, *J* = 3.8 Hz, CH), 124.08 (q, *J* = 272.8 Hz, CF_3), 123.78 (CH), 17.08 (CH_3).

^{19}F NMR (376 MHz, Chloroform-*d*) δ -62.67 (s, 3F).

LCMS(in MeOH): R_t = 2.30 min, m/z = 238.1$[M+H]^+$; HR-MS: calculated for $C_{13}H_{11}F_3N$- 238.0844, found- 238.0835 (Δ= -3.8 ppm)

IR (neat) ν = 3035.5 (w), 1591.3 (w), 1480.3 (w), 1403.9 (w), 1384.8 (w), 1333.6 (s), 1262.9 (m), 1163.7 (m), 1120.4 (s), 1094.6 (m), 1073.8 (m), 1043.0 (m), 833.2 (m), 804.3 (m), 704.3 (m), 658.7 (m), 623.8 (m)

4-(4-trifluoromethylphenyl)-3-methylpyridine, **7m**:

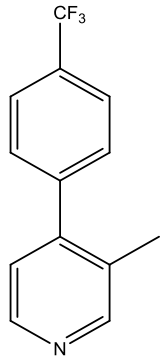

Chemical Formula: $C_{13}H_{10}F_3N$
Exact Mass: 237.08

Isolated yield: 64%

^{1}H NMR (400 MHz, Chloroform-*d*) δ 8.53 (s, 1H), 8.49 (d, *J* = 5.0 Hz, 1H), 7.71 (d, *J* = 8.0 Hz, 2H), 7.43 (d, *J* = 8.0 Hz, 2H), 7.12 (d, *J* = 5.0 Hz, 1H), 2.25 (s, 3H).

^{13}C NMR (101 MHz, Chloroform-*d*) δ 151.48 (CH), 147.75 (C), 147.53 (CH), 142.69 (app. d, *J* = 1.5 Hz, C), 130.43 (C), 130.22 (q, *J* = 32.3 Hz, C), 128.95 (2CH), 125.47 (q, *J* = 3.7 Hz, 2CH), 124.03 (q, *J* = 272.7 Hz, CF_3), 123.67 (CH), 17.07 (CH_3).

^{19}F NMR (376 MHz, Chloroform-*d*) δ -62.63 (s, 3F).

LCMS(in MeOH): R_t = 2.61 min, m/z = 238.1$[M+H]^+$; HR-MS: calculated for $C_{13}H_{11}F_3N$- 238.0844, found- 238.0843 (Δ= -0.4 ppm)

IR (neat) ν = 3033.9 (w), 1620.0 (w), 1591.4 (w), 1451.9 (w), 1321.9 (s), 1163.6 (m), 1121.5 (s), 1107.5 (s), 1069.3 (s), 1031.1 (m), 828.4 (m), 723.0 (m), 612.4 (m)

4-(2-nitrophenyl)-3-methylpyridine, **7n**:

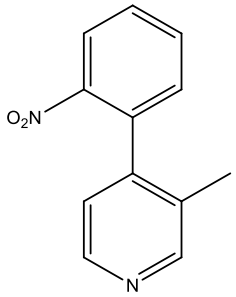

Chemical Formula: $C_{12}H_{10}N_2O_2$
Exact Mass: 214.07

Isolated yield: 39%

^{1}H NMR (400 MHz, Chloroform-*d*) δ 8.58 – 8.40 (m, 2H), 8.10 (dd, *J* = 8.2, 1.3 Hz, 1H), 7.69 (td, *J* = 7.6, 1.3 Hz, 1H), 7.59 (td, *J* = 8.2, 1.5 Hz, 1H), 7.27 (dd, *J* = 7.5, 1.5 Hz 1H), 7.03 (d, *J* = 4.9 Hz, 1H), 2.07 (s, 3H).

^{13}C NMR (101 MHz, Chloroform-*d*) δ 150.78(CH), 148.00(C), 147.29(CH), 146.02(C), 138.96(C), 133.96(CH), 133.32(CH), 131.28(CH), 130.86(C), 124.63(CH), 122.62(CH), 16.67(CH_3).

LCMS(in MeOH): R_t = 1.52 min, m/z = 215.0$[M+H]^+$; HR-MS: calculated for $C_{12}H_{11}N_2O_2$- 215.0821, found- 215.0827 (Δ= 2.8 ppm)

IR (neat) ν = 2981.2 (m), 1737.2 (w), 1591.6 (m), 1521.4 (s), 1346.3 (s), 855.3 (m), 787.4 (m), 746.6 (m), 668.6 (m), 526.6 (m)

4-(3-nitrophenyl)-3-methylpyridine, **7o**:

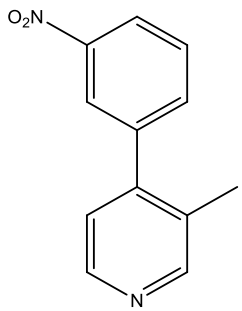

Chemical Formula: $C_{12}H_{10}N_2O_2$
Exact Mass: 214.07

Isolated yield: 70%

^{1}H NMR (400 MHz, Chloroform-*d*) δ 8.55 (s, 1H), 8.51 (d, *J* = 5.0 Hz, 1H), 8.29 – 8.24 (m, 1H), 8.20 (dt, *J* = 2.2, 0.9 Hz, 1H), 7.68 – 7.64 (m, 2H), 7.16 (d, *J* = 4.9 Hz, 1H), 2.28 (s, 3H).

^{13}C NMR (101 MHz, Chloroform-*d*) δ 151.67 (CH), 148.30 (C), 147.75 (CH), 146.61 (C), 140.61 (C), 134.61 (CH), 130.40 (C), 129.65 (CH), 123.67 (CH), 123.54 (CH), 122.98 (CH), 17.10 (CH_3).

LCMS(in MeCN): R_t=1.66 min, m/z = 215.0 $[M+H]^+$; HR-MS: calculated for $C_{12}H_{11}N_2O_2$ - 215.0821, found- 215.0830 (Δ= 4.2 ppm)

IR (neat) ν = 2981.1 (m), 1736.5 (w), 1595.8 (w), 1524.8 (s), 1346.3 (s), 855.3 (m), 787.4 (m), 746.6 (m), 668.6 (m), 526.6 (m)

4-(4-nitrophenyl)-3-methylpyridine, **7p**:

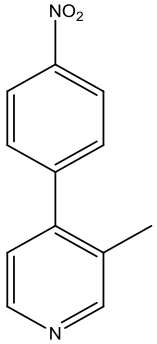

Chemical Formula: $C_{12}H_{10}N_2O_2$
Exact Mass: 214.07

Isolated yield: 79%

^{1}H NMR (400 MHz, Chloroform-*d*) δ 8.54 (s, 1H), 8.50 (d, *J* = 5.0 Hz, 1H), 8.32 – 8.27 (m, 2H), 7.52 – 7.46 (m, 2H), 7.13 (d, *J* = 5.0 Hz, 1H), 2.25 (s, 3H).

^{13}C NMR (101 MHz, Chloroform-*d*) δ 151.63 (CH), 147.65 (CH), 147.56 (C), 146.85 (C), 145.59 (C), 130.23 (C), 129.61 (2CH), 123.76 (2CH), 123.41 (CH), 17.10 (CH_3).

LCMS(in MeCN): R_t=1.69 min, m/z = 215.0 $[M+H]^+$; HR-MS: calculated for $C_{12}H_{11}N_2O_2$ - 215.0821, found- 215.0830 (Δ= 4.2 ppm)

IR (neat) ν = 2981.2 (m), 1738.1 (w), 1514.7 (s), 1347.9 (s), 855.7 (m), 836.9 (m), 814.8 (m), 738.5 (m), 697.4 (m), 577.5 (m)

4-(2-cyanophenyl)-3-methylpyridine, **7q**:

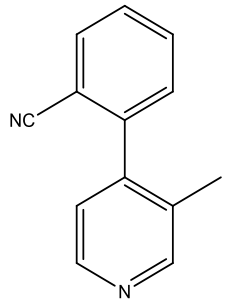

Chemical Formula: $C_{13}H_{10}N_2$
Exact Mass: 194.08

Isolated yield: 42%

^{1}H NMR (400 MHz, Chloroform-*d*) δ 8.59 (s, 1H), 8.54 (d, *J* = 5.0 Hz, 1H), 7.80 (ddd, *J* = 7.7, 1.4, 0.6 Hz, 1H), 7.69 (app. td, *J* = 7.7, 1.4 Hz, 1H), 7.53 (app. td, *J* = 7.7, 1.2 Hz, 1H), 7.36 (ddd, *J* = 7.8, 1.3, 0.6 Hz, 1H), 7.15 (d, *J* = 4.9 Hz, 1H), 2.20 (s, 3H).

^{13}C NMR (101 MHz, Chloroform-*d*) δ 151.51(CH), 147.46(CH), 145.53(C), 142.74(C), 133.19(CH), 132.81(CH), 130.98(C), 129.72(CH), 128.58(CH), 123.69(CH), 117.43(C), 112.18(C), 16.71(CH_3).

LCMS(in MeCN): R_t=1.42 min, m/z = 195.4 $[M+H]^+$; HR-MS: calculated for $C_{13}H_{11}N_2$ - 195.0922, found - 195.0932 (Δ= 5.1 ppm)

IR (neat) ν = 2227.5 (m, CN), 1590.2 (m), 1443.4 (m), 1404.6 (m), 1192.6 (w), 836.8 (m), 768.5 (s), 630.2 (m), 602.2 (m)

4-(3-cyanophenyl)-3-methylpyridine, **7r**:

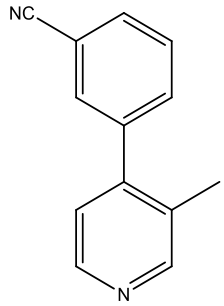

Chemical Formula: $C_{13}H_{10}N_2$
Exact Mass: 194.08

Isolated yield: 87%

^{1}H NMR (400 MHz, Chloroform-*d*) δ 8.53 (s, 1H), 8.49 (d, *J* = 5 Hz, 1H), 7.70 (dt, *J* = 6.9, 2.0 Hz, 1H), 7.62 – 7.60 (m, 1H), 7.59 – 7.55 (m, 2H), 7.10 (d, *J* = 4.9 Hz, 1H), 2.25 (s, 3H).

^{13}C NMR (101 MHz, Chloroform-*d*) δ 151.61 (CH), 147.69 (CH), 146.74 (C), 140.30 (C), 132.96 (CH), 132.01 (CH), 131.64 (CH), 130.36 (C), 129.48 (CH), 123.64 (CH), 118.36 (C), 112.90 (C), 17.08 (CH_3).

LCMS(in MeCN): R_t=1.48 min, m/z = 195.0 $[M+H]^+$; HR-MS: calculated for $C_{13}H_{11}N_2$ - 195.0922, found - 195.0915 (Δ= -3.6 ppm)

IR (neat) ν = 2981.2 (s), 2230.9 (m, CN), 1738.3 (s), 1591.6 (m), 1380.5 (s), 838.1 (m), 805.0 (s), 700.7 (s), 587.4 (m), 488.8 (m)

4-(4-cyanophenyl)-3-methylpyridine, **7s**:

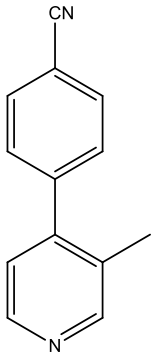

Chemical Formula: $C_{13}H_{10}N_2$
Exact Mass: 194.08

Isolated yield: 68%

^{1}H NMR (400 MHz, Chloroform-*d*) δ 8.54 (s, 1H), 8.51 (d, *J* = 5.0 Hz, 1H), 7.78 – 7.72 (m, 2H), 7.48 – 7.40 (m, 2H), 7.11 (d, *J* = 5.0 Hz, 1H), 2.25 (s, 3H).

^{13}C NMR (101 MHz, Chloroform-*d*) δ 151.66 (CH), 147.69 (CH), 147.18 (C), 143.72 (C), 132.33 (2CH), 130.19 (C), 129.39 (2CH), 123.42 (CH), 118.46 (C), 112.08 (C), 17.08 (CH_3).

LCMS(in MeOH): R_t=1.48 min, m/z = 195.0 $[M+H]^+$; HR-MS: calculated for $C_{13}H_{11}N_2$ - 195.0922, found - 195.0924 (Δ= 1.0 ppm)

IR (neat) ν = 2981.2 (m), 2228.3 (m, CN), 1738.8 (m), 1592.1 (m), 1404.49 (m), 1376.9 (m), 1230.6 (m), 826.4 (m), 559.4 (s), 516.4 (m)

3,5-dimethylpyridine-N-oxide (3,5-lutidine-N-oxide), **8**:

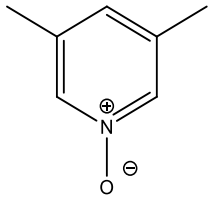

Chemical Formula: C_7H_9NO
Exact Mass: 123.07

Isolated yield: 56%

^{1}H NMR (400 MHz, Chloroform-*d*) δ 7.90 (s, 2H), 6.90 (s, 1H), 2.25 (s, 6H).

4-nitro-3,5-dimethylpyridine-N-oxide (4-nitro-3,5-lutidine-N-oxide), **9**:

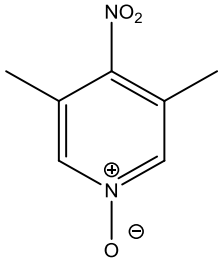

Chemical Formula: $C_7H_8N_2O_3$
Exact Mass: 168.05

Isolated yield: 63%

^{1}H NMR (400 MHz, Chloroform-*d*) δ 7.98 (s, 2H), 2.30 (s, 6H).

4-bromo-3,5-dimethylpyridine-N-oxide (4-bromo-3,5-lutidine-N-oxide), **10**:

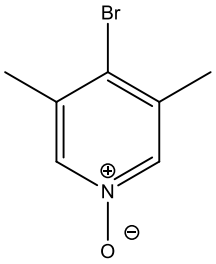

Chemical Formula: C_7H_8BrNO
Exact Mass: 200.98

Isolated yield: 58%

^{1}H NMR (400 MHz, Chloroform-*d*) δ 7.95 (s, 2H), 2.33 (d, 6H).

4-bromo-3,5-dimethylpyridine hydrochloride (4-bromo-3,5-lutidine hydrochloride), **11b**:

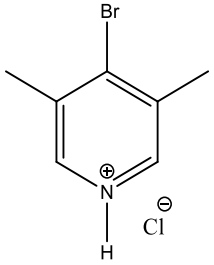

Chemical Formula: C_7H_9BrNCl
Exact Mass: 220.96

Isolated yield: 60%

^{1}H NMR (400 MHz, Methanol-d_4) δ 8.66 (s, 2H), 2.64 (s, 6H).

4-phenyl-3,5-dimethylpyridine, **12a**:

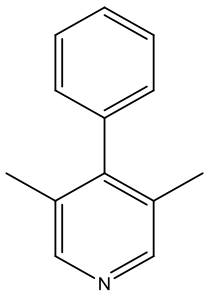

Chemical Formula: $C_{13}H_{13}N$
Exact Mass: 183.10

Isolated yield: 65%

^{1}H NMR (400 MHz, Chloroform-*d*) δ 8.34 (s, 2H), 7.48 – 7.41 (m, 2H), 7.41 – 7.34 (m, 1H), 7.14 – 7.07 (m, 2H), 2.01 (s, 6H).

^{13}C NMR (101 MHz, Chloroform-*d*) δ 149.33 (C), 148.37 (2CH), 138.10 (C), 130.81 (2C), 128.71(2CH), 128.00 (2CH), 127.51 (CH), 17.29 ($2CH_3$).

LCMS(in MeOH): R_t = 1.89 min, m/z = 184.1$[M+H]^+$; HR-MS: calculated for $C_{13}H_{13}N$- 184.1126, found- 184.1126 (Δ= 0.0 ppm)

IR (neat) ν = 2970.3 (w), 1584.3 (m), 1472.6 (m), 1441.1 (m), 1410.2 (m), 1159.4 (m), 877.8 (m), 774.7 (m), 711.3 (s), 755.4 (s), 667.0 (m), 588.8 (m), 523.9 (m)

Melting point: 85.7 – 88.0 ºC (1:9::AcOEt:Hexanes)

4-(2-methylphenyl)-3,5-dimethylpyridine, **12b**:

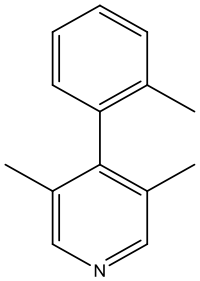

Chemical Formula: $C_{14}H_{15}N$
Exact Mass: 197.12

Isolated yield: 69%

Melting point: 70.9 – 72.1ºC, dried from 10% AcOEt solution in Hexanes.

^{1}H NMR (400 MHz, Chloroform-*d*) δ 8.34 (s, 2H), 7.32 – 7.21 (m, 3H), 6.97 – 6.90 (m, 1H), 1.95 (s, 3H), 1.93 (s, 6H).

^{13}C NMR (101 MHz, Chloroform-*d*) δ 148.94(C), 148.37(2CH), 137.57(C), 134.63(C), 130.88(2C), 130.28(CH), 127.80(CH), 127.69(CH), 126.30(CH), 19.22(CH_3), 16.87($2CH_3$).

LCMS(in MeOH): R_t=1.89 min, m/z = 198.1 $[M+H]^+$; HR-MS: calculated for $C_{14}H_{16}N$ - 198.1283, found - 198.1281 (Δ= -1.0 ppm)

IR (neat) ν = 2919.5 (w), 1584.3 (m), 1450.0 (m), 1410.1 (m), 1378.0 (m), 1156.2 (m), 881.4 (m), 764.9 (s), 752.8 (m), 600.1 (m), 462.7 (m)

Melting point: 70.9 – 72.1 ºC (1:9::AcOEt:Hexanes)

4-(3-methylphenyl)-3,5-dimethylpyridine, **12c**:

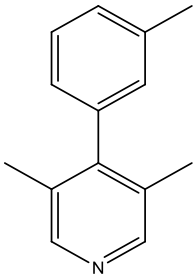

Chemical Formula: $C_{14}H_{15}N$
Exact Mass: 197.12

Isolated yield: 45%

^{1}H NMR (400 MHz, Chloroform-*d*) δ 8.32 (s, 2H), 7.32 (t, *J* = 7.5 Hz, 1H), 7.18 (d, *J* = 7.7 Hz, 1H), 6.93 – 6.86 (m, 2H), 2.38 (s, 3H), 2.01 (s, 6H).

^{13}C NMR (101 MHz, Chloroform-*d*) δ 149.45(C), 148.34(2CH), 138.31(C), 138.06(C), 130.78(2C), 128.57(CH), 128.54(CH), 128.19(CH), 125.00(CH), 21.48(CH_3), 17.29(2CH_3).

LCMS(in MeOH): R_t = 2.27 min, m/z = 198.1 $[M+H]^+$; HR-MS: calculated for $C_{14}H_{16}N$ - 198.1283, found - 198.1286 (Δ= 1.5 ppm)

IR (neat) ν = 2920.2 (w), 1583.4 (m), 1472.1 (m), 1446.9 (m), 1382.0 (m), 1156.9 (m), 885.8 (m), 796.8 (m), 763.9 (m), 746.5 (m), 711.9 (s), 591.0 (m), 455.7 (m)

Melting point: 65.2 – 66.3 ºC (1:9::AcOEt:Hexanes)

4-(4-methylphenyl)-3,5-dimethylpyridine, **12d**:

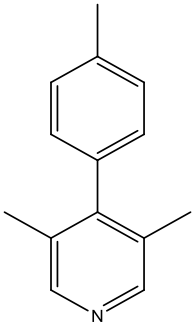

Chemical Formula: $C_{14}H_{15}N$
Exact Mass: 197.12

Isolated yield: 36%

^{1}H NMR (400 MHz, Chloroform-*d*) δ 8.34 (s, 2H), 7.30 – 7.24 (m, 2H), 7.04 – 6.98 (m, 2H), 2.42 (s, 3H), 2.09 – 1.97 (m, 6H).

^{13}C NMR (101 MHz, Chloroform-*d*) δ 149.39 (C), 148.34 (2CH), 137.14 (C), 135.06 (C), 130.97 (2C), 129.37 (2CH), 127.89 (2CH), 21.26 (CH_3), 17.33 (2CH_3).

LCMS(in MeOH): R_t= 2.27 min, m/z = 198.1 $[M+H]^+$; HR-MS: calculated for $C_{14}H_{16}N$ - 198.1283, found - 198.1280 (Δ= -1.5 ppm)

IR (neat) ν = 2920.1 (w), 1584.5 (m), 1514.2 (m), 1447.8 (m), 1407.8 (m), 1157.7 (m), 884.0 (m), 815.4 (s), 752.0 (m), 585.0 (m), 523.3 (s)

4-(2-methoxyphenyl)-3,5-dimethylpyridine, **12f**:

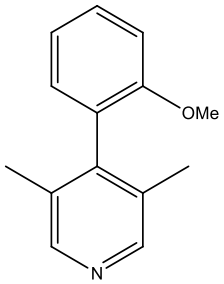

Chemical Formula: $C_{14}H_{15}NO$
Exact Mass: 213.12

Isolated yield: 47%

^{1}H NMR (400 MHz, Chloroform-*d*) δ 8.31 (s, 2H), 7.36 (ddd, *J* = 8.3, 7.3, 1.9 Hz, 1H), 7.04 – 6.94 (m, 3H), 3.71 (s, 3H), 1.98 (s, 6H).

^{13}C NMR (101 MHz, Chloroform-*d*) δ 155.91 (C), 148.04 (2CH), 146.36 (C), 131.58 (2C), 129.56 (CH), 129.28 (CH), 126.60 (C), 120.85 (CH), 111.03 (CH), 55.39 (CH_3), 16.99 ($2CH_3$).

LCMS(in MeOH): R_t= 1.69 min, m/z = 214.1 $[M+H]^+$; HR-MS: calculated for $C_{14}H_{16}NO$ - 214.1232, found – 214.1232 (Δ= 0.0 ppm)

IR (neat) ν = 2957.2 (w), 1601.6 (m), 1581.8 (m), 1435.0 (m), 1251.4 (s), 1230.1 (m), 1161.7 (m), 1120.2 (m), 1052.6 (m), 1026.4 (m), 804.7 (m), 753.8 (s), 662.6 (m), 539.4 (m)

4-(3-methoxyphenyl)-3,5-dimethylpyridine, **12g**:

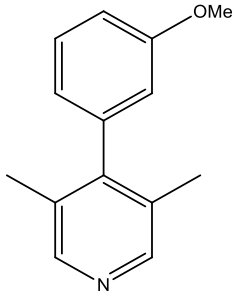

Chemical Formula: $C_{14}H_{15}NO$
Exact Mass: 213.12

Isolated yield: 49%

^{1}H NMR (400 MHz, Chloroform-*d*) δ 8.33 (s, 2H), 7.36 (dd, *J* = 8.4, 7.5 Hz, 1H), 6.91 (ddd, *J* = 8.3, 2.6, 1.0 Hz, 1H), 6.68 (app. dt, *J* = 7.5, 1.2 Hz, 1H), 6.64 (dd, *J* = 2.6, 1.5 Hz, 1H), 3.81 (s, 3H), 2.03 (s, 6H).

^{13}C NMR (101 MHz, Chloroform-*d*) δ 159.84(C), 149.14(C), 148.38(2CH), 139.49(C), 130.72(2C), 129.86(CH), 120.32(CH), 113.73(CH), 112.77(CH), 55.25(CH_3), 17.20(2CH_3).

LCMS(in MeOH): R_t= 2.03 min, m/z = 214.1 $[M+H]^+$; HR-MS: calculated for $C_{14}H_{16}NO$ - 214.1232, found – 214.1234 (Δ= 0.9 ppm)

IR (neat) ν = 3002.8 (w), 2968.7 (w), 1574.9 (m), 1466.8 (m), 1291.5 (m), 1208.1 (s), 1173.0 (m), 1054.6 (m), 1030.8 (m), 874.3 (m), 790.8 (s), 746.7 (s), 712.8 (s), 563.4 (m)

Melting point: 93.2 – 95.6 °C (1:9::AcOEt:Hexanes)

4-(4-methoxyphenyl)-3,5-dimethylpyridine, **12h**:

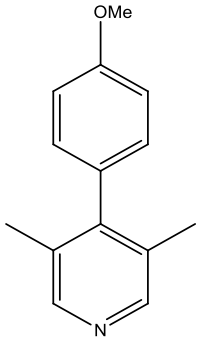

Chemical Formula: $C_{14}H_{15}NO$
Exact Mass: 213.12

Isolated yield: 56%

^{1}H NMR (400 MHz, Chloroform-*d*) δ 8.30 (s, 2H), 7.05 – 6.92 (m, 4H), 3.83 (s, 3H), 2.01 (s, 6H).

^{13}C NMR (101 MHz, Chloroform-*d*) δ 158.89 (C), 149.08 (C), 148.36 (2CH), 131.23 (C), 130.25 (C), 129.23 (2CH), 114.10 (2CH), 55.24 (CH_3), 17.35 (CH_3).

LCMS(in MeOH): R_t= 2.00 min, m/z = 214.1 $[M+H]^+$; HR-MS: calculated for $C_{14}H_{16}NO$ - 214.1232, found – 214.1227 (Δ= -2.3 ppm)

IR (neat) ν = 2958.5 (w), 1610.1 (m), 1516.0 (m), 1465.2 (m), 1292.5 (m), 1241.1 (s), 1173.7 (m), 1043.3 (m), 831.6 (m), 807.3 (m), 767.7 (m), 534.8 (m)

4-(2,4-dimethoxyphenyl)-3,5-dimethylpyridine, **12i**:

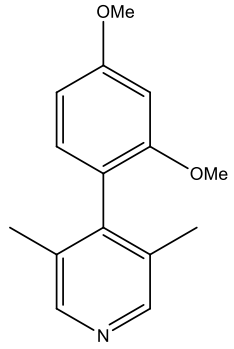

Chemical Formula: $C_{15}H_{17}NO_2$
Exact Mass: 243.13

Isolated yield: 71%

^{1}H NMR (400 MHz, Chloroform-*d*) δ 8.28 (s, 2H), 6.89 – 6.80 (m, 1H), 6.60 – 6.49 (m, 2H), 3.82 (s, 3H), 3.67 (s, 3H), 1.97 (s, 6H).

^{13}C NMR (101 MHz, Chloroform-*d*) δ 160.71 (C), 157.01 (C), 148.03 (2CH), 146.19 (C), 132.10 (2C), 130.01 (CH), 119.21 (C), 104.63 (CH), 98.81 (CH), 55.42 (CH_3), 55.38 (CH_3), 17.05 ($2CH_3$).

LCMS(in MeOH): R_t= 2.07 min, m/z = 244.2 $[M+H]^+$; HR-MS: calculated for $C_{15}H_{18}NO_2$ - 244.1338, found – 244.1337 (Δ= -0.4 ppm)

IR (neat) ν = 2958.9 (w), 1610.7 (m), 1579.6 (m), 1510.8 (m), 1304.1 (m), 1206.1 (s), 1157.0 (s), 1029.5 (m), 833.4 (m), 531.6 (m)

4-(3-trifluoromethylphenyl)-3,5-dimethylpyridine, **12k**:

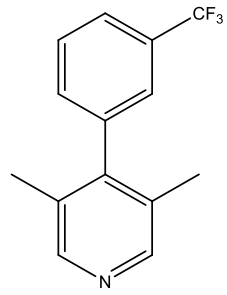

Chemical Formula: $C_{14}H_{12}F_3N$
Exact Mass: 251.09

Isolated yield: 45%

^{1}H NMR (400 MHz, Chloroform-*d*) δ 8.37 (s, 2H), 7.66 (d, *J* = 7.9 Hz, 1H), 7.60 (t, *J* = 7.8 Hz, 1H), 7.40 (s, 1H), 7.33 (d, *J* = 7.9 Hz, 1H), 2.01 (s, 6H).

^{13}C NMR (101 MHz, Chloroform-*d*) δ 148.64(2CH), 147.63(C), 138.87(C), 131.57 (app. d, *J* = 1.4 Hz, CH), 131.29 (q, *J* = 32.6 Hz, C), 130.54(2C), 129.36(CH), 124.93 (q, *J* = 3.7 Hz, CH), 124.51 (q, *J* = 3.8 Hz, CH), 123.96 (q, *J* = 275.3 Hz, CF_3), 17.24($2CH_3$).

^{19}F NMR (376 MHz, Chloroform-*d*) δ -62.65(3F).

LCMS(in MeOH): R_t= 0.87 min, m/z = 252.1 $[M+H]^+$; HR-MS: calculated for $C_{14}H_{12}F_3N$ - 252.1000, found – 252.1001 (Δ= 0.4 ppm)

IR (neat) ν = 2972.6 (w), 1742.6 (w), 1584.0 (w), 1478.4 (w), 1382.7 (w), 1328.6 (s), 1242.9 (m), 1120.3 (m), 1092.1 (s), 1074.6 (s), 1041.7 (m), 905.4 (m), 876.2 (m), 816.7 (m), 711.8 (m), 685.8 (m)

Melting point: 79.6 – 80.7 ºC (1:9::AcOEt:Hexanes)

4-(4-trifluoromethylphenyl)-3,5-dimethylpyridine, **12l**:

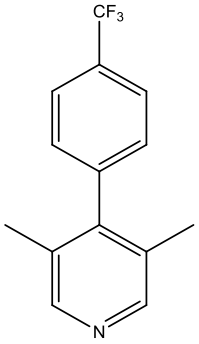

Chemical Formula: $C_{14}H_{12}F_3N$
Exact Mass: 251.09

Isolated yield: 58%

^{1}H NMR (400 MHz, Chloroform-*d*) δ 8.36 (s, 2H), 7.72 (d, *J* = 7.8 Hz, 2H), 7.26 (d, *J* = 7.8 Hz, 2H), 2.00 (s, 6H).

^{13}C NMR (101 MHz, Chloroform-*d*) δ 148.60(2CH), 147.80(C), 141.89 (app. d, *J* = 1.6 Hz, C), 130.38(2C), 129.94 (q, *J* = 32.7 Hz, C), 128.58(2CH), 125.80 (q, *J* = 3.8 Hz, 2CH), 124.06 (q, *J* = 273.0 Hz, CF_3), 17.20($2CH_3$).

^{19}F NMR (376 MHz, Chloroform-*d*) δ -62.61(3F).

LCMS(in MeOH): R_t= 2.58 min, m/z = 252.1 $[M+H]^+$; HR-MS: calculated for $C_{14}H_{12}F_3N$ - 252.1000, found – 252.1005 (Δ= 2.0 ppm)

IR (neat) ν = 2970.4 (w), 1737.2 (w), 1616.0 (w), 1584.5 (w), 1379.1 (w), 1320.6 (m), 1159.2 (m), 1105.4 (s), 1031.5 (m), 1019.2 (m), 889.8 (m), 753.8 (m), 613.5 (m)

Melting point: 89.2 – 90.4 ºC (1:9::AcOEt:Hexanes)

4-(3-nitrophenyl)-3,5-dimethylpyridine, **12n**:

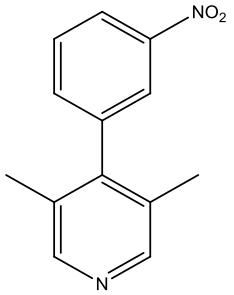

Chemical Formula: $C_{13}H_{12}N_2O_2$
Exact Mass: 228.09

Isolated yield: 53%

^{1}H NMR (400 MHz, Chloroform-*d*) δ 8.39 (s, 2H), 8.27 (ddd, *J* = 8.3, 2.3, 1.1 Hz, 1H), 8.04 (app. s, 1H), 7.69 (t, *J* = 7.9 Hz, 1H), 7.50 (dt, *J* = 7.6, 1.3 Hz, 1H), 2.03 (s, 6H).

^{13}C NMR (101 MHz, Chloroform-*d*) δ 148.77 (2CH), 148.57 (C), 146.59 (C), 139.70 (C), 134.45 (CH), 130.38 (2C), 129.99 (CH), 123.24 (CH), 122.74 (CH), 17.26 ($2CH_3$).

LCMS(in MeOH): R_t= 1.83 min, m/z = 229.1 $[M+H]^+$; HR-MS: calculated for $C_{13}H_{13}N_2O_2$ – 229.0977, found – 229.0979 (Δ= 0.9 ppm)

IR (neat) ν = 2921.2 (w), 1741.4 (w), 1587.7 (w), 1525.9 (m), 1348.4 (s), 1162.9 (m), 1091.9 (m), 880.9 (m), 736.2 (m), 700.8 (s)

Melting point: 112.4 – 113.4 ºC (1:4::AcOEt:Hexanes)

4-(4-nitrophenyl)-3,5-dimethylpyridine, **12o**:

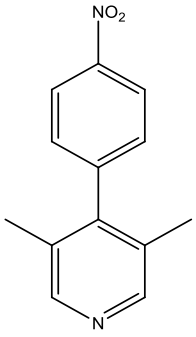

Chemical Formula: $C_{13}H_{12}N_2O_2$
Exact Mass: 228.09

Isolated yield: 42%

^{1}H NMR (400 MHz, Chloroform-*d*) δ 8.42 (s, 2H), 8.37 (d, *J* = 8.6 Hz, 2H), 7.36 (d, *J* = 8.6 Hz, 2H), 2.04 (s, 6H).

^{13}C NMR (101 MHz, Chloroform-*d*) δ 148.72 (2CH), 147.50 (C), 147.01 (C), 145.01 (C), 130.05 (2C), 129.31 (2CH), 124.17 (2CH), 17.23 ($2CH_3$).

LCMS(in MeOH): R_t= 1.89 min, m/z = 229.1 $[M+H]^+$; HR-MS: calculated for $C_{13}H_{13}N_2O_2$ – 229.0977, found – 229.0967 (Δ= -4.4 ppm)

IR (neat) ν = 1600.7 (w), 1582.9 (w), 1515.2 (s, NO_2), 1345.6 (s, NO_2), 1163.2 (w), 1102.9 (w), 856.0 (s), 776.4 (m), 748.2 (m), 702.6 (m), 588.3 (m), 459.4 (m)

4-(2-cyanophenyl)-3,5-dimethylpyridine, **12q**:

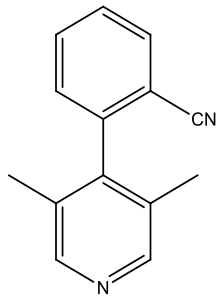

Chemical Formula: $C_{14}H_{12}N_2$
Exact Mass: 208.10

Isolated yield: 12%

^{1}H NMR (400 MHz, Chloroform-*d*) δ 8.45 (s, 2H), 7.84 (dd, *J* = 7.8, 1.4 Hz, 1H), 7.74 (td, *J* = 7.7, 1.4 Hz, 1H), 7.56 (td, *J* = 7.7, 1.2 Hz, 1H), 7.31 – 7.25 (m, 1H), 2.05 (s, 6H).

^{13}C NMR (101 MHz, Chloroform-*d*) δ 148.71 (2CH), 145.39 (C), 142.08 (C), 133.30 (CH), 133.23 (CH), 130.60 (2C), 129.25 (CH), 128.45 (CH), 117.07 (C), 112.17 (C), 16.94 ($2CH_3$).

LCMS(in MeOH): R_t= 1.31 min, m/z = 209.1 $[M+H]^+$; HR-MS: calculated for $C_{14}H_{13}N_2$ – 209.1079, found – 209.1085 (Δ= 2.9 ppm)

IR (neat) ν = 2226.2 (m, CN), 1584.3 (m), 1470.3 (m), 1444.6 (m), 1163.6 (m), 879.0 (m), 761.3 (s), 768.7 (s), 742.5 (m), 518.4 (m)

4-(3-cyanophenyl)-3,5-dimethylpyridine, **12r**:

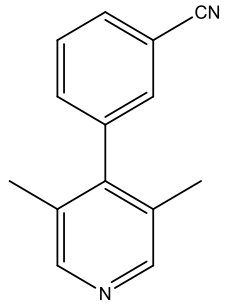

Chemical Formula: $C_{14}H_{12}N_2$
Exact Mass: 208.10

Isolated yield: 60%

^{1}H NMR (400 MHz, Chloroform-*d*) δ 8.37 (s, 2H), 7.70 (app. dt, *J* = 7.8, 1.4 Hz, 1H), 7.60 (td, *J* = 7.7, 0.6 Hz, 1H), 7.44 (app. td, *J* = 1.7, 0.6 Hz, 1H), 7.38 (dt, *J* = 7.7, 1.5 Hz, 1H), 2.00 (s, 6H).

^{13}C NMR (101 MHz, Chloroform-*d*) δ 148.74(2CH), 146.73(C), 139.42(C), 132.70(CH), 131.65(CH), 131.41(CH), 130.38(2C), 129.80(CH), 118.38(C), 113.20(C), 17.25($2CH_3$).

LCMS(in MeOH): R_t= 1.52 min, m/z = 209.1 $[M+H]^+$; HR-MS: calculated for $C_{14}H_{12}N_2$ - 209.1079, found – 252.1079 (Δ= 0.0 ppm)

IR (neat) ν = 2919.2 (w), 2228.3 (m, CN), 1585.9 (m), 1471.5 (m), 1411.1 (m), 1381.1 (m), 1159.4 (m), 877.1 (m), 805.9 (s), 701.3 (s), 598.7 (m), 496.8 (s)

4-(4-cyanophenyl)-3,5-dimethylpyridine, **12s**:

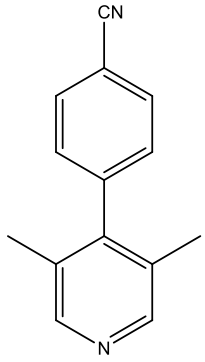

Chemical Formula: $C_{14}H_{12}N_2$
Exact Mass: 208.10

Isolated yield: 60%

^{1}H NMR (400 MHz, Chloroform-*d*) δ 8.36 (s, 2H), 7.82 – 7.71 (m, 2H), 7.31 – 7.23 (m, 2H), 2.00 (s, 6H).

^{13}C NMR (101 MHz, Chloroform-*d*) δ 148.66(2CH), 147.26(C), 143.01(C), 132.66(2CH), 130.06(2C), 129.09(2CH), 118.49(C), 111.80(C), 17.18($2CH_3$).

LCMS(in MeOH): R_t= 1.54 min, m/z = 209.1 $[M+H]^+$; HR-MS: calculated for $C_{14}H_{12}N_2$ - 209.1079, found – 252.1075 (Δ= -1.9 ppm)
IR (neat) ν = 2919.0 (w), 2227.2 (m, CN), 1570.0 (m), 1477.3 (m), 1412.7 (m), 1349.6 (m), 848.1 (s), 585.6 (s), 548.9 (s), 499.7 (m)

Melting point: 166.3 – 169.0 ºC (3:7::AcOEt:Hexanes)

References:

1: Bissantz C, Kuhn B, Stahl M, *J. Med. Chem.*, **2010**, *53*, p5061-5084.

2: McGaughey G.B, Gagne M, Rappe A.K, *J. Biol. Chem.*, **1998**, *273*, p15458-15463.

3: van der Spoel, van Buuren A.R, Tieleman D.P, Berendsen H.J.C, *J. Biomol. NMR*, **1996**, *8*, p229-238.

4: Zacharias N, Dougherty D.A, *Trends Pharmacol. Sci.*, **2002**, *23*, p281-287.

5: Hadjuk P.J, Bures M, Praestgaard J, Fesik S.W, *J. Med. Chem.*, **2000**, *43*, p3443-3447.

6: Schnur D.M, Beno B.R, Good A, Tebben A.J, *J. Med. Chem.*, **2006**, *49*, p2000.

7: Martin R, Buchwald S.L, *Acc. Chem. Res.*, **2008**, *41*, p1461-1473.

8: Wu S, He M, Zhang X, *Tetrahedron: Asymmetry*, **2004**, *41*, p2177-2180.

9: Kanthasamy K, Pfnur H, *Beilstein J. Nanotechnol.*, **2015**, *6*, 1690-1697.

10: de Gennes D.G, Prost J, In: "*The Physics of Liquid Crystals*", Oxford: Clarendon Press, **1995**, *2*, 4.

11: Lim E.C, Li Y.H, *J. Chem. Phys.*, **1970**, *52*, p6416-6422.

12: Loyd-Williams P, Giralt E, *Chem. Soc. Rev.*, **2001**, *30*, p146.

13: Trotter J, *Acta. Cryst.*, **1961**, *14*, p1135-1140.

14: Bastiensen O, *Acta. Chem. Scand.*, **1949**, *3*, p408.

15: Eaton V.J, Steele V.D, *J. Chem. Soc. Faraday Trans. 2*, **1973**, *69*, 1601-1608.

16: Imamura A, Hoffmann R, *J. Am. Chem. Soc.*, **1968**, *90*, p5379.

17: Kato M, Higashi M, Taniguchi Y, *J. Chem. Phys.*, **1988**, *89*, p5417-5421.

18: Oki K, "*Recent Advances in atropisomerism*", In: Allinger N.L, Eliel E.E, Wilen S.H (editors), "*Topics in Stereochemistry*", New York: Wiley Interscience, **1983**, *14*, p9.

19: LaPlante S.R, Fader L.D, Fandrick K.R, Fandrick D.R, Hucke O, Kemper R, Miller S.P.F, Edwards P.J, *J. Med. Chem.*, **2011**, *54*, p7005-7022.

20: Mikami K, Aikawa K, Yusa Y, Jodry J.J, Yamanaka M, *Synlett.*, **2002**, *10*, p1561-1578.

21: Christie G.H, Kenner J, *J. Chem. Soc. Trans.*, **1922**, *121*, p614-620.

22: Cahn R.S, *J. Chem. Educ.*, **1964**, *41*, 116.

23: Bringmann G, Mortimer A.P.J, Keller, P.A, Gresser M.J, Garner J, Breuning M, *Angew. Chem. Int. Ed.*, **2005**, *44*, p5384-5427.

24: Bringmann G, Menche D, Bezabih M, Abegaz B.M, Kaminsky R, *Planta. Med.*, **1999**, *65*, p757-758.

25: Sprogoe K, Stark D, Ziegler H.L, Jensen T.H, Holm-Moller S.B, Jaroszewski J.W, *J. Nat. Prod.*, **2008**, *71*, p516-519.

26: Casy A.F, *Magn. Reson. Chem.*, **1993**, *31*, p416-417.

27: Smyth J.E, Butler N.M, Keller P.A, *Nat. Prod. Rep.*, **2015**, *32*, p1562-1583.

28: Eliel,E.L., "*Stereochemistry of Carbon Compounds*", McGraw-Hill Book Company

Inc., **1962**, p22.

29: Chhabra N, Aseri M.L, Padmanabhan D, *Int. J. App. Basic. Med. Res.*, **2013**, *3*, p16-18.

30: Knoche B, Blaschke G, *Chirality*, **1994**, *6*, p221-224.

31: Zask A, Murphy J, Ellestad G.A, *Chirality*, **2013**, *25*, p265-274.

32: Boger D.L, Beresis R.T, Loiseleur O, Wu J.H, Castle S.L, *Bioorg. Med. Chem. Lett.,* **1998**, *8*, p721-724.

33: Boger D.L, Miyazaki S, Kim S.H, Wu J.H, Loiseleur O, Castle S.L, Jin Q*, J. Am. Chem. Soc.*, **1999**, *121*, p10004-10011.

34: Clayden J, *Chem. Commun.*, **2004**, *2*, p127-135.

35: Bringmann G, Menche D, Kraus J, Muhlbache J, Peters K, Peters E, Brun R, Bezabih M, Abegaz B.M, *J. Org. Chem.*, **2002**, *67*, p5595-5610.

36: Gustafson J.L, Lim D, Miller S.J, *Science*, **2010**, *328*, p1251-1255.

37: Yoon T.P, Jacobsen E.N, *Science*, **2003**, *299*, p1691-1693.

38: Meca L, Reha D, Hawlas Z, *J. Org. Chem.*, **2003**, *68*, p5677-5680.

39: Garcia J.S, Lepetit C, Canac Y, Chauvin R, Boggio-Pasqua M, *Chem. Asian J.*, **2014**, *9*, p462-465.

41: Mikami K, Aikawa K, Yusa Y, Jodry J.J, Yamanaka M, *SynLett.*, **2002**, *10*, p1561-1578.

42: Aikawa M, Mikami K, *Chem. Commun.*, **2012**, *48*, p11050-11069.

43: Oczipka P, Muller D, Leitner W, Francio G, *Chem. Sci.*, **2016**, *7*, p678-683.

44: Nagrady T, Weaver D.F, In: "*Medicinal Chemistry: A Molecular and Biochemical Approach*", New York: Oxford University Press, Inc., **2005**, *3*, p36.

44: Lai Y, Xing L, Poda G.I, Hu Yiding, *Drug Metab. Dispos.*, **2007**, *35*, p937-945.

45: Forest J, Bazylewski P, Bauer R, Hong S, Kim C.Y, Giesy J.P, Seong Khim J, Soo Changg G, *Front. Mar. Sci.*, **2014**, *1*, p1-7.

46: Hinreiner M, Ryndyk D.A, Usyvat D, Merz T, Schutz M, Richter K, *Phys. Status Solidi. B*, **2013**, *250*, p2408-2416.

47: Xia C.J, Fang C.F, Peng Z, Shi-Jie X, De-Sheng L, *Phys. Lett. A*, **2009**, *373*, p3787-3794.

48: Buerkle M, Zotti L.A, Viljas J.K, Vonlanthen D, Mischenko A, Wandlowski T, Mayor M, Schoen G, Pauly F, *Phys. Rev. B*, **2012**, *86*, p115304-115308.

49: Wang L.H, Guo Y, Tian C.F, Song X.P, Ding B.J, *Phys. Lett. A*, **2010**, *374*, p4876-4879.

50: Page P.C.B, Bartlett C.J, Chan Y, Allin S.M, McKenzie M.J, Lacour J, Garth A.J, *Org. Biomol. Chem.*, **2016**, *14*, p4220-4232.

51: Cobley C.J, Froes R.D.J, Klosin J, Qin C, Whiteker G.T, Abboud K.A, *Organometallics*, **2007**, *26*, p2986-2999.

52: Bott G, Field L.D, Sternhell S, *J. Am. Chem. Soc.*, **1980**, *102*, p5618-5626.

53: Meyer W.L, Meyer R.B, *J. Am. Chem. Soc.*¸ **1963**, *85*, p2170-2171.

54: Michinori O, Iwamura H, Hayakawa N, *Bull. Chem. Soc. Jap.*¸ **1964**, *37*, p1865-1870.

55: Colebrook L.D, Jahnke J.A, *J. Am. Chem. Soc.*¸ **1968**, *90*, p4687-4690.

56: Klaus M, Willi H, Klaemer F.G, Roth W.R, Kindermann I, Adamczako O, Wette M, Johann L, *Chem. Ber.*, **1990**, *123*, p2349-2371.

57: Lunazzi L, Mancinelli M, Mazzanti A, Lepri S, Ruzziconi R, Schlosser M, *Org. Biomol. Chem.*, **2012**, *10*, p1847-1855.

58: Wesseloh G, Wolf C, Koenig W.A, *Chirality*, **1996**, *8*, p441-445.

59: Veciana J, Crespo M.J, *Angew. Chem. Int. Ed. Engl.*, **1990**, *30*, p74-76.

60: Trapp O, *Chirality*, **2006**, *18*, p489-497.

61: Wolf C, Koenig W.A, Roussel C, *Liebigs Ann.*, **1995**, *5*, p781-786.

62: Wolf C, Hochmuth D.H, Koenig W.A, Roussel C, *Liebigs Ann.*, **1996**, *3*, p357-363.

63: Bihlmeier A, Rotzler J, Rickhaus M, Mayor M, Klopper W, *Phys. Chem. Chem. Phys.*, **2015**, *17*, p11165-11173.

64: Storch G, Maier F, Wessig P, Trapp O, *Eur. J. Org. Chem.*, **2016**, DOI:10.1002/ejoc.201600836.

65: Sherer E.C, Lee C.H, Shpungin J, Cuff J.F, Da C, Ball R, Bach R, Crespo A, Gong X, Welch C.J, *J. Med. Chem.*, **2014**, *57*, p477-494.

66: Okuom M.O, Burks R, Naylor C, Homes A.E, *J. Anal. Methods Chem.*, **2015**, ArticleID: 865605.

67: Pivonka D.E, Wesolowski S.S, *Appl. Spectrosc.*, **2013**, *67*, p365-371.

68: Grein F, *J. Phys. Chem. A*, **2002**, *106*, p3823-3827.

69: Buevich A.V, *J. Org. Chem.*, **2016**, *81*, p485-501.

70: Masson E, *Org. Biomol. Chem.*, **2013**, *11*, p2859-2871.

71: Zhang L, Peslherbe G.H, Muchall H.M, *Can. J. Chem.*, **2010**, *88*, p1175-1185.

72: Gomez-Gallago M, Martin-Ortiz M, Sierra M.A, *Eur. J. Org. Chem.*, **2011**, *32*, p6502-6506.

73: Vonlanthen D, Rotzler J, Neuberger M, Mayor M, *Eur. J. Org. Chem.*, **2010**, *1*, p120-133.

74: Akiyama M, Watanabe T, Kakihana M, *J. Phys. Chem.*, **1986**, *90*, p1752-1755.

75: Dynes J.J, Baudais F.L, Boyd R.K, *Can. J. Chem.*, **1985**, *63*, p1292-1299.

76: Egolf D.S, Jurs P.C, *Anal. Chem.*, **1990**, *62*, p1746-1754.

77: Barich D.H, Pugmire R.J, Grant D.M, Iulliuci R.J, *J. Phys. Chem. A*, **2001**, *105*, p6780-6784.

78: Leroux F, *ChemBioChem*, **2004**, *5*, p644-649.

79: Jia J, Wu H-S, Chen Z, Mo Y, *Eur. J. Org. Chem.*, **2013**, *3*, 611-616.

78: Sullivan J.J, Jones A.D, Tanji K.K, *J. Chem. Inf. Comput. Sci.*, **2000**, *40*, 1113-1127.

80: Peralta-Inga Z, Murray J.S, Politzer P, *J. Org. Chem.*, **2001**, *66*, 6919-6925.

81: Hansch C, Leo A, Taft R.W, *Chem. Rev.*, **1991**, *91*, 165-195.

82: Byron D.J, Gray G.W, Wilson R.C, *J. Chem. Soc. C*, **1966**, 831-836.

83: Byron D.J, Gray G.W, Wilson R.C, *J. Chem. Soc. C*, **1966**, 837-840.

84: Schneider H.J, Hoppen V.J, *J. Org. Chem.*, **1978**, *43*, 3866.

85: Busing W.R, *Acta. Cryst. A*, **1983**, *39*, 340-347.

86: Wu X, Anbarasan P, Neumann H, Beller M, *Angew. Chem. Int. Ed.*, **2010**, *49*, 9047-9050.

87: Kang H, Facchetti A, Stern C.L, Rheingold A.L, Kassel W.S, Marks T.J, *Org. Lett.*, **2005**, *7*, p3721-3724.

88: Conejo-Garcia A, Pisani L, Nunez M.C, Catto M, Nicolotti O, Leonetti F, Campos J.M, Gallo M.A, Espinosa A, Carotti A, *J. Med. Chem.*, **2011**, *54*, 2627-2645.

89: Diemer V, Helene C, Defoin A, Fort A, Boeglin A, Carre C, *Eur. J. Org. Chem.*, **2008**, *10*, 1767-1776.

90: Feast W.J, Tsibouklis J, *Polym. Int.*, **1994**, *35*, 67-74.

91: Bonin H, Fouquet E, Felpin F, *Adv. Synth. Catal.*, **2011**, *353*, 3063-3084.

92: Joule J.A, Mills K, In: "*Heterocyclic Chemistry*"*,* John Wiley&Sons, **2010**, 146.

93: Kassanova A.Z, Krasnokutskaya E.A, Beisembai P.S, Filimonov V.D, *Synthesis*, **2016**, *48*, 256-262.

94: Espino G, Kurbangalieva A, Brown J.M, *Chem. Commun.*, **2007**, 1742-1744.

95: Walker S.D, Barder T.E, Martinelli J.R, Buchwald S.L, *Angew. Chem. Int. Ed.*, **2004**, *43*, 1871-1876.

96: Andon R.J.L, Cox J.D, Herington E.F.G, *Trans. Faraday. Soc.*, **1954**, *50*, 918-927.

97: Espinosa S, Bosch E, Rosés M, *Anal. Chem.*, **2000**, *72*, 5193-5200.

98: Espinosa S, Bosch E, Rosés M, *Analytica Chimica Acta*, **2002**, *454*, 157-166.

99: Dewar M.J.S, Grisdale P.J, *J. Am. Chem. Soc.*, **1962**, *84*, 3539-3541.

100: Campanelli A.R, Domenicano A, Ramondo F, *J. Phys. Chem. A*, **2012**, *116*, 8209-8217.

101: Schulman E.M, Christensen K.A, Grant D.M, Walling C, *J. Org. Chem.*, **1974**, *39*, 2686-2690.

102: Greenwood N.N, In: "*Spectroscopic Properties of Inorganic and Organometallic Compounds*", London: The Chemical Society, **1971**, *4*, 298-299.

103: Cavallo G, Metrangolo P, Milani R, Pilati T, Priimagi A, Resnati G, Terraneo G, *Chem. Rev.*, **2016**, *116*, 2478-2601.

104: Williams D.H, Fleming I, In: "*Spectroscopic Methods in Organic Chemistry*"*,* New York: The McGraw-Hill Companies Inc., **2008**, *6*, 38.

105: Fuson N, Josien M-L, Shelton E.M, *J. Am. Chem. Soc.*, **1954**, *76*, 2526-2533.

106: Hoffmann R.V, In: "*Organic Chemistry: An Intermediate Text*", Hoboken, New Jersey: Wiley Interscience, **2004**, *2*, 167.

107: Olah G.A, Surya Prakash G.K, Shih J.G, Krishnamurthy V.V, Mateescu G.D, Liang G, Sipos G, Buss V, Gund T.M, Schleyer PvR, *J. Am. Chem. Soc.*, **1985**, *107*, 247-255.

108: Reid K.S.C, Lindley P.F, Thornton J.M, *FEBS Lett*., **1985**, *190*, 209-213.